JRC SCIENTIFIC AND POLICY REPORTS

Particle Measurement Programme. Volatile Particle Remover Calibration Round Robin.

Final Report

Author:
Athanasios Mamakos

Editors:
Giorgio Martini, Alois Krasenbrink

2012

EMRP
European Metrology Research Programme
Programme of EURAMET
The EMRP is jointly funded by the EMRP participating countries within EURAMET and the European Union

Report EUR 25512 EN

Joint
Research
Centre

European Commission
Joint Research Centre
Institute for Energy and Transport

Contact information
Giorgio Martini
Address: Joint Research Centre, Via Enrico Fermi 2749, TP 441, 21027 Ispra (VA), Italy
E-mail: giorgio.martini@jrc.ec.europa.eu
Tel.: +39 0332 789293

http://iet.jrc.ec.europa.eu/
http://www.jrc.ec.europa.eu/

This publication is a Reference Report by the Joint Research Centre of the European Commission.

JRC73454

EUR 25512 EN

ISBN 978-92-79-26416-0 (pdf)
ISBN 978-92-79-26417-7 (print)

ISSN 1831-9424 (online)
ISSN 1018-5593 (print)

doi: 10.2788/49253

Luxembourg: Publications Office of the European Union, 2012

Printed in Italy

TABLE OF CONTENTS

1 INTRODUCTION 6
1.1 Background 6
1.2 History of the Particle Measurement Programme 6
1.3 From PMP to legislation 7
1.4 Scope of the PMP VPR Round Robin 8
1.5 Elements of the PMP VPR Round Robin 9
2 EXPERIMENTAL 11
2.1 Golden Instrumentation 11
2.1.1 Golden Volatile Particle Remover 11
2.1.2 Golden Aerosol Generator 12
2.1.3 Golden Condensation Particle Counter 13
2.2 Calibration Setups 14
2.2.1 Reference setup 14
2.2.2 Calibration setups at the different labs 16
2.2.3 Dilution Factor Measurements 30
3 Characterization of the Golden Instrumentation at JRC 31
3.1 GVPR 31
3.2 GAG 33
3.3 GCPC 38
4 Round Robin Results 40
4.1 GVPR dilution factor 40
4.2 Particle Concentration Reduction Factors 41
4.2.1 Stability of the concentrations in the calibration setup 41
4.2.2 Calculations 42
4.2.3 Golden instrumentation results 44
4.2.4 Results with alternative CPCs 49
4.2.5 Results with alternative generators 54
4.2.6 Additional investigations 60
5 CONCLUSIONS 68
6 Nomenclature 70
7 REFERENCES 72
8 ANNEX A 75
8.1 Description of the minimum required calibration work to be performed at each participating laboratory 75
9 ANNEX B 77
9.1 Original calibration certificate of the GCPC (Page 1/2) 77
9.2 Original calibration certificate of the GCPC (Page 2/2) 78
9.3 Calibration certificate of the GCPC after the failure at LAT (Page 1/2) 79
9.4 Calibration certificate of the GCPC after the failure at LAT (Page 1/2) 80
9.5 Calibration certificate of the GCPC after the failure at AEAT (Page 1/2) 81
9.6 Calibration certificate of the GCPC after the failure at AEAT (Page 2/2) 82
9.7 Calibration certificate of the GCPC after the failure at VW (Page 1/2) 83
9.8 Calibration certificate of the GCPC after the failure at VW (Page 2/2) 84

ACKNOWLEDGMENTS

The authors would like to acknowledge T. Tzamkiozis (LAT), L. Ntziachristos (LAT), Barouch Giechaskiel (AVL), A. Bergmann (AVL), D. Scheder (Horiba), K. Lenz (Horiba), U. Dierks (Horiba), D. Schreiber (EMPA), P. Dimopoulos (EMPA), D. Imhof (Matter Aerosol), M. Kasper (Matter Aerosol), P. Quincey (NPL), J. Tompkins (NPL), D. Sarantaridis (NPL), I. Marshall (AEAT), J. Southgate (AEAT), S. Carli (VW), S. Usarek (VW), D. Hitzler (Maha), H.-G. Horn (TSI) and E. Lamminen (Dekati) for making this work possible and for the fruitful discussions. TSI Inc. is gratefully acknowledged for the supply of the TSI 3790 Condensation Particle Counter that was employed as the "golden" particle detector in the campaign. Dekati Ltd. is also acknowledged for the support throughout the measurement campaign.

The experimental work conducted at JRC was partially funded by the EMRP-ENV02 PartEmission project. The EMRP is jointly funded by the EMRP participating countries within EURAMET and the European Union.

1 INTRODUCTION

1.1 Background

Automotive exhaust Particulate Matter (PM) was long recognized as a harmful pollutant (EPA, 2009), and has been subject to continuously tighter legislation, world-wide. The automotive exhaust PM was traditionally determined gravimetrically, following dilution in a Constant Volume Sampler (CVS) (Berg, 2003). The tightening of the PM limits, however, raised concerns regarding the sensitivity of the legislated gravimetric procedure (Andersson et al., 2001; Zervas et al., 2005).

In Europe, the Euro 4 limits which entered into force in 2005, were set at 25 mg/km for Light Duty (LD) vehicles and 20 mg/kWh for Heavy Duty (HD) engines. These figures corresponded to a 82% (LD) and 94% (HD) reduction over the first legislative step in 1992. Yet, the Clean Air For Europe (COM 446, 2005) study suggested that significant negative impacts of automotive exhaust PM will persist even with effective implementation of the Euro 4 legislation.

In response, the European Commission requested a further tightening of the PM limits to necessitate the installation of very efficient wall-flow Diesel Particulate Filters (DPF) to all diesel vehicles. Recognizing though that the gravimetric procedure might not be sensitive enough to discriminate between wall-flow and the less efficient flow-through particulate filter designs, the European Commission requested the introduction of a complementary particle number drawing from the Particle Measurement Programme (PMP).

1.2 History of the Particle Measurement Programme

The Paticle Measurement Programme (PMP) was first established in 2001 on the initiative of several European countries, with the objective of developing a worldwide harmonized procedure for the measurement of particle number in engine exhaust and an improved mass based measurement procedure. Since then it has evolved in a large scale collaborative project conducted in the framework of the United Nations Economic Council for Europe (UN-ECE) GRPE (Working Party on Pollution and Energy) managed by a UN-ECE Working Group chaired by the UK Department of Transport. The PMP Working Group currently comprises several Governments (including France, Germany, the Netherlands, Japan, Korea, Sweden, Switzerland, UK), the European Commission, automotive industry, aerosol instrumentation manufacturers, national emission laboratories and research institutes.

The PMP project was divided in three different phases (Giechaskiel et al., 2012). The first phase (2001-2002) was devoted to the development of test protocols for the assessment of different candidate sampling. conditioning and measurement approaches. The actual evaluation of the different techniques was conducted in the follow-up second phase of the project, which concluded in 2003 and recommended two complementary measurement procedures:

1. A gravimetric filter mass procedure largely based on the refinements envisaged in the US 2007 legislation (Federal Register, 2001), the most important being:
    a. The mandatory use of a High Efficiency Particulate Filter (HEPA) and recommended use of a charcoal scrubber to condition the dilution air of the CVS.
    b. Use of a pre-classifier (e.g. cyclone) in the sampling line to remove coarse mode particles (cut-off size at 2.5 to 10 μm).
    c. Tighter control of the sample temperature (47±5°C for at least 0.2 s)
    d. Tighter control of the filter face velocity (50 to 80 cm/s)
    e. Removal of the back-up filter
2. A non-volatile Particle Number (PN) method, based on hot dilution and thermal treatment of samples drawn from the CVS. The main elements are:
    a. A Volatile Particle Remover (VPR), consisting of:
        i. A hot diluter allowing dilution of at least 10:1 at temperatures above 150°C.

ii. An Evaporation Tube (ET) maintained at a fixed wall temperature between 300 and 400°C.

iii. A second diluter operating at ambient temperatures to cool down the thermally treated sample and at the same time further reduce the vapour pressures of the evaporated material, to reduce the risk of homogeneous nucleation.

b. A Condensation Particle Counter (CPC) exhibiting a 50% counting efficiency at 23 nm, to reduce the risk of volatile nucleated particle interference in the measurements.

The last phase of the PMP consisted of several inter-laboratory exercises, aiming at the evaluation of the repeatability and reproducibility of the recommended methodologies, for both LD and HD applications.

The PMP LD inter-laboratory study was launched in 2004 and concluded in 2006 (Andersson et al., 2007). In this study, a DPF-equipped diesel passenger car utilizing fuel-borne catalyst and a reference "golden" PN measurement system were circulated to nine laboratories where it was tested following a prescribed test protocol (Andersson and Clarke, 2004). The results obtained suggested that the proposed PN methodology exhibited an intra-laboratory (40%) and inter-laboratory (25%) variability similar to other gaseous pollutants (CO and HC) and better than the revised PM method (55% and 35% respectively) (Giechaskiel et al., 2008a). To a large extent, the variability in the PN results reflected a true variability in the vehicle particle emissions, as the method was found to be sensitive enough to identify different DPF fill states as well as the effect of different preconditioning approaches (Giechaskiel et al., 2007). Different PN systems employed in parallel with the reference instrumentation showed differences within ±30% (2 standard deviations of the differences between the systems) (Giechaskiel et al., 2008b).

A similar study was launched in 2007 to assess the performance of the methodology in HD applications. In this HD inter-laboratory validation exercise, a Euro III HD engine retrofitted with a diesel oxidation catalyst and a DPF was circulated to five European laboratories, together with two reference "golden" PN systems to be installed in the CVS tunnel and the Partial Flow Dilution System (PFDS) of each lab (Giechaskiel et al., 2009a). The study was concluded in 2009, with the results revealing that the PN emissions depended significantly on the test cycle, ranging from as low as 10^9 #/kWh over the hot start World-harmonized Heavy duty Transient Cycle (WHTC) to as high as 7.5×10^{11} #/kWh over a cold start repetition of the same cycle. On the other hand, the gravimetric procedure could hardly identify the large changes in the concentration of the emitted particles, with the PM results lying at the background levels. Over the cold start WHTC, the inter-laboratory variability of the PN method was estimated to be 30% and 50% for the CVS and the PFDS, respectively, while the intra-laboratory variability was 20% in both cases. Over the hot-start cycles, where the cycle-average emissions were at least one order of magnitude lower (approaching the background levels lying in the range of 3×10^8 to 8×10^8 #/kWh), the intra- and inter-laboratory variabilities increased by up to 80% partly due to the different background levels and over high load test cycles due to passive regeneration of the DPF (Andersson et al., 2010). Results obtained with additional PN instrumentation agreed to those of the golden instruments generally agreed within ±30%, but some larger differences (of up to 55%) were observed with some systems.

A similar HD study (PMP HD Round Robin), was launched in 2008. In this exercise, a different Euro III HD engine, equipped with an alternative, less efficient DPF is circulated to 12 laboratories. The main difference from the previous two campaigns, is that the participating laboratories employ their own commercial equipment as well as commercially available fuel and lubricating oil. The study is expected to conclude within 2012.

1.3 From PMP to legislation

Following the successful implementation of the PMP LD and HD inter-laboratory study, which verified the superior performance of the PN methodology compared to the revised gravimetric procedure, the PN method was introduced in the both the LD (UNECE Regulation 83; Commission

Regulation 692/2008) and the HD (UNECE Regulation 49, Commission Regulation 715/2007), European legislation.

The regulation has also introduced specifications for the different components of the PN measurement systems. More specifically, with respect to the Condensation Particle Counter (CPC), the instrument shall:

- Operate under full flow operating conditions (i.e. not incorporate internal splitting of the sampled aerosol flow);
- Have a linear response to particle concentrations over the full measurement range in single particle count mode;
- Have a counting accuracy of ±10% across the range 1 cm^{-3} to the upper threshold of the single particle count mode of the PNC against a traceable standard;
- Have counting efficiencies at particle sizes of 23 nm (±1 nm) and 41 nm (±1 nm) electrical mobility diameter of 50% (±12%) and > 90% respectively.

With respect to the Volatile Particle Remover (VPR), it shall:

- Be capable of diluting the sample in one or more stages to achieve a particle number concentration below the upper threshold of the single particle count mode of the PNC (typically 10000 #/cm^3) and a gas temperature below 35 °C at the inlet to the PNC;
- Include an initial heated dilution stage which outputs a sample at a temperature of ≥ 150°C and ≤ 400°C and dilutes by a factor of at least 10;
- Achieve a Particle Concentration Reduction Factor (*PCRF* - defined as the ratio of the number concentration of mono-disperse solid particles upstream and downstream of the VPR) for particles of 30 nm and 50 nm electrical mobility diameters, that is no more than 30% and 20% respectively higher, and no more than 5% lower than that for particles of 100 nm electrical mobility diameter for the VPR as a whole;
- Also achieve > 99.0% vaporisation of 30 nm tetracontane ($CH_3(CH_2)_{38}CH_3$) particles, with an inlet concentration of ≥ 10000 cm^{-3}, by means of heating and reduction of partial pressures of the tetracontane.

It should also be stressed at this point, that the regulatory requirements for the VPR systems differ from the original PMP specifications. In particular, the PMP protocol requested dilution factor measurements based on flow or trace gas measurements but also specified particle penetration requirements (<40% at 30 nm, <30% at 50 nm and <20% at 100 nm).

1.4 Scope of the PMP VPR Round Robin

The recently introduced PN measurement methodology introduced also some calibration requirements for a metric (particle number) that currently does not have a traceable standard. This raises some concerns with respect to the accuracy of the instrument calibrations, and accordingly the comparability of results obtained using different commercial systems. In line with that, the experimental data collected in the PMP LD and HD inter-correlation studies using different PN systems in parallel to the golden instrumentation, revealed systematic differences which could reach up to 55% (Giechaskiel et al., 2008b; Anderson et al., 2010) and were mainly attributed to uncertainties in the dilution factors and the particle losses.

Dedicated calibration experiments conducted at JRC to determine the *PCRF* of the golden instrumentation of the PMP LD and HD inter-correlation studies, revealed a number of potential sources of uncertainty in such calibration experiments (Giechaskiel et al., 2009b). More, specifically:

- The inlet pressure of the VPR generally affects the achieved *PCRF* and Dilution Factors (DF), with different VPR designs exhibiting different dependence on the inlet pressure.
- Accordingly, operation of the calibration setup in under-pressure, requires the use of two CPCs or one and flow compensation with a pump of equal flow, to ensure equal inlet pressure conditions, when measuring the upstream and downstream concentrations.

- Thermal treatment of the sodium chloride aerosol employed in the calibration experiments, resulted in particle shrinkage. This highlighted the importance of employing thermally stable aerosols, to avoid structural changes in the ET of the VPR system under calibration. While particle shrinkage should not affect the number concentrations, it may result in less efficient particle detection especially if a large cut-off size CPC is employed (i.e. one complying with the regulatory requirements).

Following the dissemination of the results in a PMP meeting, a questionnaire was circulated to different instrumentation manufacturers in order to collect information on the calibration procedures employed. The collected information, indicated that different manufacturers employ different calibration aerosols, different conditioning of the aerosol and also different aerosol instrumentation and calibration setups. These different implementations raised concerns regarding the comparability of the calibration certificates issued by the different manufacturers. Accordingly, it was decided within the PMP working group to launch an inter-laboratory correlation study aiming at the assessment of the different VPR calibration procedures established by the different manufacturers.

1.5 Elements of the PMP VPR Round Robin

The study was organized by the Joint Research Centre (JRC) of the European Commission, that also provided the "golden" VPR system and aerosol generator. The "golden" VPR (GVPR) was a prototype two stage ejector system with an intermediate ET by Dekati. The "Golden" Aerosol Generator (GAG) was a PALAS DNP 3000 graphite spark generator. The "golden" instrumentation also included a TSI 3790 CPC (GCPC) which was provided by TSI Inc.

The dual ejector system was selected on the ground that its dilution factor is very sensitive to the inlet pressure and the composition of the sampled gas, thus constituting the *PCRF* and DF calibration rather challenging. The GVPR was sent to Dekati Ltd. before the campaign for inspection and introduction of a pressure transducer (Keller EV120) at the inlet. The graphite spark generator was selected on the ground that it produces dry (and hydrophobic) carbon particles that were also expected to be thermally stable, therefore requiring no pretreatment. The GCPC was complying with the European legislation requirements and accordingly had a nominal cut-off size at 23 nm, which constituted its response sensitivity to particle size changes. Accordingly, its use for *PCRF* calibration, especially at 30 nm, could provide information on the stability of the calibration aerosols, since any shrinkage would result in a reduced detection efficiency downstream of the GVPR.

Following some preliminary investigations at JRC, which also served to investigate the most suitable operating conditions of the GAG, the golden instrumentation was circulated to nine laboratories together with a description of the minimum calibration work required (Annex A). JRC repeated some tests in the middle and at the end of the campaign. The exact test sequence is illustrated in Table 1. A "golden" engineer from JRC visited each lab in order to assist in the set-up the golden instrumentation and verify its proper performance.

The minimum calibration work requested by each lab included:

1. Measurement of the dilution factor using a trace gas
2. Measurement of the *PCRF* at 30, 50 and 100 nm using aerosol generated by the GAG at specified operating parameters, using two CPCs (one of them being the GCPC) alternatively sampling upstream and downstream of the GVPR.
3. Measurement of the *PCRF* at 30, 50 and 100 nm using the calibration approaches established at each lab.

Following discussions within the PMP group, it was deemed unnecessary to examine the volatile removal efficiency of the GVPR, since experimental (Giechaskiel et al., 2009b) and theoretical (Giechaskiel and Drossinos, 2010) investigations suggested that the regulated requirement can be easily met with this system.

Table 1: Test sequence and additional experimental investigations conducted at each lab.

Laboratory	**Test dates**	**Alternative calibration aerosol**	**Additional investigations**
JRC	08/2010	-	Definition of the test protocol, Calibration of the GCPC
LAT	12/2010	Thermally treated diesel exhaust	-
AVL	01/2011	Thermally treated mini-CAST	Linearity cross-checks, polydisperse characterization with SMPS
Horiba	03/2011	Thermally treated mini-CAST, sodium chloride	Size classification of non-neutralized particles
EMPA	04/2011	Sodium chloride, Palladium	Tandem DMA measurements, linearity cross-checks
Matter Aerosol	05/2011	Thermally treated CAST	*PCRF* at 15 nm
JRC	07/2011	-	-
NPL	09/2011	-	Calibration of the GCPC against a traceable electrometer
AEAT	10/2011	Thermally treated CAST	Linearity cross checks
VW	12/2011	PALAS DNP 3000	Linearity cross checks
Maha	02/2012	PALAS DNP 2000	Thermal treatment of graphite particles, linearity cross checks
JRC	03/2012	-	-

2 EXPERIMENTAL

2.1 Golden Instrumentation

2.1.1 Golden Volatile Particle Remover

The Golden Volatile Particle Remover (GVPR) was a dual ejector system by Dekati Ltd. (Figure 1). The operation principle of the ejector dilutor is illustrated in Figure 2. Pressurized diluent flows at high speed around an ejector nozzle and causes a pressure drop which draws a sample through the nozzle. For a given nozzle geometry, the mass flowrate of diluent and sampled gas, which define the dilution factor, depend on the pressure, the temperature and the chemical composition of the diluent and the sample (Giechaskiel et al. 2004).

The system was shipped to Dekati Ltd. before the start of the study for inspection and installation of a pressure transducer (Keller EV120) at the inlet. The first diluter incorporated a dilution air heater and a heating blanket. The ET had an internal volume of 67 cm^3 (length 7 cm, diameter 3.5 cm) which for the nominal sample flowrate of the secondary ejector diluter (~5 lpm) corresponded to a minimum residence time of 0.4 s. The second diluter had an identical geometry with the primary one and was connected as close as possible to the ET, using no insulation.

The laboratories were requested to employ purified air as diluent at an overpressure of 2 bar (which corresponds to the nominal operating pressure of the two dilutors). The temperature controllers of the primary dilution air heater, the heating blanket and the ET, were pre-set at 150, 150 and 300°C, throughout the campaign. The laboratories were requested to establish an inlet pressure at 3 kPa below ambient, in their calibration setup. It was also requested from each lab to take all possible measures to avoid pressure build up at the outlet of the ejectors due to venting of the excess flow (that could also affect the dilution factor – Giechaskiel et al. 2004).

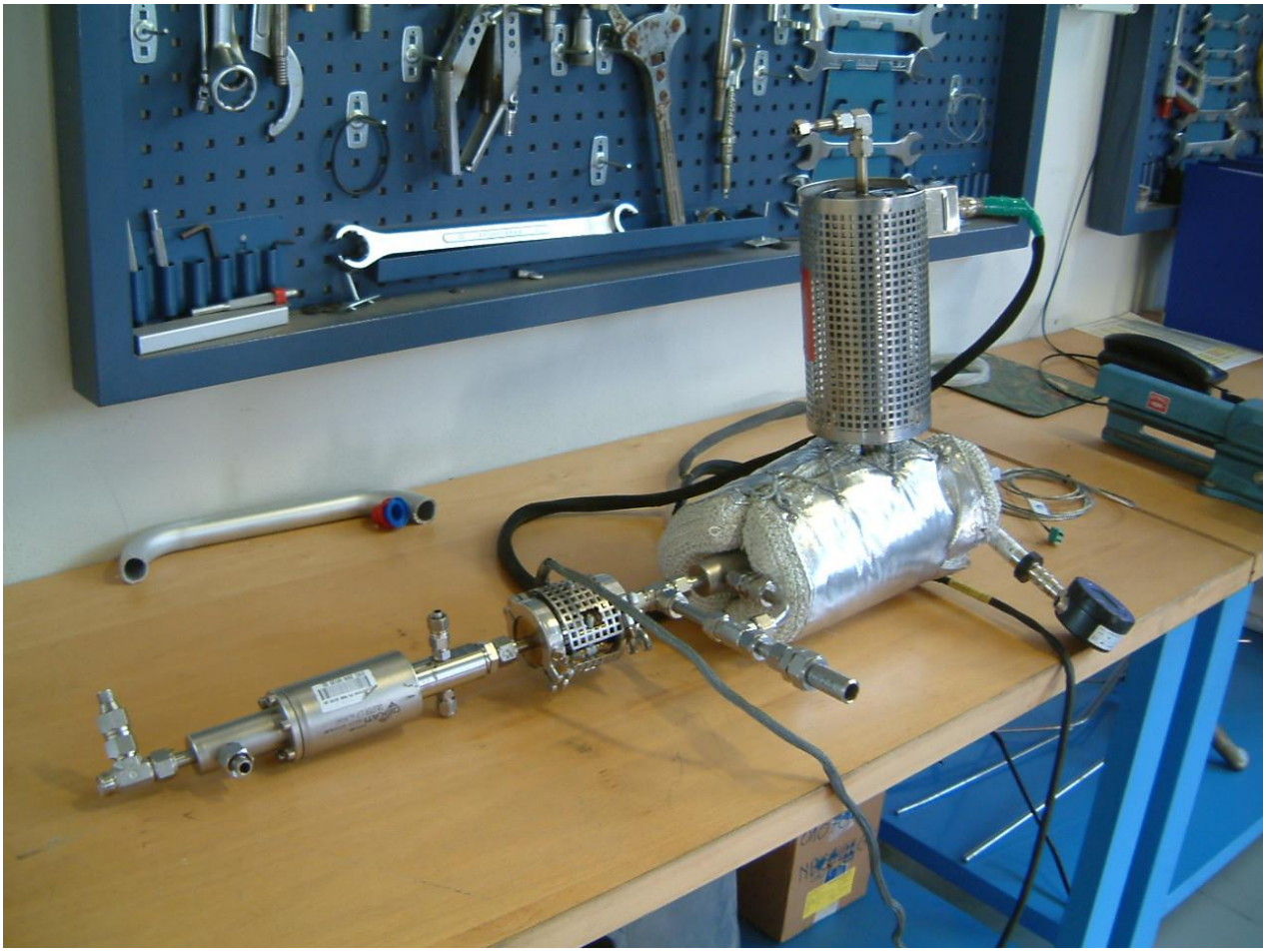

Figure 1: Golden Volatile Particle Remover (GVPR) fully assembled.

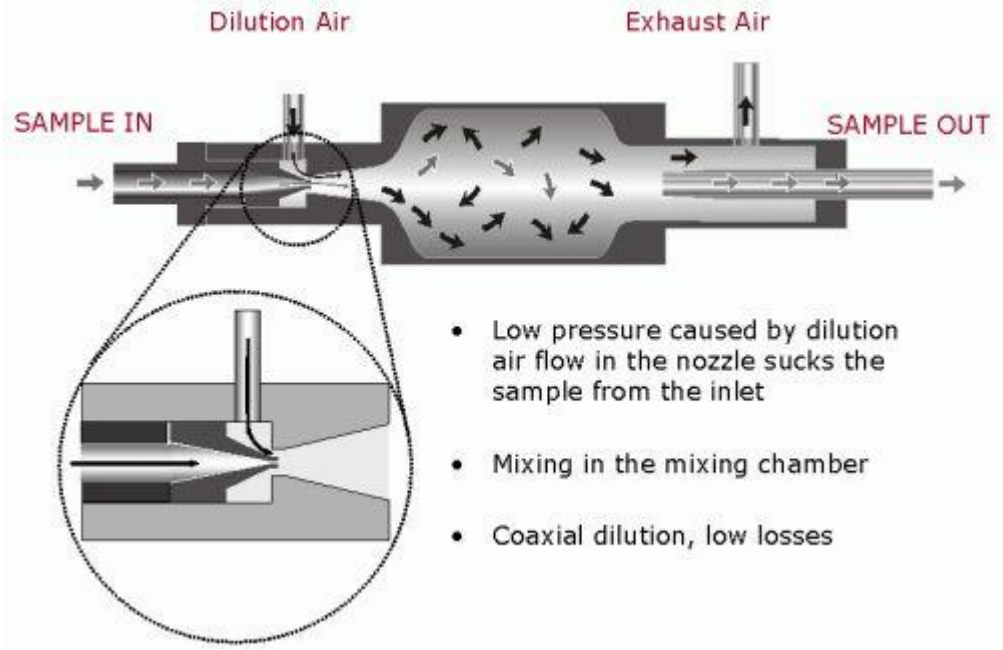

Figure 2: Operating principle of the ejector dilutor.

The temperature controller of the dilution air heater malfunctioned before the tests at AVL and was replaced by another one provided by Dekati. The ET also failed during the tests at VW and was replaced by an identical one shipped by Dekati Ltd.

2.1.2 Golden Aerosol Generator

The Golden Aerosol Generator (GAG) employed in the study was a PALAS DNP300 graphite spark generator (Figure 3). Particles in this generator are produced in a spark discharge between two graphite electrodes. A stream of nitrogen flowing through the space between the electrodes transports the carbon evaporated in the spark. The carbon vapor then condenses to fine primary particles which subsequently coagulate to form bigger agglomerates. The peak size of the produced aerosol strongly depends on the concentration of the primary particles (which controls the coagulation rate) which can be controlled by means of varying the spark frequency. An internal dilution stage employing air as a diluent can suppress the rate of coagulation and thus provides an additional control of the produced size distribution.

The operating settings of the GAG employed in this inter-laboratory study, were selected in dedicated experiments at JRC. The settings employed in the measurement campaign are summarized in Table 2. No problem was encountered with the GAG during the campaign.

Table 2: Operating settings of the GAG employed for the *PCRF* measurements at 30, 50 and 100 nm at the different laboratories.

Parameter	30 nm	50 nm	100 nm
Air flowrate [lpm]	6	3	3
Nitrogen flowrate [lpm]	3	3	3
Current [mA]	0.75	2	2
Energy	Medium	Medium	Medium

Figure 3: Golden Aerosol Generator (GAG) - PALAS DNP 3000 spark generator.

2.1.3 Golden Condensation Particle Counter

The Golden Condensation Particle Counter (GCPC) circulated to the different participating laboratories was a TSI 3790 CPC, supplied by TSI Inc (Figure 4). The GCPC is designed around the requirements laid down in the European legislation (UNECE Regulation 83). It operates at 1 lpm sample flowrate and has nominal detection efficiencies at 23 nm and 41 nm of 50% and >90% respectively. The certified by TSI counting efficiencies, as indicated in the accompanying certificate (Annex B), were 58.9% (23 nm) and 92.4% (41 nm), determined using emery oil particles. The GCPC was also calibrated at JRC using both graphite and emery oil particles. The results of this calibration work (Mamakos et al., 2011a) verified the calibration certificate for emery oil (54% at 23 nm and 92% at 41 nm) but suggested much lower detection efficiencies for graphite (32% at 23 nm and 75% at 41 nm). Theoretical considerations suggested that the effect of particle affinity to butanol is amplified at the low saturation ratios employed in PMP-compliant CPCs (Giechaskiel et al., 2011; Mamakos et al., 2011a) and that the deteriorated efficiency for graphite could be reproduced by a contact angle of 10°.

Figure 4: Golden Condensation Particle Counter (GCPC) – TSI 3790 CPC

Unfortunately, the GCPC malfunctioned thrice during the measurement campaign (at LAT, AEAT and VW) and was shipped to TSI for the necessary maintenance and re-calibration. Figure 5 compares the certified detection efficiencies at 23 and 41 nm as well as the linearity of the unit after each calibration (the calibration certificates issued after each calibration are appended in Annex B, together with the original one).

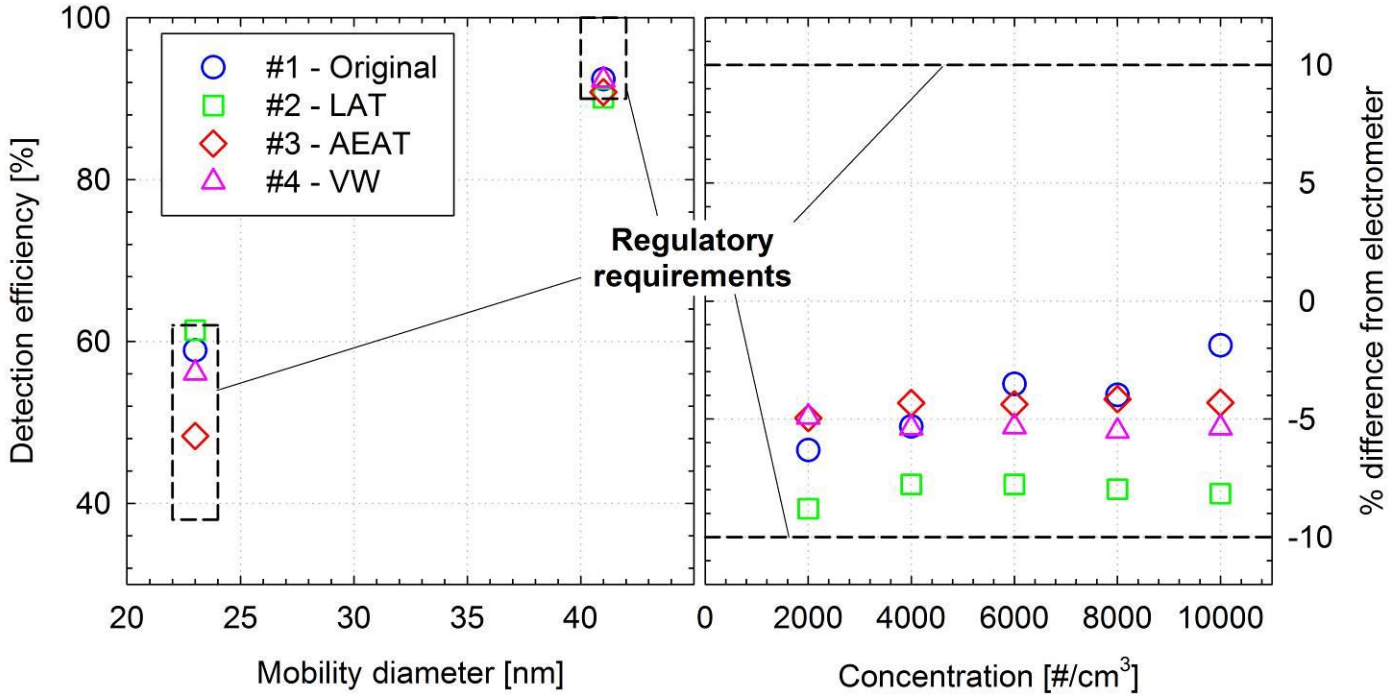

Figure 5: Comparison of the original calibration certificate (blue dots) to those after the three maintenances of the GCPC. Linearity checks (left-hand panel) were conducted using 55 nm emery oil particles.

2.2 Calibration Setups

2.2.1 Reference setup

Figure 6 illustrates the requested experimental setup for the calibration experiments with the golden instrumentation. The laboratories had to ensure two sampling points for size-classified calibration aerosol, one for the GVPR and another one for a CPC monitoring the upstream concentration. A control valve upstream of the two sampling points would allow for a control of the inlet pressure of the GVPR. The laboratories had to apply their best practices to ensure sufficient mixing between the size-classified aerosol and the necessary make-up air (preliminary investigations at JRC suggested that a 1 m long tube downstream of a needle valve should suffice). The laboratories had to supply purified shop air at an over-pressure of 2 bars in the GVPR. It was furthermore requested that the calibration aerosol produced by the GAG at the specified operating conditions (Table 2), would not be thermally treated.

At least two CPCs, one of them being the GCPC, should be employed in this "reference" calibration setup, sampling alternatively upstream and downstream of the GVPR. The two CPCs should operate at the same flowrate (1 lpm), and if not the flows should be compensated (i.e. by the use of an additional pump). It was also recommended to employ a third CPC (monitor CPC) always sampling downstream of the GVPR, to keep trace of any changes in the dilution factor and/or inlet concentration during the calibration tests.

Table 3 provides some additional information on the exact configuration of the reference calibration setup employed in the different laboratories.

Table 3: Details of the "reference" calibration setup employed at the different laboratories.

Laboratory	Size classifications				Operating pressure	Dilution	Alternative CPC	Monitor CPC
	DMA setup	Neutralizer	Sheath flowrate [lpm]	Sample flowrate [lpm]				
JRC	Tandem DMA: Grimm 5.5-900 / TSI 3081	0.1 mCi ^{241}Am / 10 mCi ^{85}Kr	3/ 10	1/ 1	Underpressure	Upstream of TDMA	TSI 3010	TSI 3790
LAT	TSI 3081	2 mCi ^{85}Kr	10	0.9	Underpressure	Upstream of DMA	TSI 3010	TSI 3776
AVL	TSI 3085	10 mCi ^{85}Kr	7	0.7	Underpressure	Upstream of DMA	TSI 3790	-
Horiba	TSI 3081	10 mCi ^{85}Kr	10	0.8	Underpressure	Upstream of DMA	Mass Flow Controller	-
EMPA	TSI 3071	16.2 mCi ^{63}Ni	22	1.6	Underpressure	Upstream of DMA	TSI 3790	TSI 3010
Matter Aerosol	TSI 3071	2 mCi ^{85}Kr	15	1.5	Underpressure	Upstream of DMA	TSI 3010	TSI 3010
JRC	Tandem DMA: Grimm 5.5-900 / TSI 3081	0.1 mCi ^{241}Am / 10 mCi ^{85}Kr	3/ 10	1/ 1	Underpressure	Upstream of DMA	TSI 3010	TSI 3025A
NPL	TSI 3081	10 mCi ^{85}Kr	10	1	Underpressure	Upstream of DMA	TSI 3775 & 0.7 lpm MFC	TSI 3022
AEAT	TSI 3081	2 mCi ^{85}Kr	10	1	Underpressure	Upstream of DMA	TSI 3010	-
VW	TSI 3081	2 mCi ^{85}Kr	15	1.5	Underpressure	Downstream of DMA	TSI 3772	-
Maha	TSI 3081	10 mCi ^{85}Kr	18	1.8	Overpressure	Downstream of DMA	TSI 3790	TSI 3790
JRC	Tandem DMA: Grimm 5.5-900 / TSI 3081	0.1 mCi ^{241}Am / 10 mCi ^{85}Kr	3/ 10	1/ 1	Underpressure			

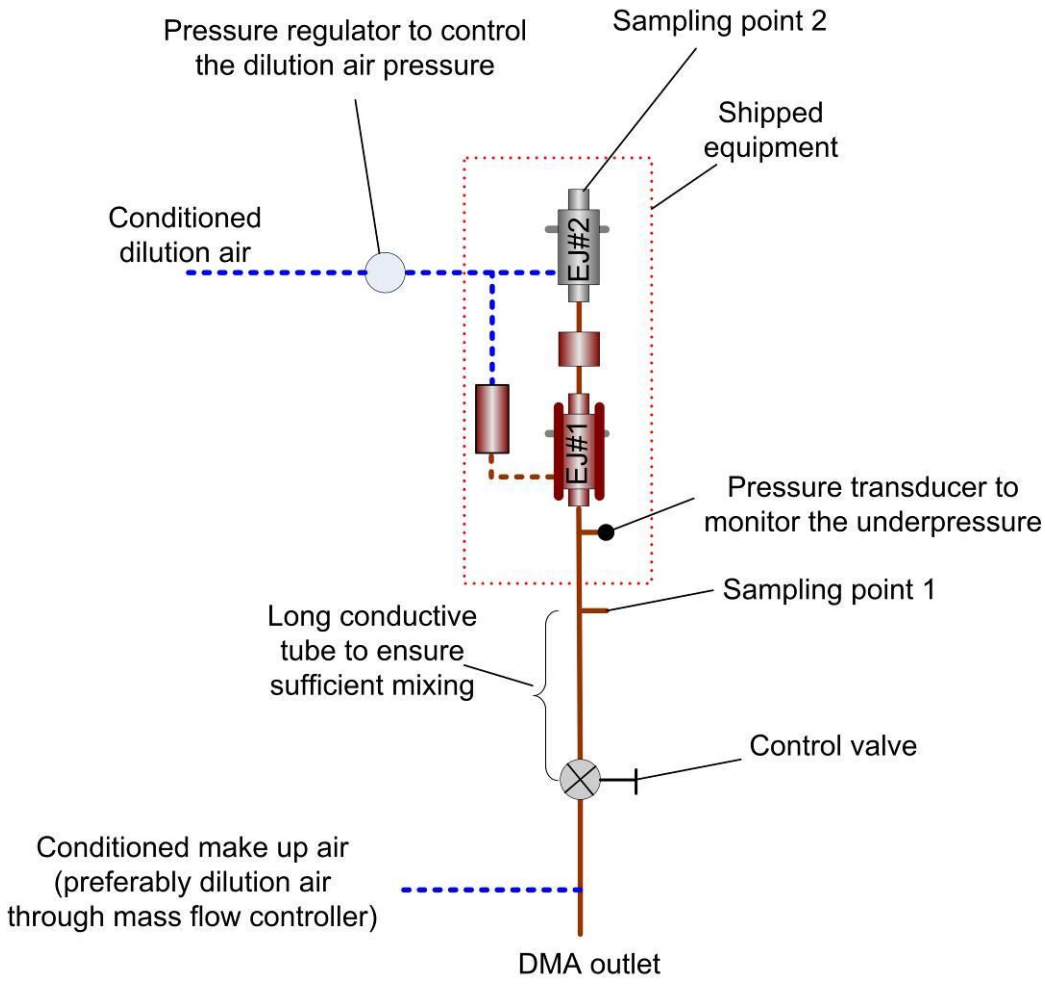

Figure 6: Requested setup for the calibration with the reference instrumentation.

2.2.2 Calibration setups at the different labs

The exact implementation of the "reference" calibration setup differed from laboratory to laboratory. Furthermore, most laboratories performed some additional investigations. This section describes the different calibration setups employed at the different labs and gives an overview of the additional investigations conducted.

- **JRC**

A schematic of the calibration setup employed at JRC for the *PCRF* measurements of the GVPR is illustrated in Figure 7. Graphite aerosol generated in the GAG was first diluted in a dilution bridge and then passed through a TSI 1035900 impactor (equipped with a 0.071 cm nozzle) to remove particles having an aerodynamic diameter larger than approximately 1 μm. The particles were then size classified in a tandem DMA (TDMA) setup, consisting of a Grimm 5.5-900 DMA connected in series with a TSI 3081 DMA. This TDMA configuration effectively minimizes the contribution of larger, multiply-charged particles in DMA-classified aerosols. In these experiments, the Grimm-DMA and the TSI-DMA were equipped with a 0.1 mCi ^{241}Am (Grimm's 5.522) and a 10 mCi 85Kr neutralizer neutralizer (manufactured by Eckert and Ziegler GmbH), respectively. The Grimm-DMA operated at a fixed sheath flowrate of 3 lpm, while the sheath flowrate of the TSI-DMA and the sample flowrate of the whole TDMA system were set at 10 lpm and 1 lpm, respectively.

The particles classified in this TDMA system were first mixed with some conditioned (HEPA-filtered, dehumidified and charcoal, scrubbed) dilution air supplied by a Mass Flow Controller (MFC), in a TSI 3077 neutralizer. The diluted and neutralized extracted sample was subsequently throttled in a needle valve in order to maintain the sample pressure of the GVPR at -3 kPa gauge. Three CPCs in total were employed in the calibration experiments. Two of them (GCPC and a TSI 3010 CPC) were alternatively sampling upstream and downstream of the GVPR, while a third one (TSI 3790 CPC) was

always monitoring the concentration downstream of the GVPR. A Druck DPI 605 pressure calibrator was also employed to monitor the dilution air pressure of the two ejectors with an accuracy of ±0.05%.

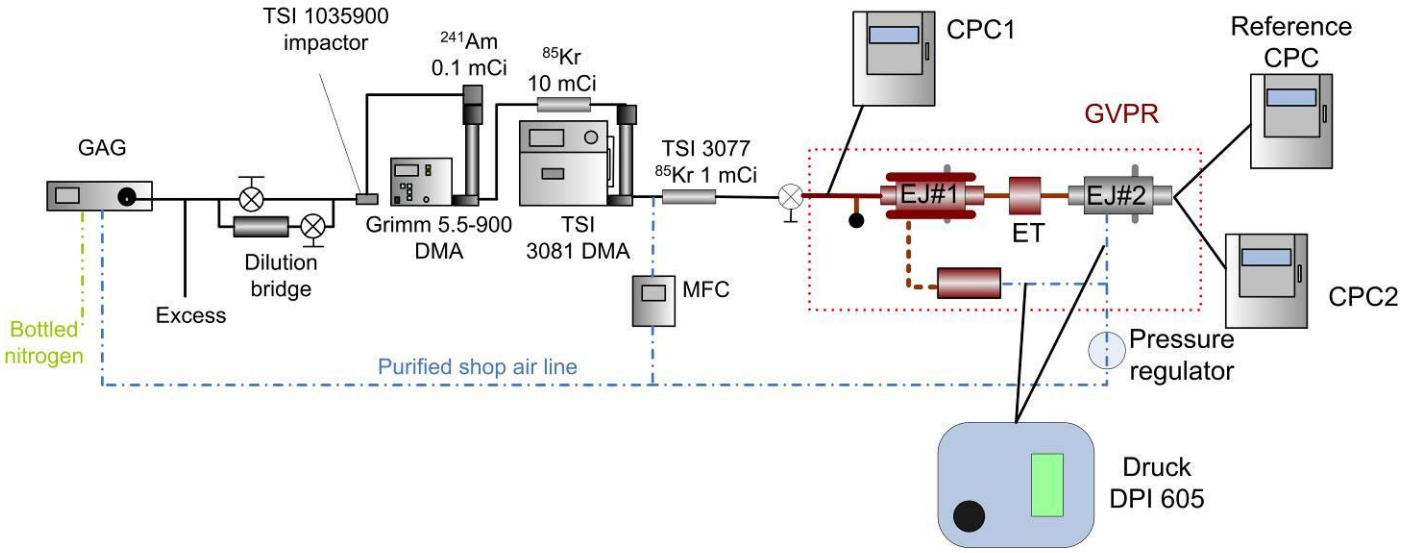

Figure 7: Calibration setup employed at JRC for the *PCRF* measurements.

JRC also performed some dedicated experiments to characterize the size distributions of the aerosol produced by the GAG generator. An in-house PAO generator operating on the condensation-evaporation principle was also employed in selected tests to cross compare the multiple charged fractions of graphite aggregates to that of spherical PAO droplets. A schematic of the setup employed is illustrated in Figure 8. The residence time of the produced polydisperse aerosol before its dilution in a simple dilution bridge was controlled by means of a) employing conductive silicon tubes of different length and b) controlling the sample flowrate through the use of an external pump and a needle valve to control the flow. The size distribution was measured with a TSI 3936L10 SMPS consisting of the TSI 3081 DMA, and a TSI 3010 CPC (in which case the Grimm-DMA was disconnected). The same SMPS unit was also employed to characterize the multiply-charged fractions of particles classified in the Grimm-DMA.

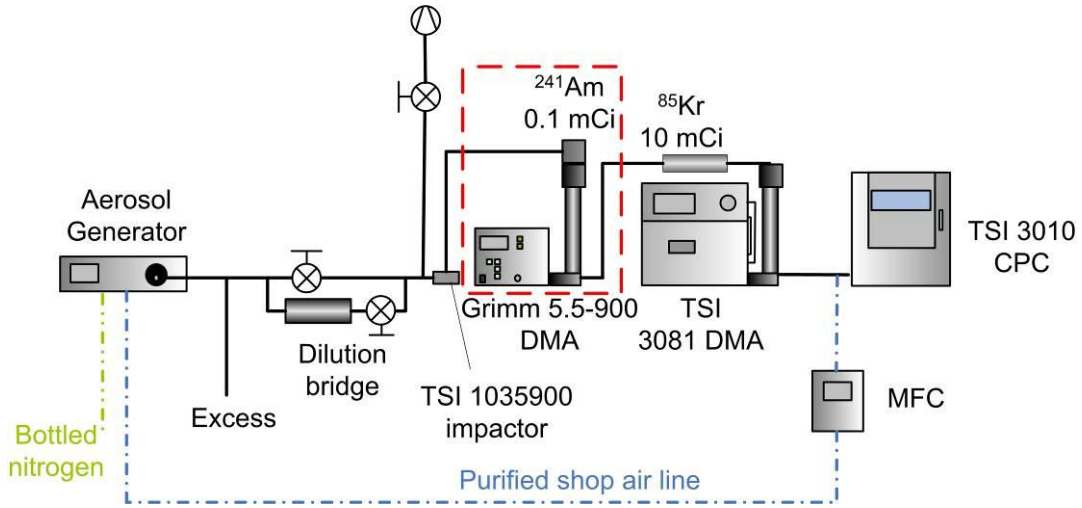

Figure 8: Calibration setup employed at JRC for the characterization of the size distributions produced by the GAG.

The linearity performance of the TSI 3010 and GCPC was cross checked with 85 and 100 nm graphite particles using the calibration setup shown in Figure 9.

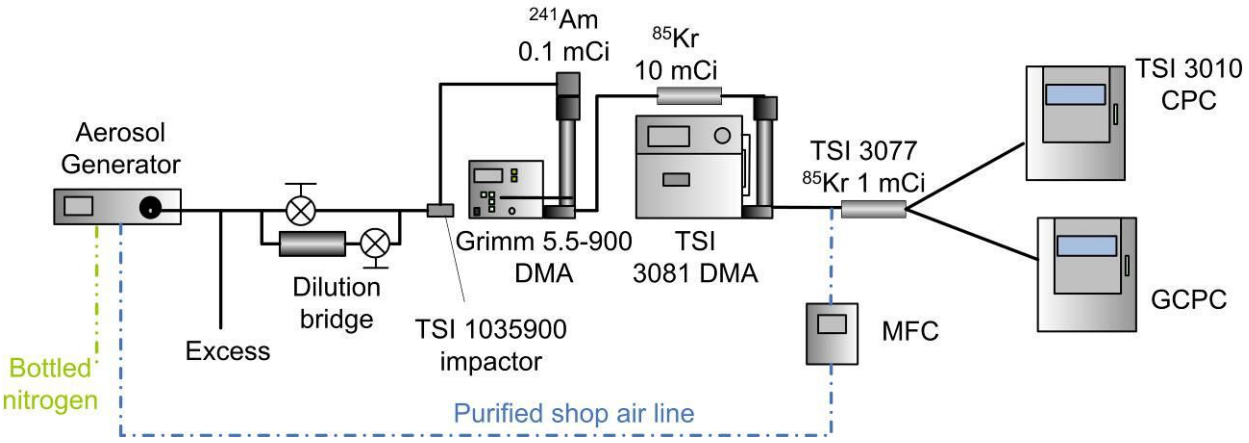

Figure 9: Calibration setup employed at JRC for the cross check of the linearity performance of the GCPC and the TSI 3010 CPC.

- **LAT**

LAT performed some *PCRF* calibration experiments using diesel engine exhaust particles produced by a Toyota 1.4 lt Euro 5 diesel engine. The engine was equipped with high-pressure common rail fuel system, a variable geometry turbocharger and an intercooler, and operated at 50 Nm load and 2750 rpm. The exhaust was diluted in a Constant Volume Sampler operating at 6.6 Nm^3/min and then thermally treated in a Dekati thermodenuder operating at the nominal setting of 250°C and 10 lpm (DMA operated at 1 lpm and the remaining 9 lpm were sampled by a pump).

The configuration of the aerosol instrumentation was the same to that employed in the GAG measurements and is illustrated in Figure 10. LAT employed a TSI 3010 CPC (d_{50} at 10 nm) in addition to the GCPC with the two sampling alternatively upstream and downstream of the GVPR. They also employed a TSI 3776 CPC (d_{50} at 2.5 nm) sampling always downstream of the GVPR, to monitor the stability of the generated aerosol and the dilution factor.

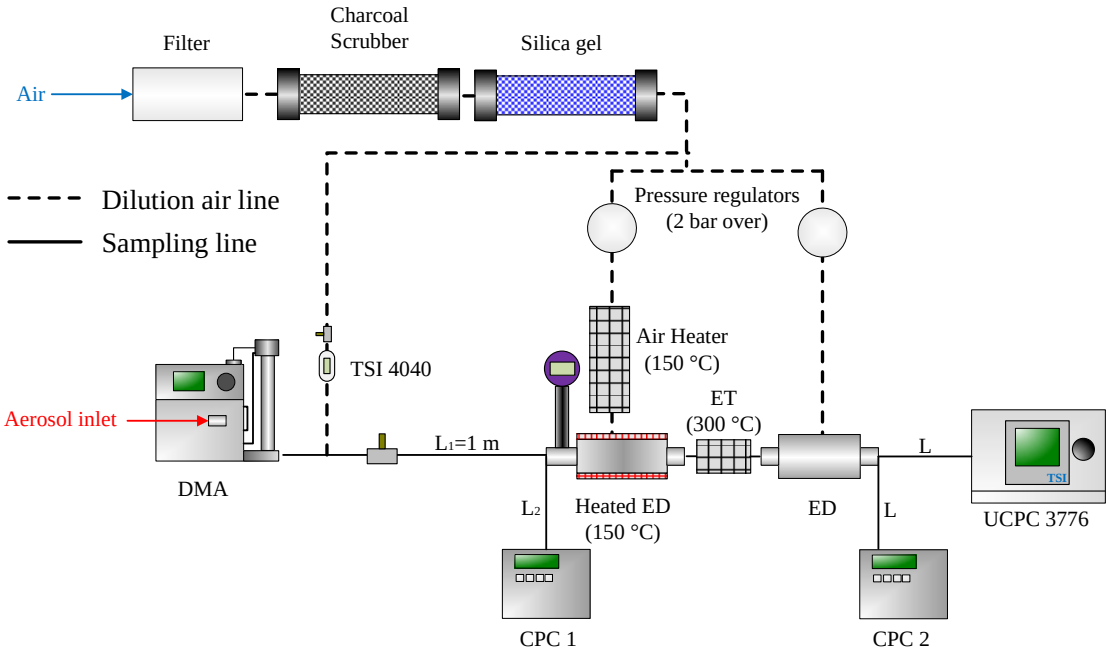

Figure 10: Calibration setup employed at LAT

- **AVL**

AVL also employed a new compact version of the CAST (Combustion Aerosol Standard – Jing, 1999) generator (commercialized as mini-CAST) in their calibration experiments. The operating principle of the CAST generator is illustrated in the schematic in Figure 11. It produces soot particles in a propane diffusion flame quenched by a flow of nitrogen.

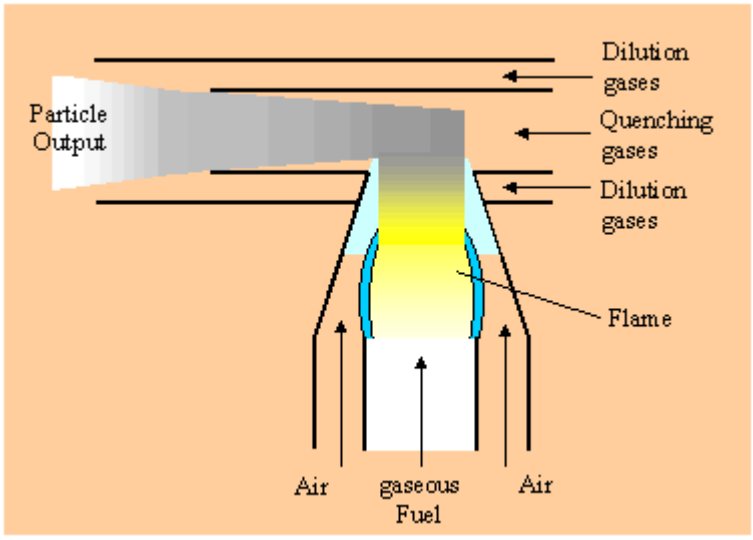

Figure 11: Operating principle of the CAST burner.

The aerosol produced from the mini-CAST was diluted ~3.5 times with diluted air at ≥150°C and then thermally treated at 350°C. Both the mini-CAST and the GAG were employed for the *PCRF* measurements using two calibration setups. The first one was in accordance with the requirements of the inter-laboratory study and is illustrated in Figure 12. A notable deviation from the recommended setup was the use of a needle valve directly at the inlet of the GVPR to control the inlet pressure. This configuration should effectively increase the *PCRF* value by the particle losses in this needle valve. One additional TSI 3790 CPC was employed monitoring the upstream concentrations when the GCPC was sampling downstream and vice versa.

The alternative configuration, a schematic of which is shown in Figure 13, was the one employed by AVL for the calibration of their units. They employ two CPCs, one of which (TSI 3790) always monitors the upstream concentration while the second (TSI 3771 – d_{50} at 10 nm) measures alternatively downstream and upstream of the VPR. A pump through a Mass Flow Controller compensates for the different flows when the VPR system is bypassed.

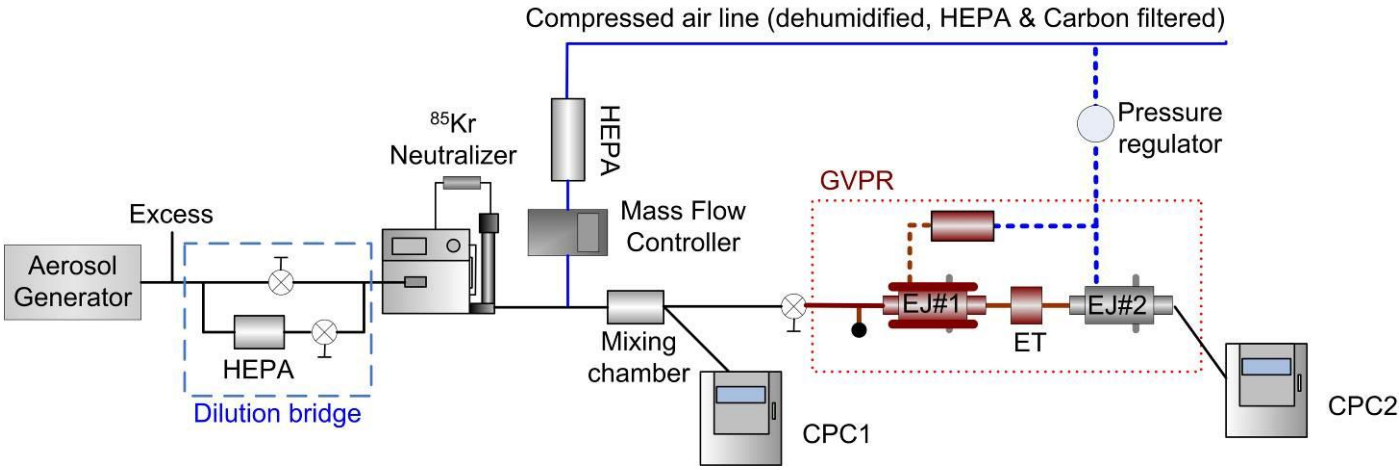

Figure 12: Implementation of the reference calibration setup at AVL.

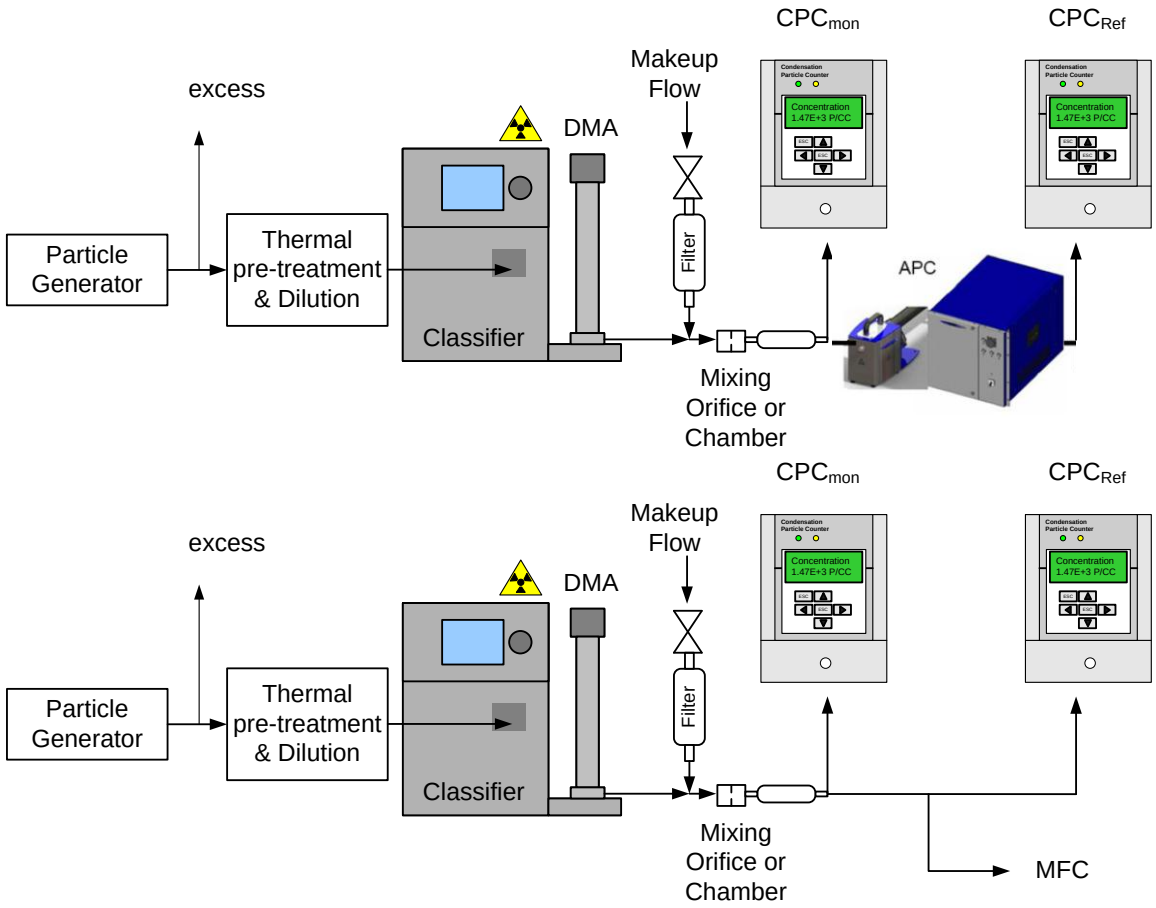

Figure 13: Alternative *PCRF* calibration setup employed at AVL.

AVL also performed some tests to cross-check the linearity of the GCPC with the two CPCs employed for their calibrations (a TSI 3790 and a TSI 3775, d_{50}=4 nm), using both graphite (GAG) and thermally treated diffusion flame propane soot (mini-CAST) aerosol. The experimental setup for these calibration tests is illustrated in Figure 14. The same setup was also employed to measure the detection efficiency of the GCPC using a calibrated TSI 3775 CPC as a reference.

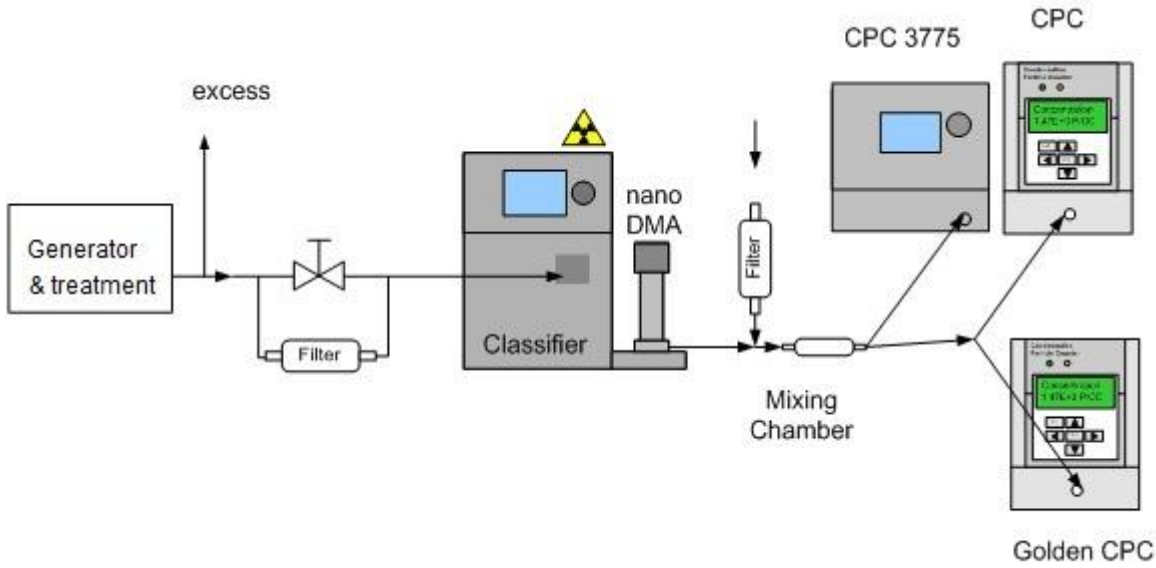

Figure 14: Experimental setup employed at AVL for the CPC linearity checks and the GCPC detection efficiency measurements.

AVL also performed some size distribution measurements upstream and downstream of the GVPR sampling thermally treated propane soot (mini-Cast) and graphite (GAG) polydisperse aerosol.

For these tests the TSI 3085 DMA operated in scanning mode (Scanning Mobility Particle Sizer) using the TSI 3771 CPC for particle detection. The DMA operated at sheath and sample flowrates of 3 and 0.3 lpm, respectively.

- **Horiba**

Horiba employed two additional aerosol generators for the calibration of the GVPR. These were a mini-CAST generator (Figure 11) and a sodium chloride generator (Figure 15) commercialized by Horiba Ltd. as LCU (Linearity Check Unit). In the LCU generator, a sodium chloride solution is aerosolized in a TSI 3076 Collison nebulizer and subsequently pass through a heated tube maintained at wall temperature of 100°C, a heat exchanger and a silica gel drier. The mini-CAST was modified to incorporate an evaporating tube operating at 350°C. The concentrations were adjusted by means of controlling the dilution gas flows in the mini-CAST generator (Figure 11), which in these calibration experiments resulted in a dilution factor of 10:1.

The experimental setup employed for the *PCRF* measurements is illustrated in Figure 16. The polydisperse aerosol produced by the different generators first passed through a dilution bridge to control the number concentration and subsequently size classified in a TSI 3081 DMA equipped with a 10 mCi ^{85}Kr neutralizer. The classified particles where mixed with HEPA filtered dilution air supplied through a Mass Flow Controller (MFC) in a TSI flow splitter (TSI 3708). A needle valve, upstream of the splitter, was employed to control the inlet pressure of the GVPR. The number concentrations upstream and downstream f the GVPR were measured using a single CPC. A MFC was employed to compensate for the CPC flow whenever the latter was sampling downstream of the GVPR. Horiba also performed *PCRF* measurements using a TSI 3776 CPC (d_{50} at 2.5 nm) in place of the GCPC.

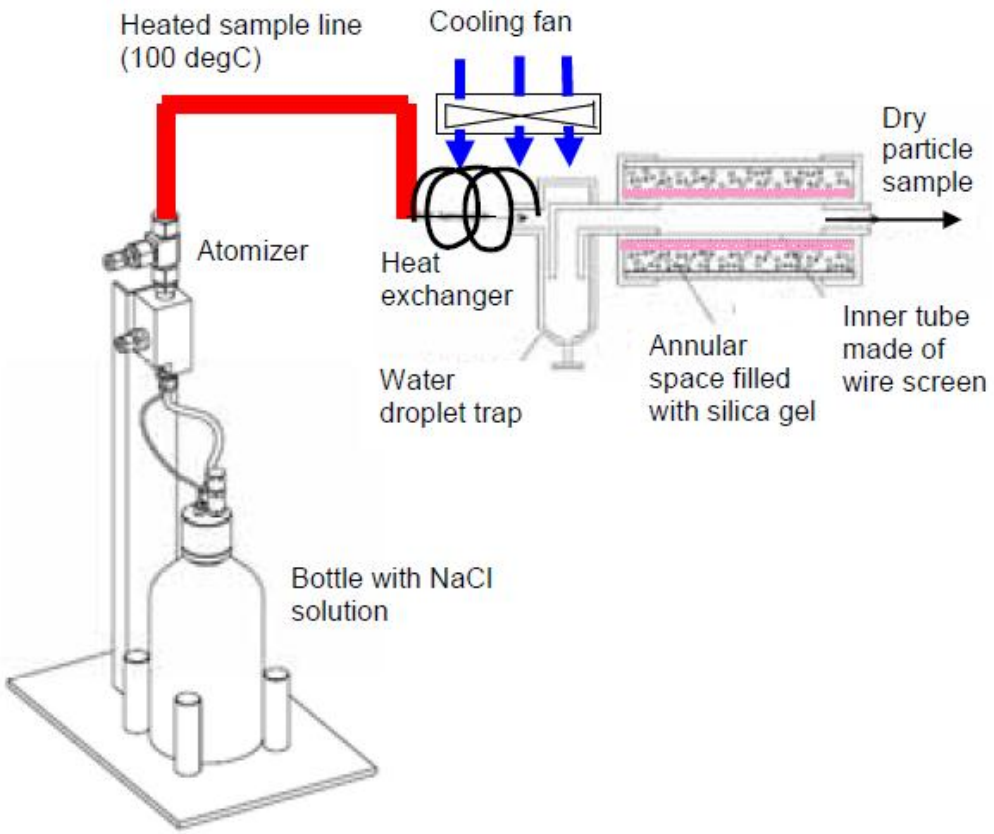

Figure 15: Horiba Linearity Check Unit (LCU).

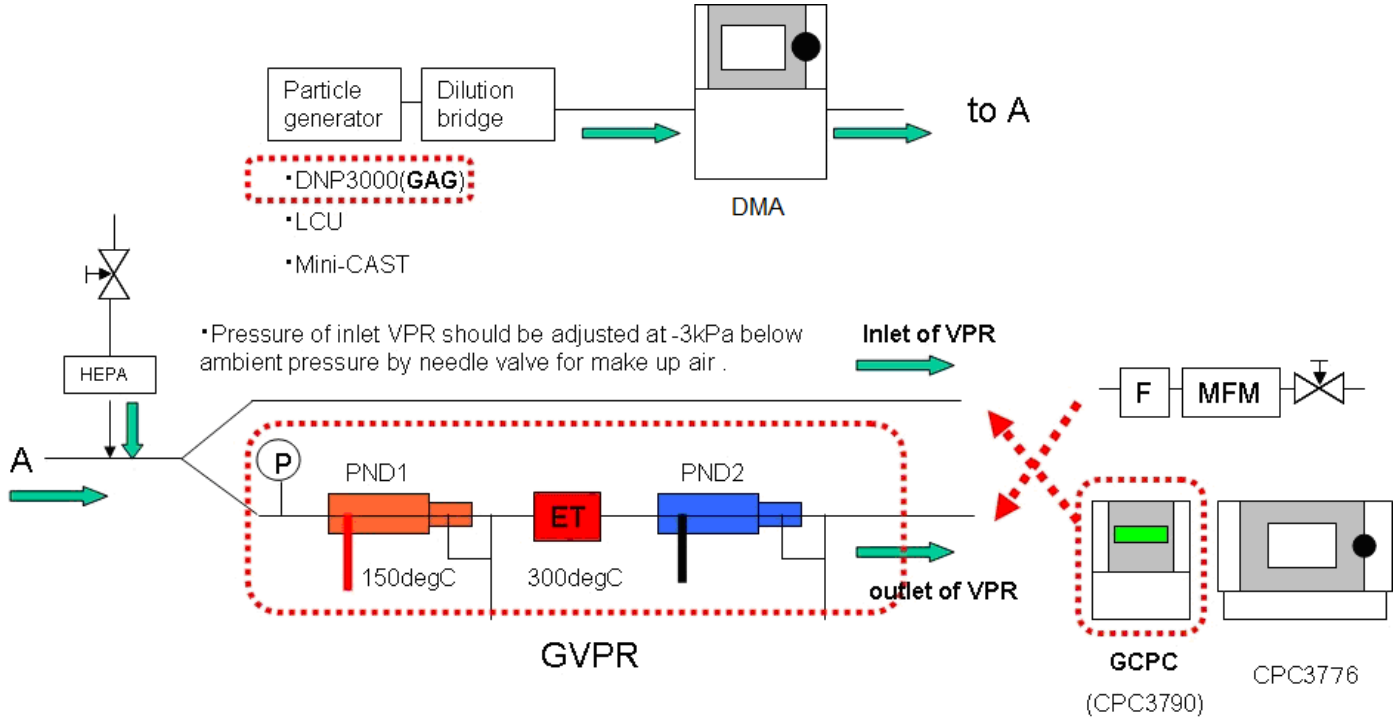

Figure 16: Calibration setup employed at Horiba

- **EMPA**

EMPA employed two additional aerosol generators for the calibration of the GVPR. The first one produced sodium chloride particles from a water solution in a TSI 3076 Collison nebulizer. The generated sodium chloride aerosol was neutralized and subsequently dried in a silica gel column. The second alternative generator was an in-house palladium generator, operating on the glow-wire technique (Gotoh et al., 1990). The heat released by applying an electric current on a palladium wire, resulted in evaporation of palladium. The palladium vapour is carried by a clean air flow and subsequently nucleates forming palladium particles as the temperature decreases.

The schematic in Figure 17 illustrates how the reference calibration setup was implemented at EMPA. The polydisperse aerosol produced from all three generators first passed through a dilution bridge to control the number concentrations. The calibration aerosol was size classified in a TSI 3071 DMA operating at a sheath flowrate of 22 lpm and a sample flowrate of 1.6 lpm. The size classified aerosol was then mixed with filtered dilution air supplied by a mass flow controller in a 2 m long conductive silicon tube (inner diameter of 6 mm). A needle valve downstream of this mixing point, maintained the pressure at 3 kPa below ambient. Two TSI 3790 CPCs (the GCPC and a second one by EMPA) were alternatively sampling upstream and downstream, of the GVPR, in the calibration tests with graphite (GAG) and palladium particles. In the calibration tests with sodium chloride particles, two TSI 3022 CPCs (d_{50} at 7 nm). In all cases, a third CPC (TSI 3010 – d_{50} at 10 nm) was always sampling downstream of the GVPR to check the stability of the particle concentrations. Before the actual *PCRF* tests, a TSI SMPS (3071 DMA and CPC 3025) system (operating at a sheath flowrate of 9 lpm, a sample flowrate of 1.6 lpm, and a scan time of 300 s) was employed to measure the size distribution of the polydisperse aerosol produced by the generators and the size classified aerosol employed for the *PCRF* measurements.

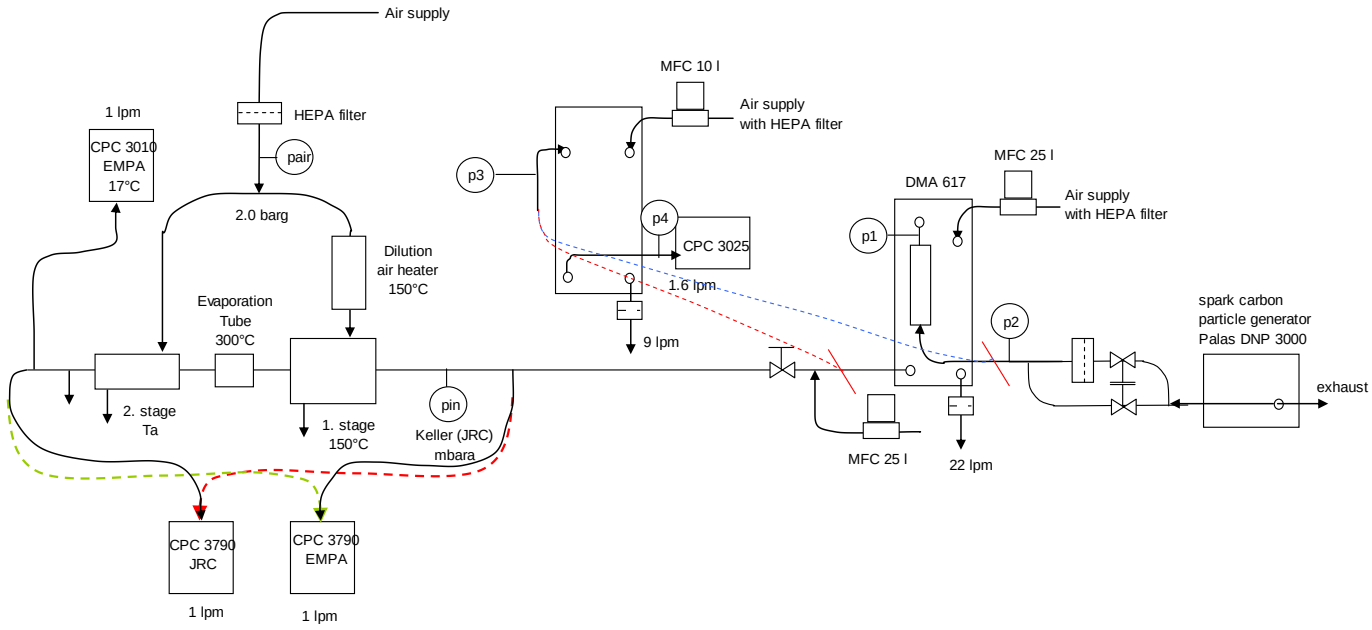

Figure 17: Implementation of the reference calibration setup at EMPA.

EMPA also performed *PCRF* calibration measurements with graphite particles classified in a Tandem DMA setup, illustrated in Figure 18. The only difference from the setup depicted in Figure 17 is that graphite particles were classified in two TSI 3071 DMAs connected in series (the second one operating at 9 lpm sheath flow and 0.9 lpm sample flowrate). A TSI 3034 SMPS was also employed in these tests, to measure the size distribution upstream of the first DMA, in between the two DMAs and downstream of the tandem DMA setup.

EMPA measured also the size distributions of size classified graphite particles upstream and downstream of the GVPR in dedicated tests, using the setup illustrated in Figure 19. In these tests, the size distributions were measured with the TSI 3071 DMA connected on a TSI 3010 CPC. The DMA operated at 9 lpm sheath flow, 1 lpm sample flow, and 300 s scan time. The GCPC was sampling upstream of the GVPR when the SMPS was sampling downstream of the GVPR, and vice versa, to compensate for the flows.

EMPA also performed linearity checks of the GCPC against their own TSI 3790 CPC using 30, 50 and 100 nm graphite and palladium particles. The setup employed for these tests is illustrated in Figure 20. The same setup was also employed for the linearity cross checks of the two TSI 3022 CPC using 30, 50 and 100 nm sodium chloride particles.

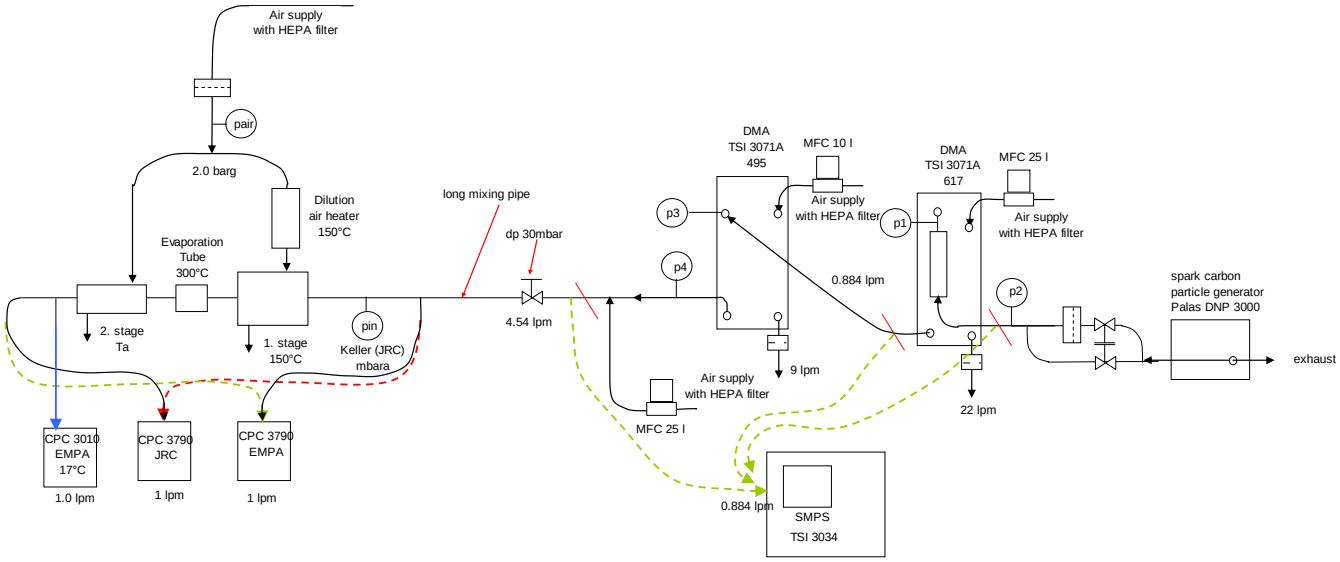

Figure 18: *PCRF* calibration measurements with graphite particles classified in a Tandem DMA setup.

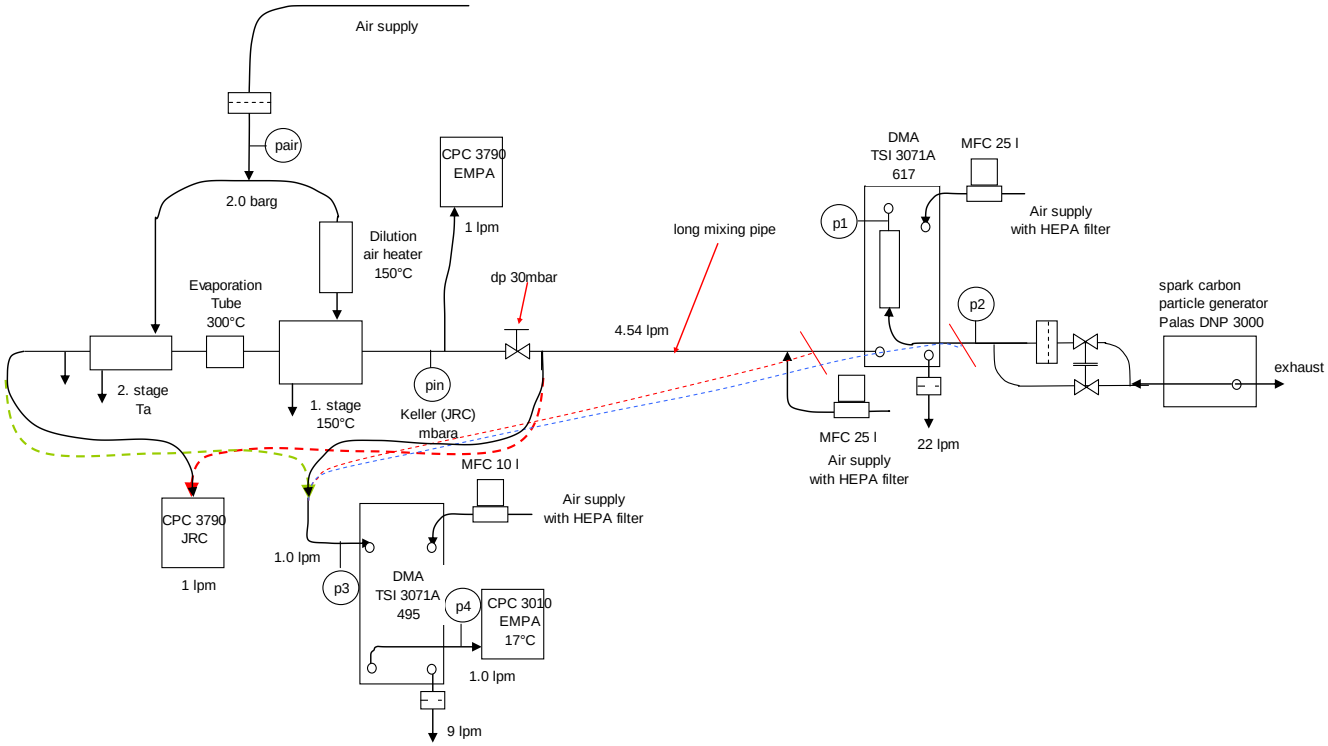

Figure 19: Setup employed at EMPA for the size distribution measurements of size classified graphite particles upstream and downstream of the GVPR.

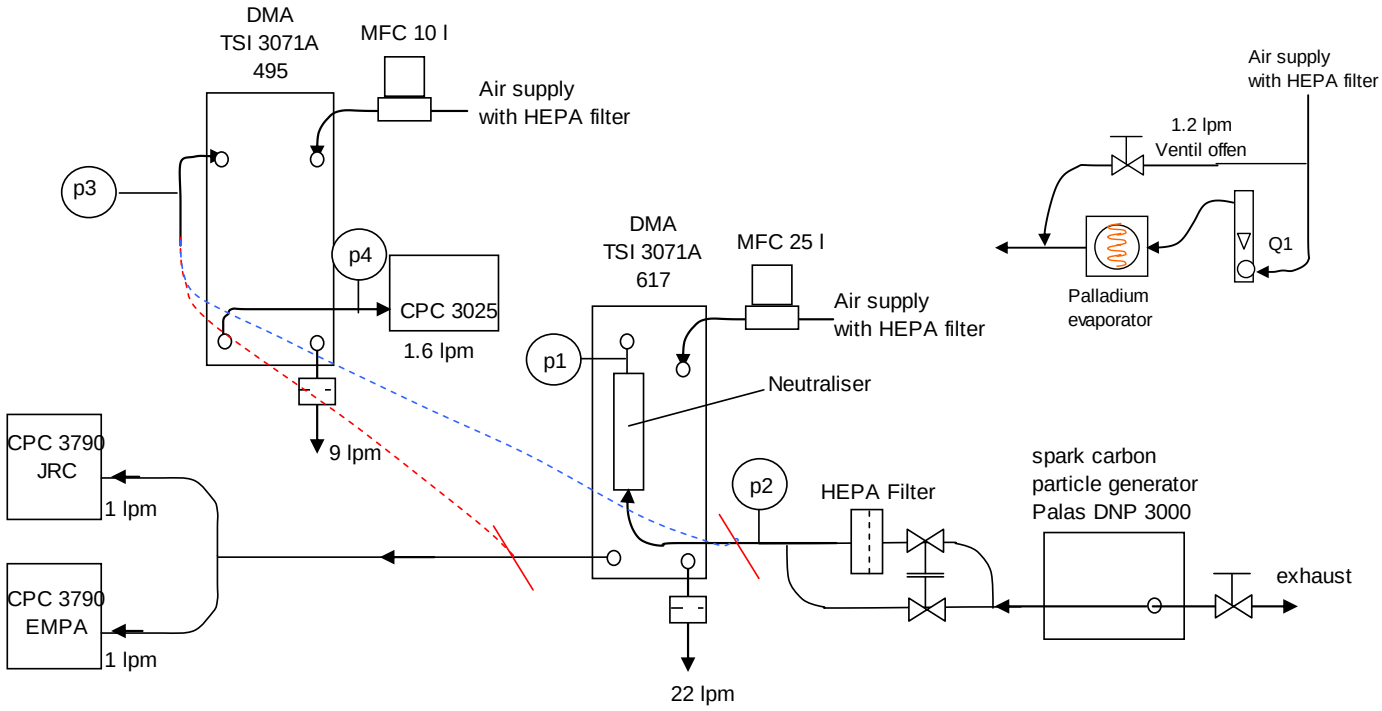

Figure 20: Experimental setup employed for the linearity checks of the GCPC against the TSI 3790 CPC of EMPA.

- **Matter Aerosol**

Matter Aerosol performed *PCRF* measurements of the GVPR using the GAG and a CAST generator. The experimental setup employed for both materials is illustrated in Figure 21. The generated polydisperse aerosol was first diluted with filtered shop air supplied by a Mass Flow Controller (MFC) and subsequently neutralized in a 2 mCi ^{85}Kr source (TSI 3077 neutralizer). In the tests with CAST, the aerosol was also thermally treated in an Evaporating Tube (ET) operating at a wall temperature of 300°C and subsequently diluted by 2.5-3.5 times. The neutralized aerosol was

subsequently size classified in a TSI 3071 DMA operating at a sheath flowrate of 15 lpm and a sample flowrate of 1.5 lpm. The size classified aerosol was then mixed with the necessary make-up filtered air supplied by a second MFC in a 2 m long conductive silicon tube (inner diameter of 6 mm). A needle valve was installed upstream of the GVPR to control the inlet pressure at 3 kPa below ambient. Matter Aerosol employed three CPCs for the calibrations. One was the GCPC while the other two were TSI 3010 (d_{50} at 10 nm) models. One TSI 3010 was sampling always downstream of the GVPR to check the stability of the aerosol concentrations and GVPR dilution, while the other one was sampling upstream of the GVPR when the GCPC was sampling downstream and vice versa.

Matter Aerosol also performed *PCRF* measurements with neutral particles. For these investigations, they passed the DMA classified particles through a second 10 mCi ^{85}Kr neutralizer (TSI 3077A) to establish a bipolar charge distribution and then from an in-house electrostatic precipitator to remove all charged particles. *PCRF* measurements were conducted at 30, 50 and 100 nm for both generators (GAG and CAST) as well as for both (singly) charged and neutral particles. In addition, Matter Aerosol performed *PCRF* measurements with 15 nm singly charged graphite particles.

Matter Aerosol employed a TSI 3936 SMPS system (consisting of a TSI 3081 DMA, a TSI 3010 CPC and a TSI 3077A 10 mCi ^{85}Kr neutralizer) to measure the size distribution of the size classified particles (i.e. downstream of the DMA in Figure 21) before each *PCRF* test. The SMPS operated at a sheath flowrate of 10 lpm, a sample flowrate of 1 lpm and a scan time of 300 s.

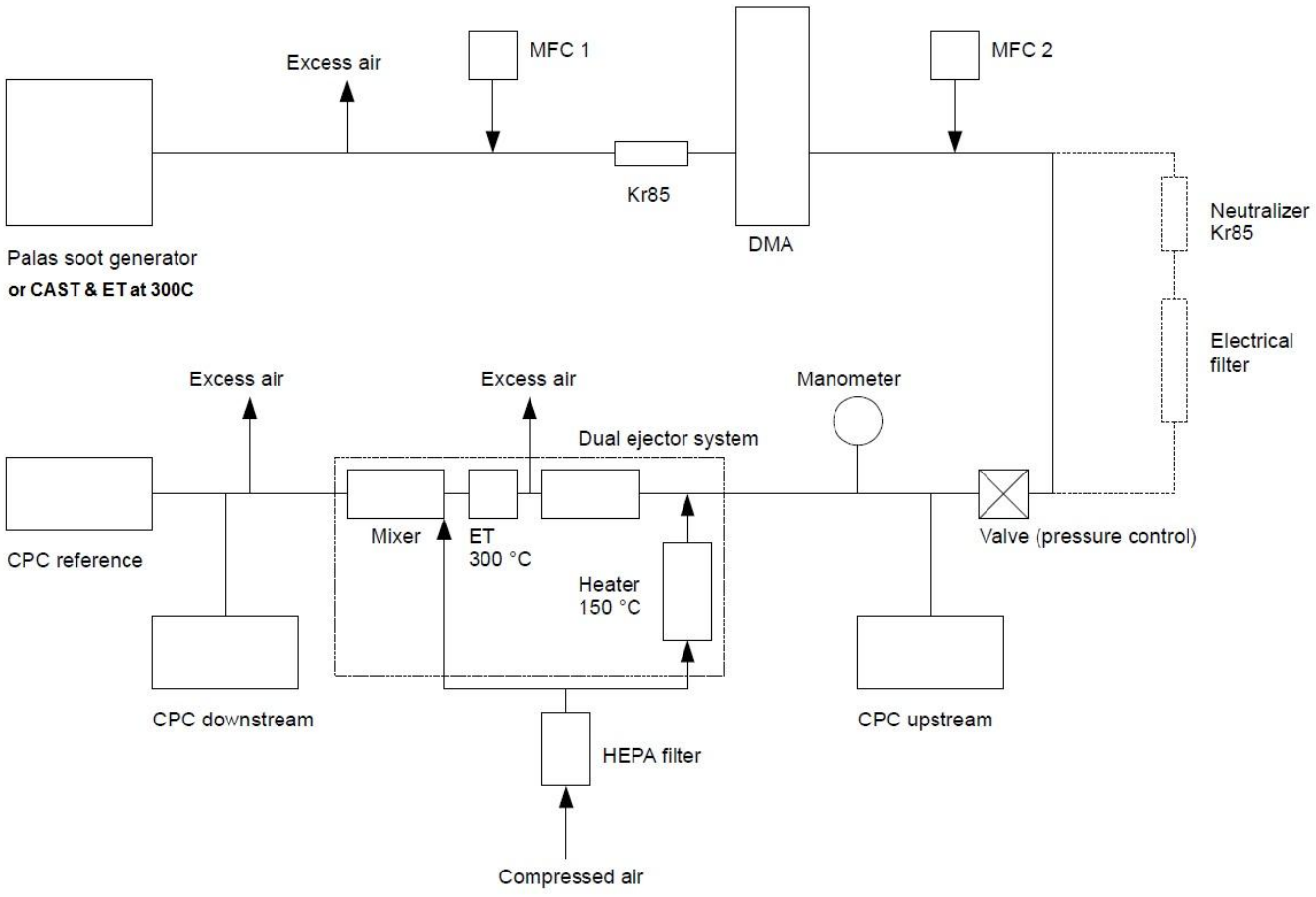

Figure 21: Calibration setup employed at Matter Aerosol.

- **NPL**

NPL performed *PCRF* measurements of the GVPR with the GAG only. The experimental setup employed for these measurements is illustrated in Figure 22. The polydisperse graphite aerosol produced in the GAG was first diluted and subsequently size-classified in a TSI 3081 DMA (that incorporated a 10 mCi ^{85}Kr neutralizer - TSI 3077A) operating at a sample flowrate of 1 lpm and sheath flowrates of 10 lpm or 20 lpm. The classified particles were mixed with purified shop air supplied through a mass flow controller in a 1 m long conductive silicon tube.

NPL employed three CPCs for the *PCRF* measurements. A TSI 3022A CPC (d_{50} at 7 nm) was always monitoring the concentrations downstream of the GVPR to check the stability of the diluted calibration aerosol concentrations. A TSI 3775 CPC (d_{50} at 4 nm) was sampling upstream of the GVPR when the GCPC was measuring the downstream concentrations and vice versa. Since the 3775 CPC operated at 0.3 lpm flowrate, a mass flow controller was employed in parallel sampling a 0.7 lpm in order to compensate for the different flow of the GCPC.

Each CPCs was calibrated against a Grimm 5.705 electrometer using 30, 50 and 100 nm graphite particles.

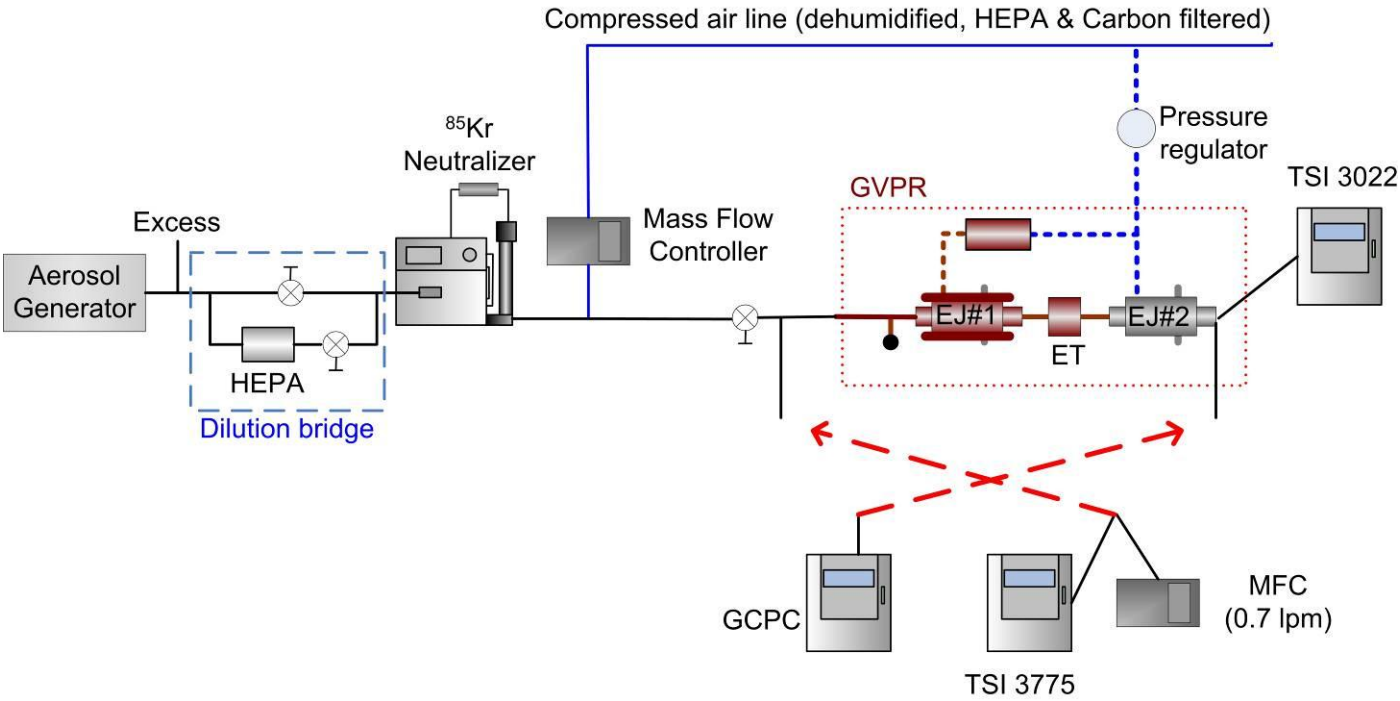

Figure 22: Calibration setup employed for the *PCRF* measurements of the GVPR at NPL.

- **AEAT**

AEAT employed a mini-CAST generator in addition to the GAG for the calibration of the GVPR. The experimental setup employed for their calibration experiments is illustrated in Figure 23. In the tests with the GAG a dilution bridge was employed to control the concentration levels. In the tests with the CAST generator the concentration were controlled by adjusting the CAST dilution air. The resulting dilution ratios at 30, 50 and 100 nm were 7.9:1, 7.7:1 and 6:1.

The polydisperse aerosol was neutralized in a TSI 3077 neutralizer (2 mCi ^{85}Kr) and then size classified in a TSI 3081 DMA operating at a sheath flowrate of 10 lpm and a sample flowrate of 1 lpm. The necessary make-up air was supplied from HEPA-filtered ambient air using a needle valve to control the flow. The two flows passed through a needle valve employed to control the inlet GVPR pressure and mixed in a 1.5 m long conductive silicon tube (6 mm inner diameter). A TSI 3010 CPC (d_{50} at 10 nm) was employed in addition to the GCPC alternatively sampling upstream and downstream of the GVPR.

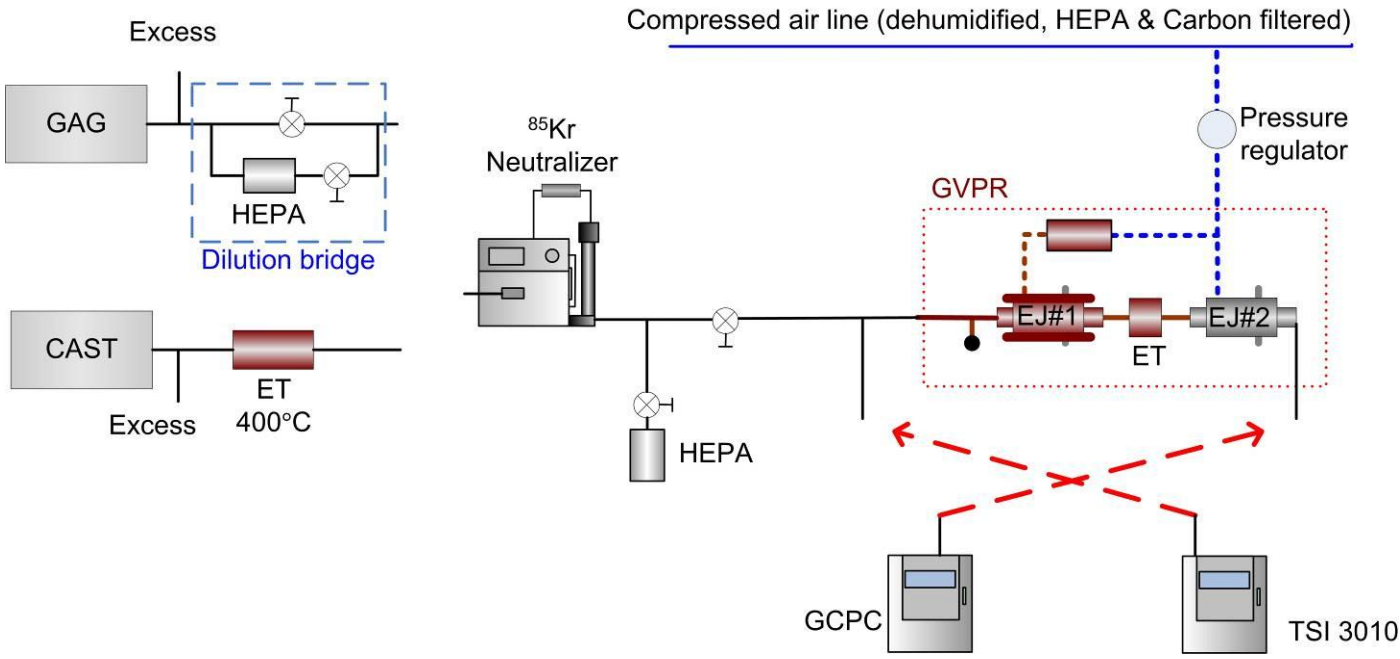

Figure 23: Calibration setup employed at AEAT for the *PCRF* measurements of the GVPR.

AEAT also performed dedicated tests to cross compare the two CPCs employed at 30, 50 and 100 nm, using both aerosol generators. The experimental setup for these checks is illustrated in Figure 24.

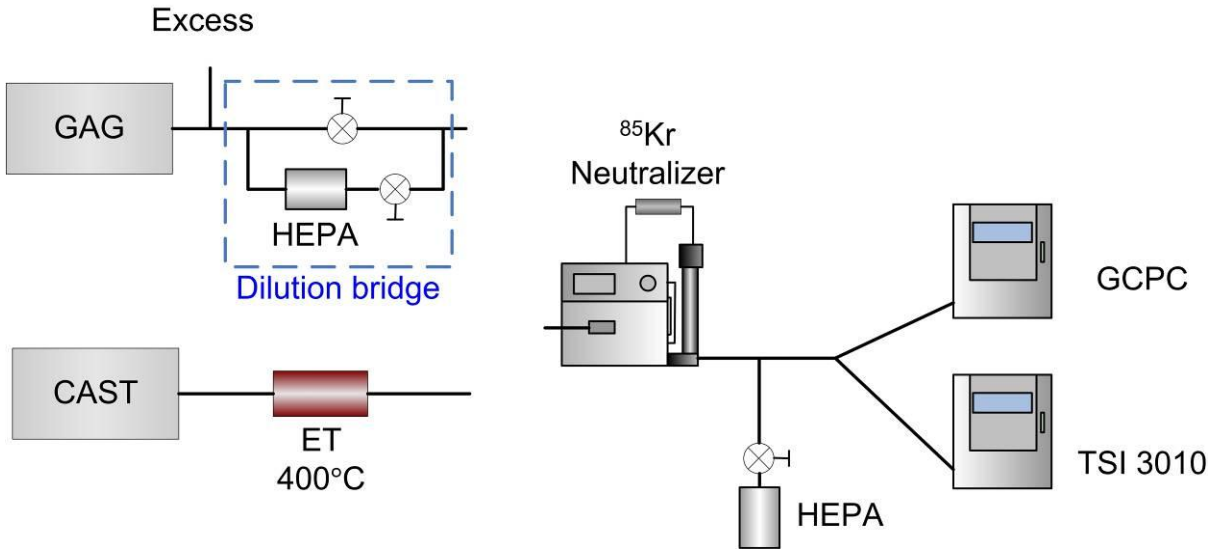

Figure 24: Experimental setup employed at AEAT for the cross check of

- **VW**

VW performed calibration experiments with the GAG and a mini-CAST generator. The calibration setup employed is illustrated in Figure 25. The polydisperse aerosol produced by the GAG was directly fed to a TSI 3081 DMA equipped with a 2 mCi ^{85}Kr neutralizer (TSI 3077), operating at a sheath flowrate of 15 lpm and a sample flowrate of 1.5 lpm. In the tests with the mini-CAST, the aerosol was thermally treated at 350°C and subsequently diluted (10:1) using shop air supplied by a Mass Flow Controller that was purified in a TSI 3074 filtered air supply (dehumidified, charcoal scrubbed and HEPA filtered).

The concentration of the size classified particles was reduced at desirable levels using a dilution bridge at the outlet of the DMA. The necessary make-up air was provided through an HEPA filter using a needle valve to control the flowrate. The two flows were mixed in a TSI 3708 flow splitter. A needle valve was installed upstream of this splitter to control the inlet pressure of the GVPR at -3 kPa gauge.

Two CPCs were employed for the *PCRF* measurements. In the tests with the GAG, the two CPCs employed were the GCPC and a TSI 3772 (d_{50} at 10 nm), which were sampling alternatively upstream and downstream of the GVPR. In the tests with the mini-CAST, the two CPCs employed were two TSI 3790 which however were operating at an elevated temperature difference of 17°C to bring their nominal cut-off size at 10 nm. The modified CPCs employed to measure the upstream concentrations was found to behave non-linearly and its indications were corrected based on dedicated linearity cross-checks (see section 4.2.6.5Figure 63).

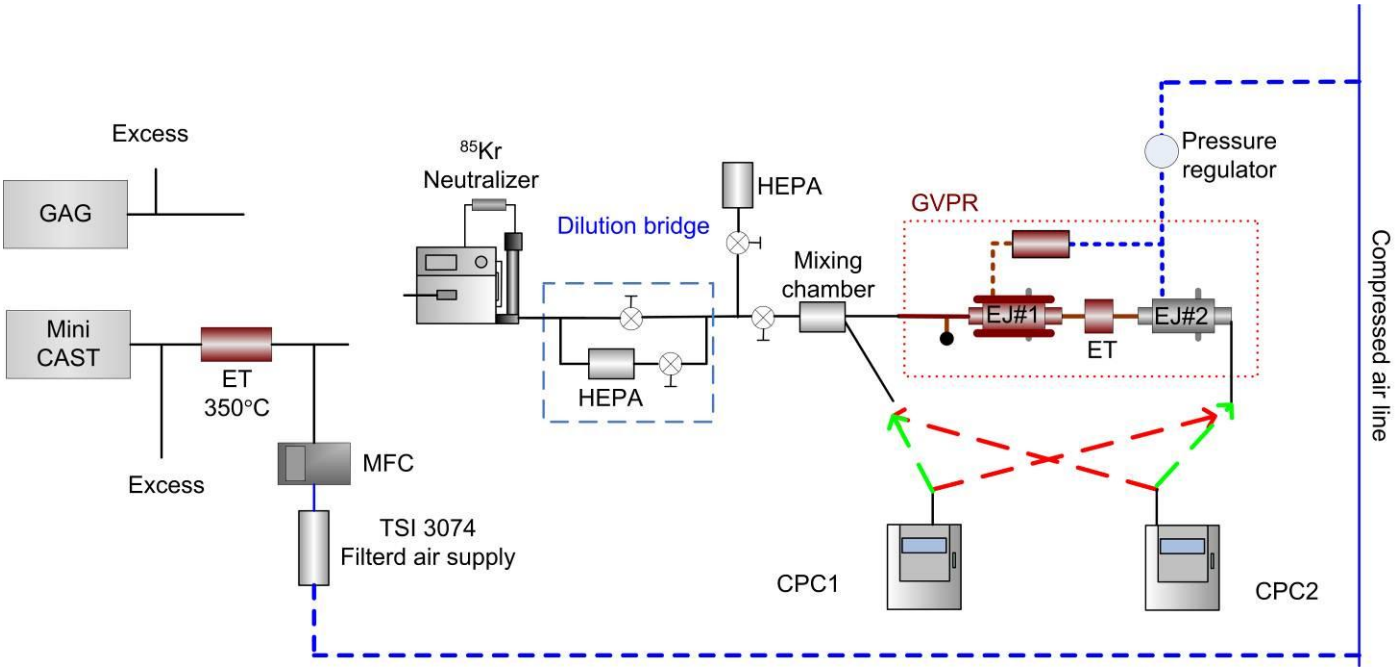

Figure 25: Calibration setup employed at VW.

- **Maha**

Maha performed calibration tests with the GAG and a PALAS DNP 2000 graphite spark generator, which is an older version of the GAG. The operating parameters of DNP 2000 employed for the calibration tests are summarized in Table 4. The experimental setup employed is illustrated in Figure 26. In all tests, the excess flow from the generators was vented through a valve to maintain the calibration setup at overpressure (down to the needle vale used to control the sample pressure of the GVPR). The aerosol produced by the DNP 2000 generator, was thermally treated in same tests by means of passing it through an evaporating tube operating at a wall temperature of 400°C and subsequently diluting it with conditioned air at ambient temperature (dilution factor 2:1).

Table 4: Operating settings of the second DNP 2000 generator employed at Maha for the *PCRF* measurements at 30, 50 and 100 nm.

Parameter	30 nm	50 nm	100 nm
Air flowrate [lpm]	40	40	25
Nitrogen flowrate [lpm]	8.5	8.5	5.4
Frequency [Hz]	65	75	105

The polydisperse aerosol was then size-classified in a TSI 3081 DMA equipped with a TSI 3077 neutralizer (2 mCi ^{85}Kr), operating at a sheath flowrate of 18 lpm and a sample flowrate of 1.8 lpm. The classified particles where subsequently diluted in a dilution bridge. The necessary make-up air was supplied by the compressed shop air line through a needle valve, which further diluted the classified particles. Part of the diluted sample was vented and the remaining was throttled in a needle valve to drop the pressure at -3 kPa (gauge).

Three TSI 3790 CPCs (one being the GCPC) were employed for the *PCRF* measurements. One was always sampling downstream of the GVPR to check the stability of the diluted aerosol concentrations. The other two (GCPC, Maha_3790) where employed sampling alternatively upstream and downstream of the GVPR. In some tests with the DNP2000, the Maha_3790 operated at an elevated temperature difference of 17°C (saturator temperature of 39°C and condenser temperature of 22°C).

A TSI 3034 SMPS was also employed to measure the size distribution of the generated polydisperse aersols (DNP 3000 and thermally treated DNP 2000). The same SMPS was also employed to measure the polydisperse size distributions downstream of the GVPR, as well as the distribution of the size classified particles employed for the calibration of the GVPR.

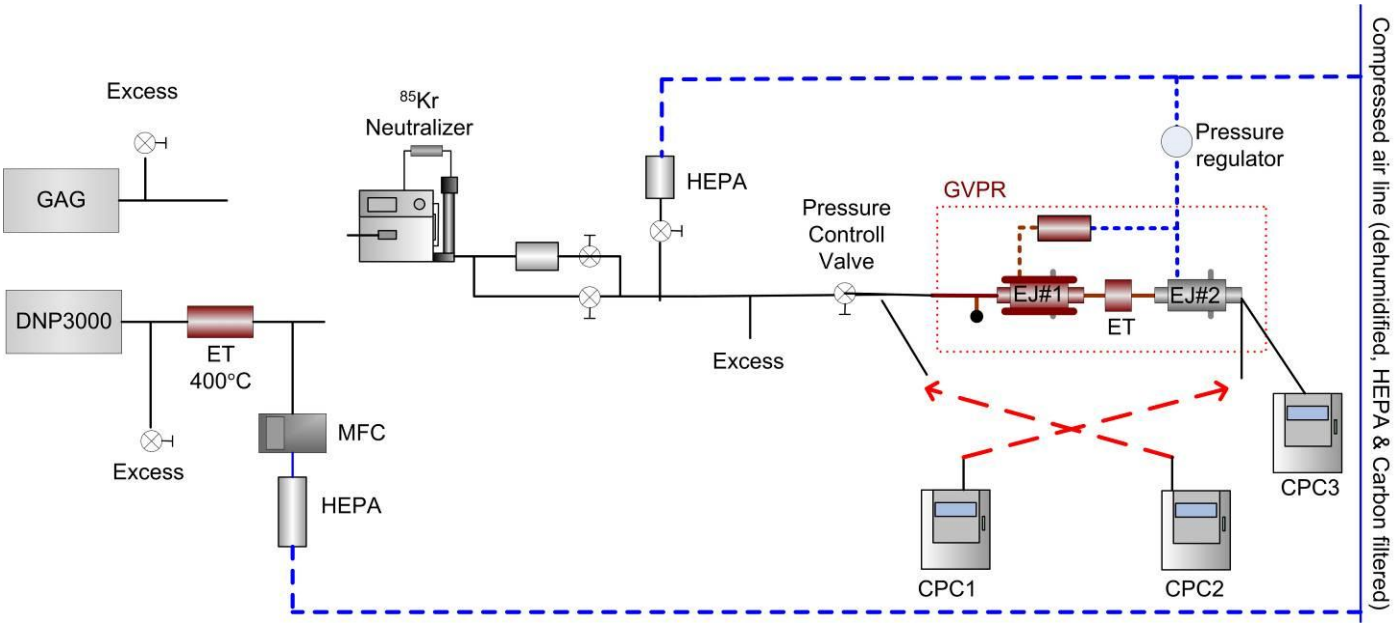

Figure 26: Calibration setup employed at Maha for the *PCRF* measurements.

The linearity of the three CPCs employed in the calibration experiments was cross compared using thermally treated graphite particles produced in the DNP 2000 generator. The experimental setup employed for these tests is illustrated in Figure 27. Checks were conducted at 30, 50 and 100 nm and for the unmodified and modified Maha_3790 CPC.

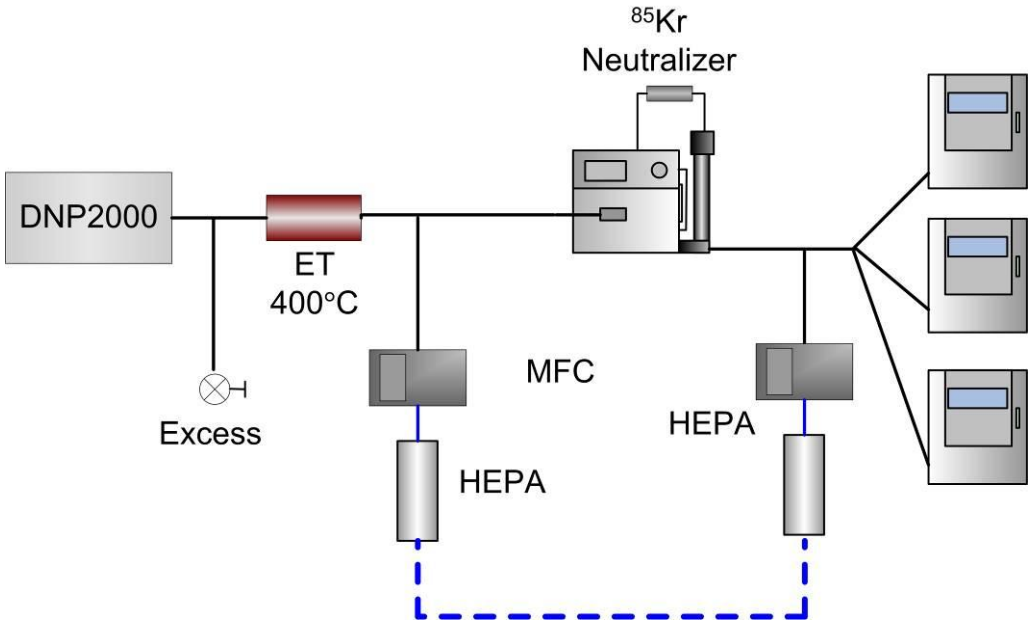

Figure 27: Calibration setup employed for the linearity checks of the three CPCs employed at Maha.

2.2.3 Dilution Factor Measurements

The participating laboratories were requested to also perform some dilution factor measurements using a gas analyzer. Table 5: summarizes the calibration gas compositions employed in the different laboratories and the chemical compound measured (trace gas).

Table 5: Trace gas employed for the dilution factor at each lab and chemical composition of the calibration gas.

Laboratory	**Trace gas**	**Chemical composition**
JRC	CO_2	14% CO_2 in N_2
LAT	NO_x	1069 ppm NO_x in N_2
AVL	CO	4.8% CO, 19% CO_2, 76.2% N_2
Horiba	NO	10000 ppm NO in N_2
EMPA	NO	980 ppm NO in N_2
Matter Aerosol	-	-
NPL	CO	5% CO, 20% O_2, 75% N_2
AEAT	CO	900 ppm CO in N_2
VW	-	-
Maha	-	-

3 Characterization of the Golden Instrumentation at JRC

3.1 GVPR

JRC performed some dedicated experiments at the beginning of the campaign to investigate the effect of sample pressure and dilution air pressure on the dilution factor. The trace gas employed in these measurements was CO_2 supplied by a calibration bottle containing 13.99%(±0.05%) CO_2 in nitrogen. The concentrations measured downstream of the VPR ranged from 1700 to 2690 ppm CO_2, while the background was measured to be 400 ppm. The dilution factor was calculated as:

$$DF = \frac{C_{upstream} - C_{background}}{C_{downstream} - C_{background}} \qquad \text{Eq. 1}$$

Figure 28 presents the measured dilution factors of the GVPR as a function of the sample pressure at dilution air pressures of 200 kPa (blue dots), 215 kPa (red dots) and 185 kPa (green dots). The dilution air pressures corresponded to the nominal set point (200 kPa) and a ±7.5% deviation around this value, which was considered as typical uncertainty in Bourdon pressure gauges employed in the participating laboratories for the control of the dilution air. The dilution factor at ambient sample pressure was found to be 75:1 to 76:1, and was little affected by a ±7.5% uncertainty in the dilution air pressure (less than 1% change in the dilution factor). However, small deviations of the sample pressure from ambient, had a strong effect on the dilution factor. In that respect, a sample underpressure of 2.7 kPa (at the nominal dilution air pressure) resulted in a 14% increase of the dilution factor (88:1).

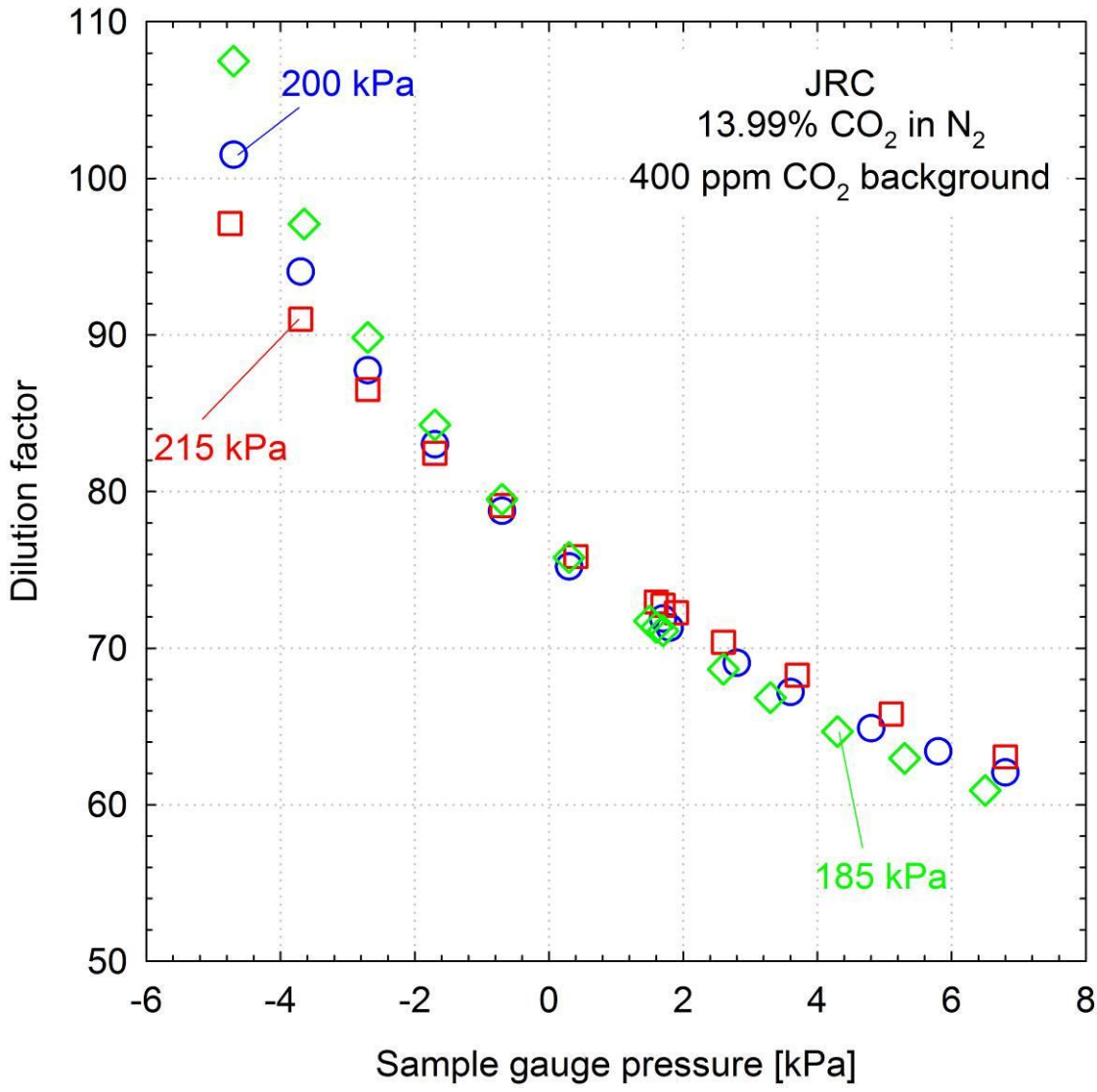

Figure 28: Measured dilution factors of the GVPR at JRC as a function of the sample pressure (horizontal axis) at three different dilution air overpressures (different symbols).

The results also showed that as the sample pressure deviates from ambient levels, the dilution factor becomes more sensitive on variations of the dilution air pressure. More specifically, a ±7.5% uncertainty in the dilution air pressure resulted in a ±2.5 % uncertainty in the dilution factor at a sample underpressure of 2.7 kPa, and ±6 % uncertainty in the dilution factor at a sample underpressure of 4.7 kPa.

The dilution factor of the ejector diluters also depends on the chemical composition of the sampled gas (Giechaskiel et al., 2004). In order to get an estimate of the associated error, some calculations were performed following the numerical model developed by Giechaskiel et al. (2004). An exact calculation of the dilution factor with this model requires information on the geometry of the ejector nozzle as well as the experimental determination of two coefficients accounting for non-idealities (non-isentropic flows). This information was not available for the two ejectors of the GVPR. Accordingly, the model was only employed to calculate the relative effect of chemical composition (percentage changes in the dilution factor from the base case of ambient air) using the ejector design investigated by Giechaskiel et al. (2004). For the calculations we assumed two of these ejector types operating at the nominal pressures and temperatures as described in Table 6.

Table 6: Input parameters employed in the ejector model calculations.

Non-isentropic coefficient for ejector inlet (k_s)	0.99
Non-isentropic coefficient for dilution air (k_{da})	0.7
First ejector	
Inlet pressure	96.3 kPa
Inlet temperature	30°C
Dilution air pressure	300 kPa
Dilution air temperature	150°C
Second ejector	
Inlet pressure	99.3 kPa
Inlet temperature	300°C
Dilution air pressure	300 kPa
Dilution air temperature	30°C

The results of these calculations are shown in Figure 29 for the different calibration gasses employed in the campaign (Table 5). In good agreement with the experimental results (Giechaskiel et al., 2009b) and theoretical predictions of Giechaskiel et al. (2004), the magnitude and direction of the error appears to mainly depend on the molecular weight of the calibration gas. Gases containing high concentrations of CO_2 have higher molecular mass compared to air and this generally results in an overestimation of the dilution factor (up to ~3% in the case of AVL). On the other hand, calibration gases containing traces of chemical compounds in nitrogen, have smaller molecular weight than air and this results in lower dilution factors (~2%). However, the overall effect was estimated to be generally smaller than ±2%.

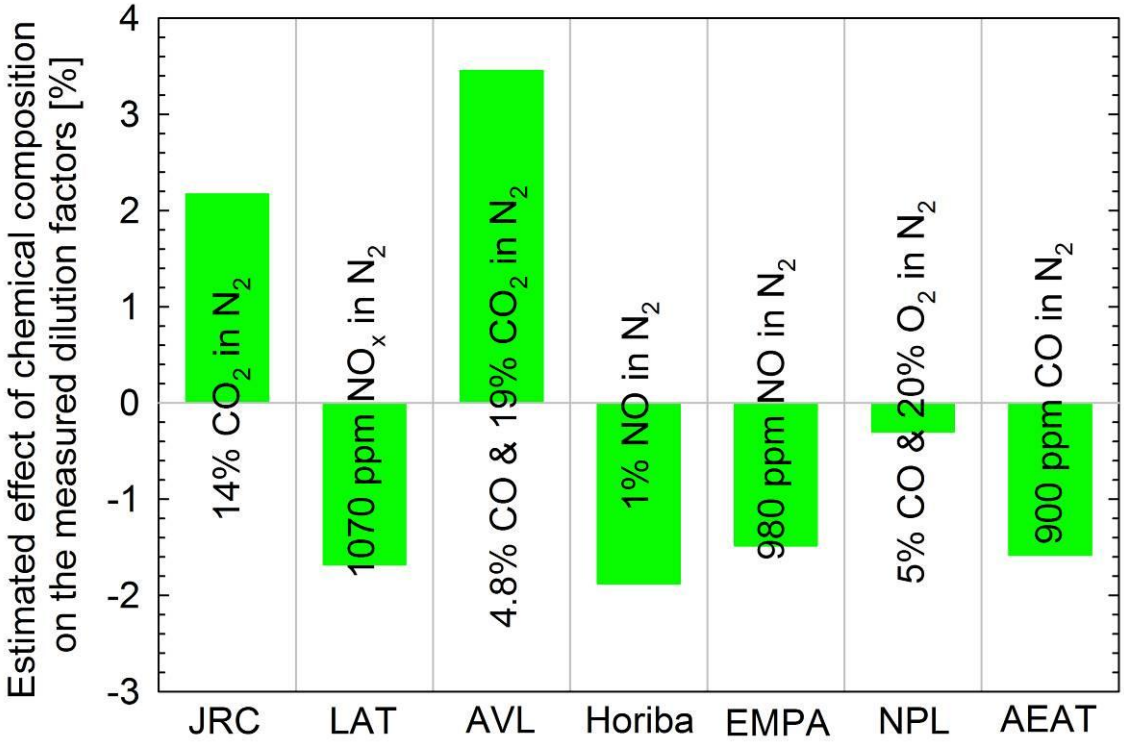

Figure 29: Estimated error in the measured dilution factor due to the different chemical composition of the calibration gas from ambient air.

3.2 GAG

JRC performed some dedicated experiments at the start of the experimental campaign to identify the operating parameters of the GAG that would result in suitable size distributions for the calibration of the GVPR at 30, 50 and 100 nm. The two points that were eventually selected were:

1. 3 lpm N_2, 6 lpm air and 0.75 mA for the calibration tests at 30 nm.
2. 3 lpm N_2, 3 lpm air and 2 mA for the calibration tests at 50 and 100 nm.

The selected nitrogen flow was the minimum possible with the GAG in order to minimize the consumption of N_2. The air flow-rate only serves for dilution of the produced aersosol and was maintained as low as possible in order to achieve concentrations typical to those produced by other aerosol generators (i.e. CAST). The adjustable current output of the high voltage supply has a direct effect on the size distribution, with the peak particle size increasing with increasing the applied current. The two values selected resulted in size distributions peaking below 30 nm (set point 1 – 0.75 mA) and 50 nm (set point 2 – 2 mA). This is a desirable property in order to maintain the fraction of multiple charged particles (classified in the DMA) low.

The characterization of the produced size distribution was found to be a rather challenging task, because of the very high number concentrations produced that laid to significant coagulation. For example, Figure 30 illustrates the strong effect of the residence time on the produced distributions at the two operating conditions that were finally selected. The situation is more clearly shown in Figure 31, which shows the actual change of the total number concentration, the geometric standard deviation and the geometric mean diameter of the size distribution with increasing residence time.

A 3.6 s residence time was sufficient to reduce the total number concentration produced at the second set point (3 lpm N_2, 3 lpm air and 2 mA) by almost 75% and shift the peak size from 25 nm to 45 nm. This change was due to the combined effect of particle coagulation and diffusion losses. The effect was less pronounced in the distribution produced at the first set point (3 lpm N_2, 6 lpm air and 0.75 mA) due to the lower initial number concentrations (6×10^7 #/cm^3 compared to 15×10^7 #/cm^3). The lower concentrations were due to a) the lower voltage that resulted in lower production rates of primary graphite particles and b) due to the higher internal dilution of 3:1 (6 lpm air and 3 lpm N_2) compared to 2:1 (3 lpm air and 3 lpm N_2). The peak size at this first set point changed from 18 nm at

0.1 s residence time to 26 nm at 3.6 s. It should be stressed here that a residence time of 3.6 s is quite high. Based on the DMA flows and tubing employed at the different labs, the maximum expected residence time in the GVPR calibration was less than 2 s (AVL).

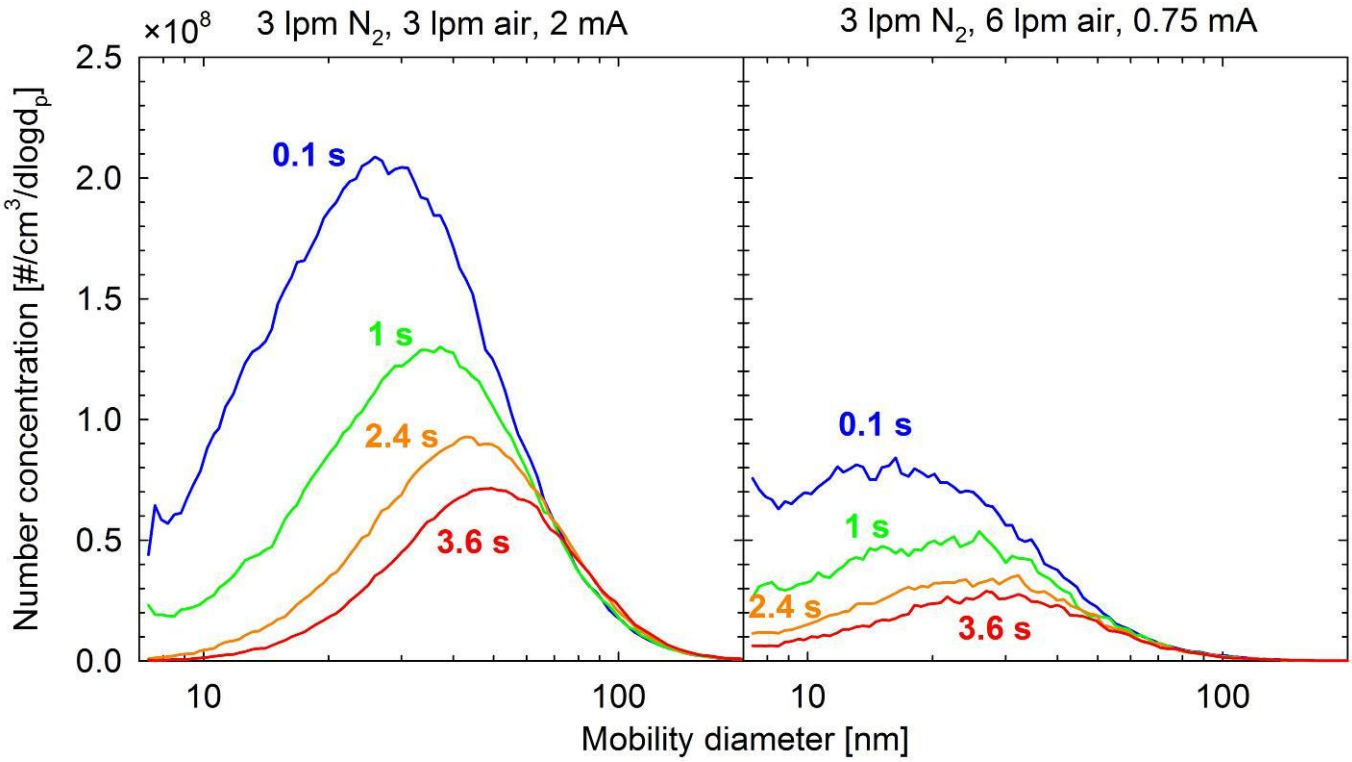

Figure 30: Size distributions of the polydisperse aerosol produces by the GAG at the two set points as a function of the residence time.

JRC also conducted some Tandem-DMA measurements in order to quantify the fraction of multiple charged particles. These investigations were conducted at the maximum residence time investigated (3.6 s) and should therefore correspond to a worst case condition. The measured TDMA distributions are shown in the top panels of Figure 32 (uncorrected for multiple charges) and Figure 33 (corrected for multiple charges). Some TDMA measurements conducted with spherical PAO particles are also shown on the bottom of these two figures for reference

Focusing first on the uncorrected for multiple charges distributions (Figure 32) of size-classified graphite particles, one can identify three peaks. The middle peak, with the highest number concentration, corresponds to singly charged particles at the selected (desired) particle size. The peak at larger sizes corresponds to larger, doubly-charged particles that are classified at the same DMA voltage with the singly charged particles of the desired size. The peak at smaller sizes corresponds to doubly charged particles at the selected (desired) particle size. Therefore, this peak should not be present when the results are corrected for multiple charges. Indeed, this peak is substantially reduced in the multiple charged corrected distributions shown in Figure 33, but not completely removed. Interestingly, the correction algorithm works very well for spherical PAO particles shown in the bottom panels. This indicates that the aggregate graphite particles produced by the GAG acquire more charges than spherical droplets of the same mobility diameter. Similar effects of particle morphology on bipolar charge distributions has been observed in other studies (Rogak and Flagan, 1992; Lall and Friedlander, 2006, Maricq, 2007). This different charging behaviour of aggregate particles can affect the accuracy of size distribution measurements (Lall and Friedlander, 2006) as well as of corrections applied in calibration experiments with size-classified particles (Giechaskiel et al., 2009b; Giechaskiel et al., 2009c). It should be mentioned that TSI ltd. is supplying a correction algorithm that is based on the idealized case of long prolate spheroids (Wen et al., 1984) and requires information on the primary particle size. However, this algorithm was not available at JRC and therefore could not be assessed.

Despite the uncertainties associated with the multiple-charge correction algorithm, the corrected size spectrums shown in Figure 33 suggest that the fraction of multiply-charged particles that would interfere in the GVPR calibration experiments at 30, 50 and 100 nm would be ~9%, ~12% and ~8%, respectively. Since these Tandem-DMA measurements were conducted at the longest expected residence time of the generated polydisperse aerosol (i.e. at the maximum expected geometric mean diameter - Figure 31), these figures should rather correspond to worst case conditions.

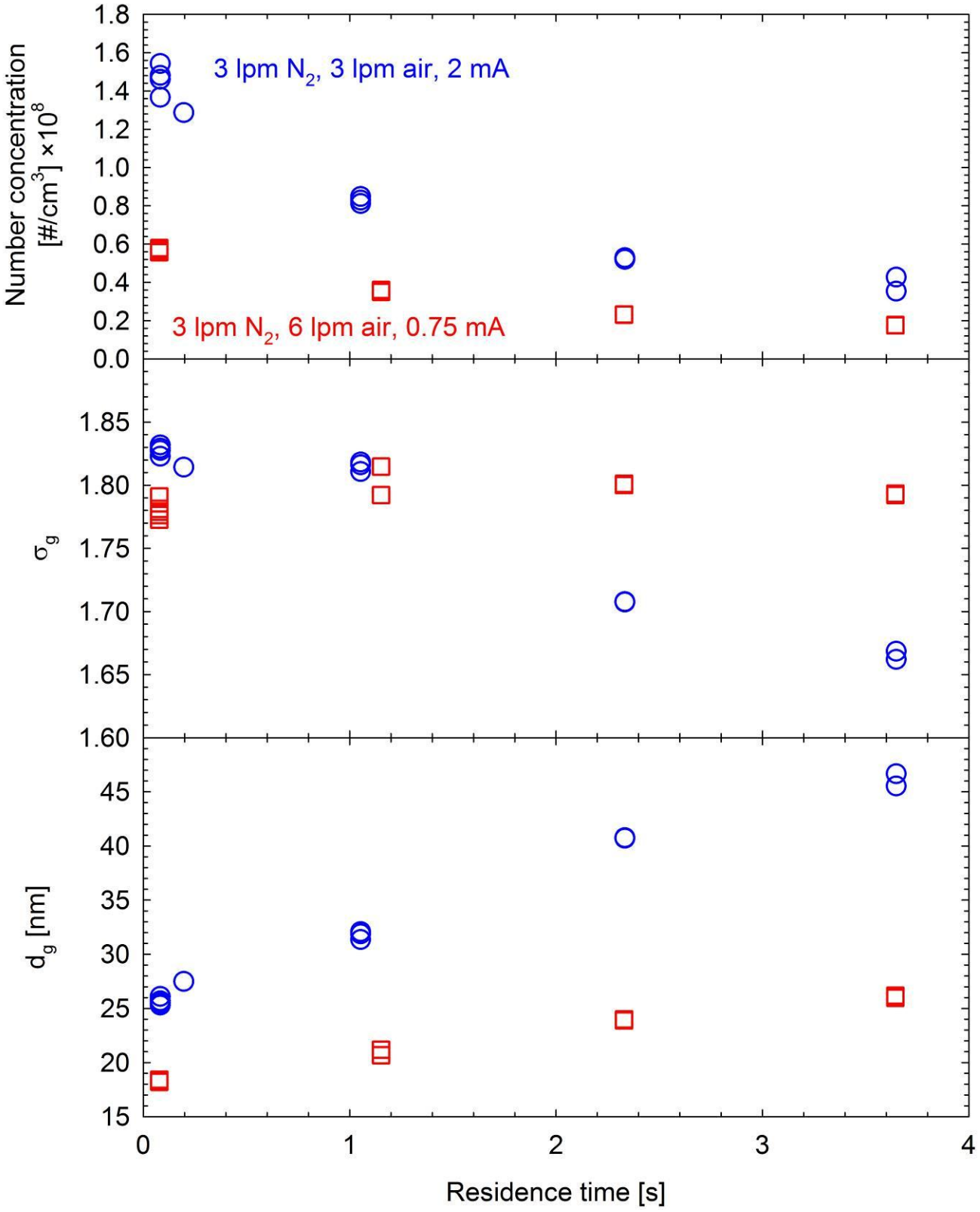

Figure 31: Effect of the residence time on the geometric mean diameter (lower panel), the geometric standard deviation (middle panel) and the total number concentration (upper panel) of the polydisperse aerosol produced by the GAG at the two selected operating conditions.

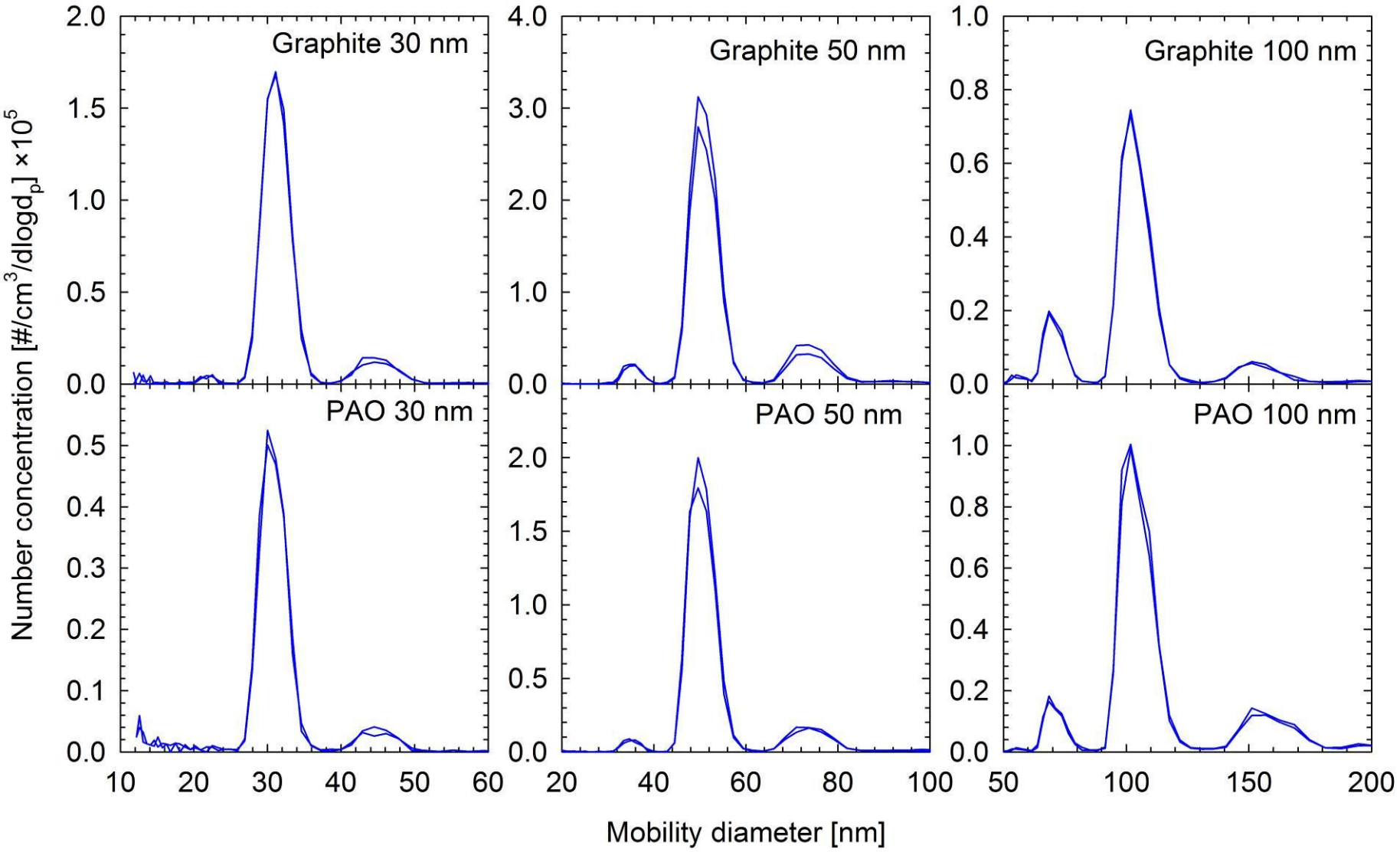

Figure 32: Tandem-DMA responses of graphite (upper panels) and PAO (lower panels) particles at 30 (left panels), 50 (middle panels) and 100 nm (right panels). The responses are not corrected for multiple charges.

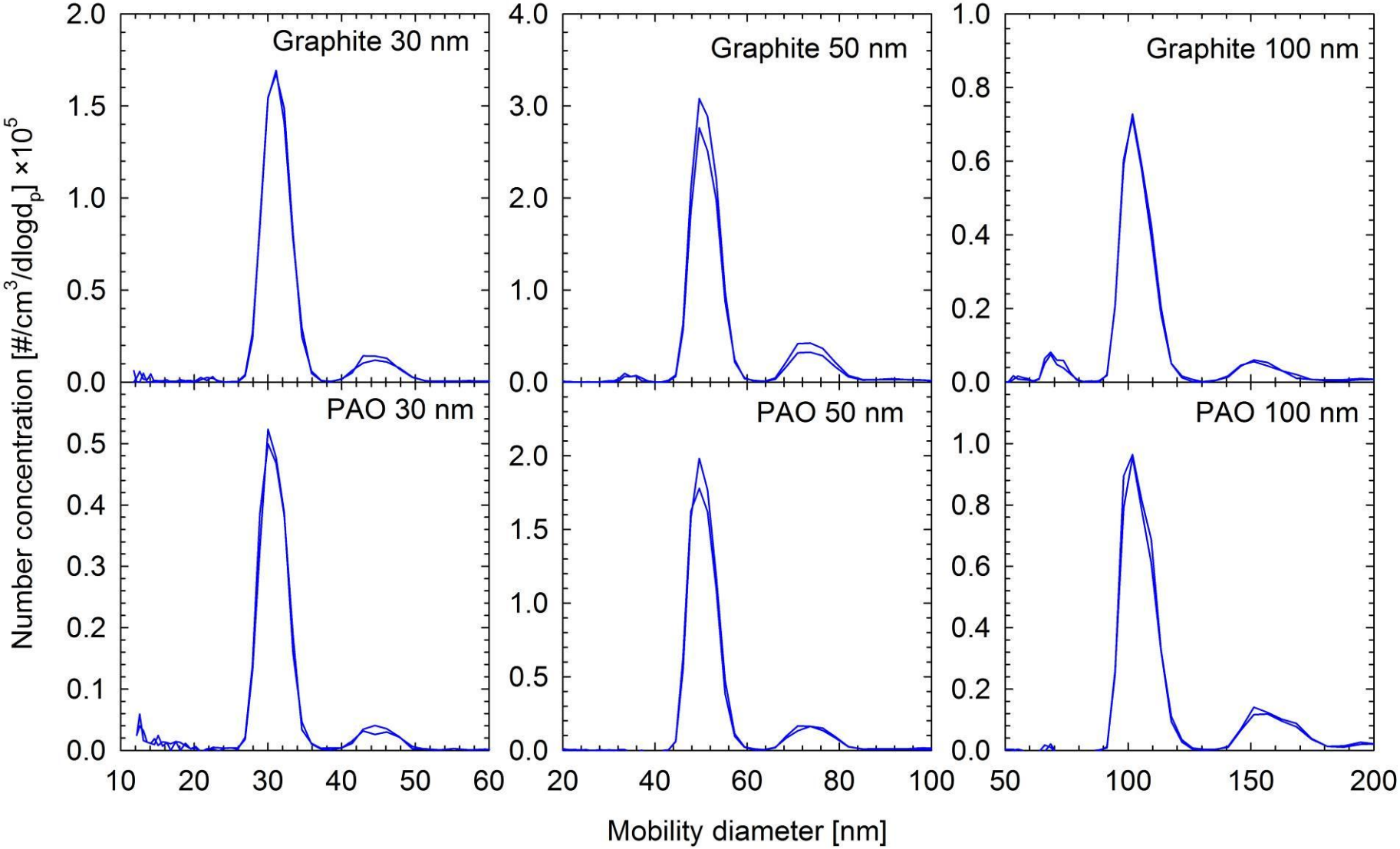

Figure 33: Tandem-DMA responses of graphite (upper panels) and PAO (lower panels) particles at 30 (left panels), 50 (middle panels) and 100 nm (right panels). The responses are corrected for multiple charges incorporated in the TSI's inversion algorithm.

3.3 GCPC

The GCPC was thoroughly characterized at JRC before the start of the campaign and the results were presented in detail elsewhere (Mamakos et al., 2011a). This section will only provide an summary of the calibration results.

The linearity of the GCPC was checked against a TSI 3068B electrometer, over an extended concentration range of 300 to 10000 #/cm^3. In order to increase the sensitivity of the electrometer at low concentrations (<2000 #/cm^3), the electrometer operated at elevated flowrates and was supplied with doubly-charged particles taking advantage of the Tandem-DMA setup (Mamakos et al., 2011a). Figure 34 summarizes the results of the linearity checks with 100 nm graphite particles. The percentage difference between the GCPC and the electrometer concentrations lied with -10% and -14% over the entire concentration range examined (300-10000 #/cm^3). The results suggest a very linear behaviour and not trend could be identified with decreasing number concentrations.

The absolute differences (-12% on average) were quite high however, and most importantly lied outside the regulatory requirements of ±10%. The certificate issued by the manufacturer suggested a ~5% underestimation of the number concentrations based on measurements with 55 nm emery oil particles. The calibration experiments conducted at JRC suggested a reduced detection efficiency of the GCPC for graphite particles compared to emery oil, even at very large sizes. This is evident in Figure 35, which compares experimentally determined counting efficiencies of the GCPC for these two different particle materials.

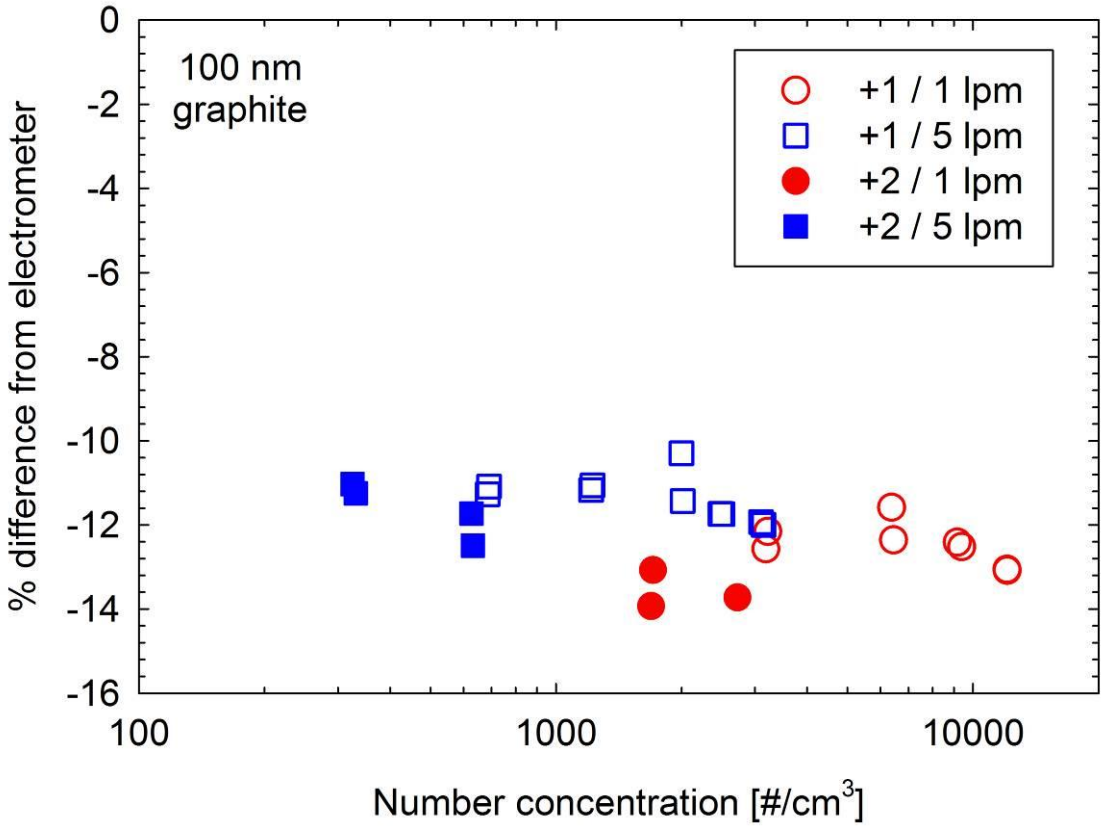

Figure 34: Linearity checks of the GCPC against a TSI 3068B electrometer using 100 nm graphite particles (Mamakos et al., 2011a).

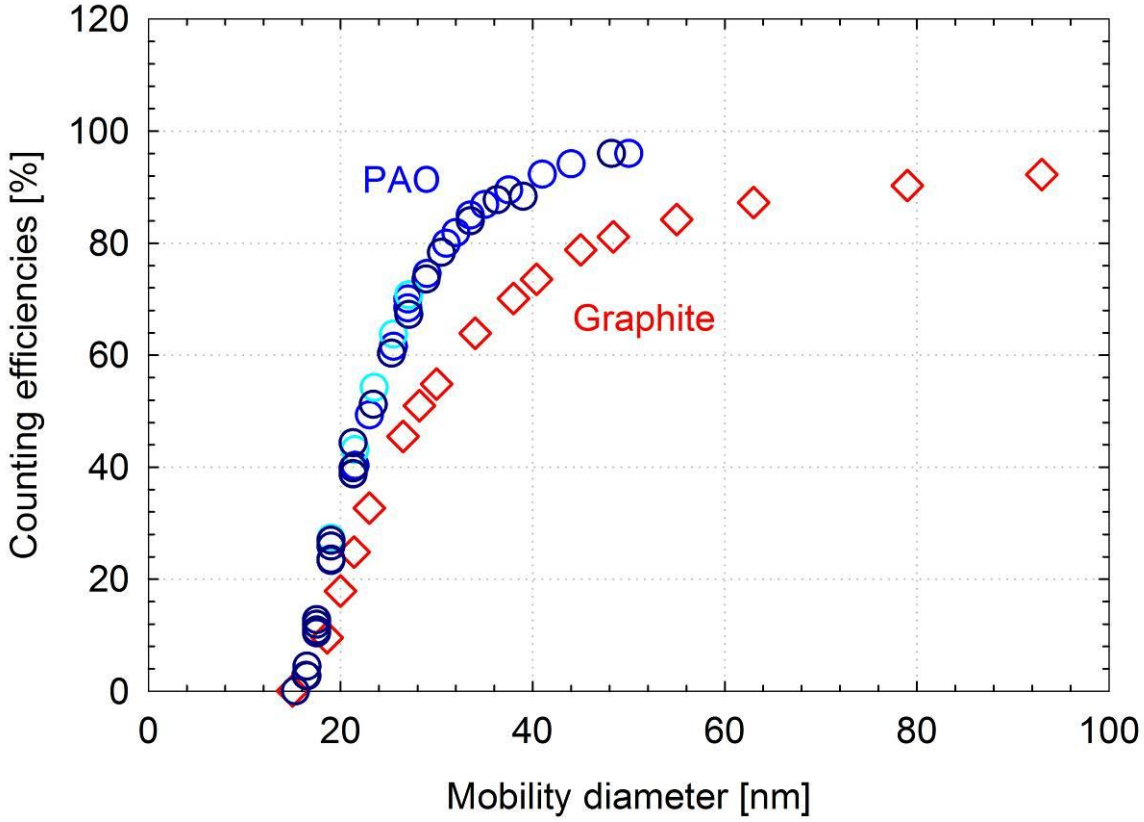

Figure 35: Experimentally determined counting efficiencies of the GCPC for graphite (red symbols) and emery-oil (blue sumbols) particles.

4 Round Robin Results

4.1 GVPR dilution factor

Only seven out of the ten laboratories measured the dilution factor of the GVPR using trace gases (Table 5). The reported dilution factors are summarized in Figure 36. One of the laboratories (EMPA) actually performed the measurements at a lower sample underpressure (2 kPa instead of 3 kPa), condition which according to the experimental investigations conducted at JRC (Figure 28) should result in a ~5% underestimation of the dilution factor. Accordingly the results from EMPA were scaled up by 5%.

Overall, the dilution factors averaged at 90.5:1, with the individual differences from this average value being generally less than ±3%. One notable exception was the measurement at AEAT which exceeded the overall average dilution factor by 8%. The consideration of the effect of chemical composition (as quantified by the numerical model of Giechaskiel et al. (2004) - Figure 29) had a minimal effect with the average dilution factor from all labs averaging again at 90.5:1, but slightly increased the individual differences (±4.5% for all labs except AEAT where the difference reached 10%).

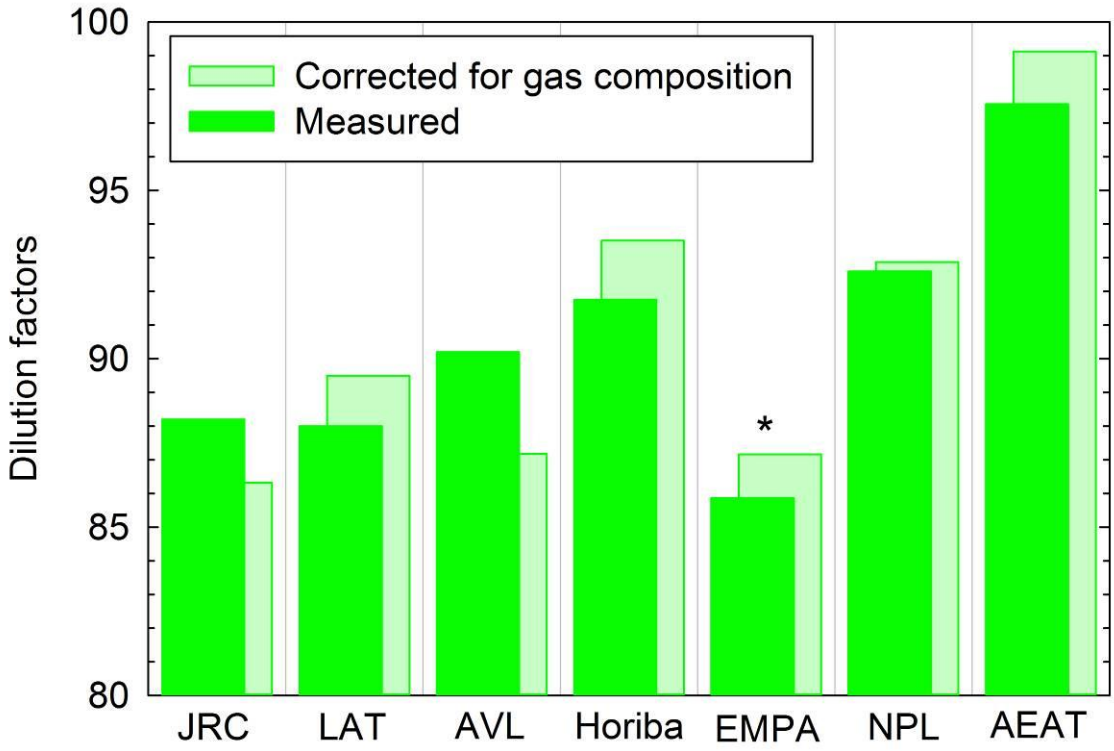

Figure 36: Measured dilution factors (bars in dark green) of the GVPR and corrected figures for the chemical composition of the calibration gas (Figure 29). * The dilution factor measurements at EMPA were conducted at a lower sample under-pressure of 2 kPa, and were accordingly corrected by 5% to account for this (Figure 28).

4.2 Particle Concentration Reduction Factors

4.2.1 Stability of the concentrations in the calibration setup

For the calibration of the GVPR with the reference instrumentation, the laboratories were requested to employ two CPCs sampling alternatively upstream and downstream of the GVPR. The two CPCs should operate at the same nominal flowrates, otherwise an additional pump or mass flow controller should be employed to compensate for the different flowrates. However, and since the calibration setup was at underpressure in almost all laboratories (the only exception being Maha), small differences in the sample flowrates of these two CPCs could result in a) changes of the DMA sample flowrate and accordingly the concentration of the calibration aerosol and b) small changes at the inlet pressure of the GVPR which could affect the dilution factor. Furthermore, the high dilution air flowrates required for the operation of the GVPR (~40 lpm of dilution air supplied to each of the two ejectors) typically led to periodic fluctuations of the dilution air pressure and accordingly the GVPR dilution.

The situation is illustrated in Figure 37 which shows the real time recordings of a CPC sampling downstream of the GVPR system during some preliminary calibration experiments conducted at JRC. This "reference" CPC was found to measure systematically higher concentrations (5-10%) whenever the GCPC was sampling downstream (and accordingly the alternative CPC was sampling upstream). The sample flowrates of the two CPCs were measured with a bubble flowmeter and found to be 1.02 lpm (GCPC) and 0.97 lpm (alternative CPC).

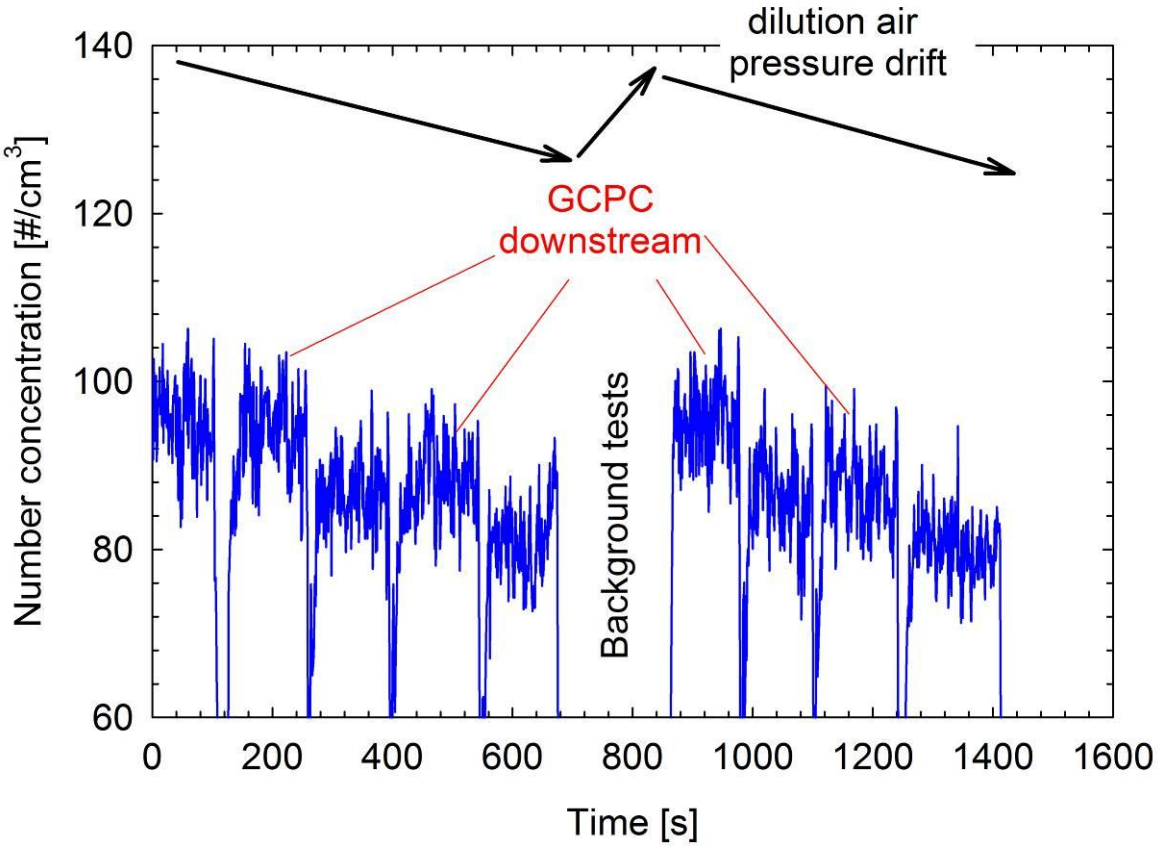

Figure 37: Recorded number concentrations downstream of the GVPR during some preliminary calibration experiments conducted at JRC. The black arrows on the top indicate qualitatively the changes in the dilution air pressure during the measurements (ranging between 205 kPa to 195 kPa).

It is also interesting to note that the concentrations were found to follow the changes in the dilution air pressure which was gradually decreasing from 205 kPa to 195 kPa (overpressure) in a periodic fashion. This drift in the dilution air pressure affected somehow the dilution factor (e.g. Figure 28) but mainly the sample flowrate. Small changes in the sample flowrate resulted in changes in the DMA sample flowrate (and accordingly the DMA transfer function and concentration of

extracted samples) and the dilution of the classified particles with the fixed make-up air supplied by a mass flow controller.

This example situation depicted in Figure 37, illustrates how sensitive the calibration setup can be in maladjustments of the flows when changing sampling positions. Accordingly it was recommended that a third CPC would be employed in the calibrations (if possible) monitoring always the concentration downstream of the GVPR. This approach was only adopted in 6 out of the 10 labs (JRC, LAT, EMPA, Matter Aerosol, NPL and Maha).

4.2.2 Calculations

Each laboratory submitted the average number concentrations measured with all of the CPCs they have employed over each sequence of upstream and downstream sampling. Whenever a monitor CPC was employed (which was the case in 6 out of 10 labs), its indications were employed to calculate the drift of the concentrations over the test sequence:

$$C_i = N \frac{C_i^{mon}}{\sum_{k=1}^{N} C_k^{mon}} \qquad \text{Eq. 2}$$

where, N is the number of repetitions (i.e. concentrations measurements), C_i^{mon} is the average number concentration measured with the "monitor" CPC (downstream of the GVPR) over the i^{th} repetition. In case no monitor CPC was employed, no correction for the concentration drift was possible (C_i assumed to equal 1)

The average concentrations measured with the other two CPCs measuring alternatively upstream and downstream of the GVPR where then divided with the calculated concentration drift (C_i). Then all upstream concentrations where corrected for the change of the flowrate due to the 3 kPa underpressure[1]:

$$C_{up} = C_{indicated} \cdot \frac{p_{down} - \Delta p}{p_{up} - \Delta p} \qquad \text{Eq. 3}$$

Where p_{down} is the pressure downstream of the GVPR and p_{up} is the pressure upstream of the GVPR. Δp is the pressure drop across the CPC that was only known for TSI 3790 CPCs (2.3 kPa - Wang and Horn, 2008) and thus assumed to be zero in all other CPC models.

The particle concentration reduction factors (*PCRF*) were then calculated for each CPC separately (GCP and alternative) as the ratio of upstream to downstream concentrations for all sequential exchanges of sampling positions (taking into account the concentration drifts -eq. 2, and pressure effects - eq. 3). The average value served as the *PCRF* for this particular calibration experiment. The standard deviation of the calculated *PCRF* values was also determined and served as an estimate of the measurement stability (s_{stab}).

4.2.2.1 Uncertainty analysis

Most laboratories performed only one repetition of *PCRF* measurements which allowed for the calculation of the mean value and the measurement stability (s_{stab}) as defined in the previous section. Some labs however, perform two or even three repetitions with each setup/diameter. The standard deviation of the mean *PCRF* values determined at each repetition was employed as a surrogate of the measurement repeatability (s_{rep}). The measurement stability in this case, was considered to be the maximum from the different test repetitions:

[1] AVL measured the upstream concentration, upstream of the needle valve controlling the GVPR sample pressure. In this setup the pressure difference at the two sampling locations of the CPC was lower but measured (~1.3 kPa).

$$PCRF^{av} = \frac{1}{J}\sum_{i=1}^{J} PCRF_i \qquad \text{Eq. 4a}$$

$$s_{\text{rep}} = \sqrt{\frac{\sum_{i=1}^{J}\left(PCRF_i - PCRF^{av}\right)^2}{J-1}} \qquad \text{Eq. 4b}$$

$$s_{\text{stab}} = \max\left(s_{stab}^{i}\right) \qquad \text{Eq. 4c}$$

where J is the number of test repetitions.

Another source of uncertainty that was considered in the analysis relates to the contribution of background. The later was determined at each lab by means of supplying the GVPR with particle free air (e.g. setting the DMA voltage at zero). The contribution of background was estimated by means of applying the conservation of mass principle on the second ejector (the concentrations at the first ejector would be too high to be affected by the background concentration):

$$m_{in}^{2nd} C_{in}^{2nd} + m_{da} C_{da} = m_{out}^{2nd} C_{out}^{2nd} \qquad \text{Eq. 5}$$

where C_{in}^{2nd}, C_{da} and C_{out}^{2nd} are the aerosol mass concentrations at the inlet, dilution air and outlet of the second ejector which are considered to be equal to the number concentrations (a valid assumption for solid particles at the low concentrations employed where coagulation is insignificant), while m_{in}^{2nd}, m_{da} and m_{out}^{2nd} are the sample, dilution air and outlet mass flowartes.

Equation 5 can also be written in the form:

$$C_{in}^{2nd} + \left(PCRF_2 - 1\right)C_{da} = PCRF_2 \cdot C_{out}^{2nd} \qquad \text{Eq. 6}$$

where $PCRF_2$ stands for the particle concentration reduction factor of the second ejector.

If the background concentration was zero, the outlet concentration would be equal to:

$$C_{out,ideal}^{2nd} = \frac{C_{in}^{2nd}}{PCRF_2} = \frac{C_{in}^{1st}}{PCRF} \qquad \text{Eq. 7}$$

where, C_{in}^{1st} is the number concentration at the inlet of the first ejector that is at the inlet of the GVPR.

For a non-zero background, the outlet concentration would be equal to:

$$C_{out}^{2nd} = \frac{C_{in}^{2nd} + \left(PCRF_2 - 1\right)C_{da}}{PCRF_2} = \frac{C_{in}^{1st}}{PCRF} + \frac{\left(PCRF_2 - 1\right)}{PCRF_2} C_{da} \qquad \text{Eq. 8}$$

Therefore the effect of background on the calculated *PCRF* would be of the order of:

$$s_{bckg} \cong PCRF \cdot \frac{\frac{C_{in}^{1st}}{C_{out,ideal}^{2nd}} - \frac{C_{in}^{1st}}{C_{out}^{2nd}}}{\frac{C_{in}^{1st}}{C_{out,ideal}^{2nd}}} = PCRF \cdot \frac{\frac{\left(PCRF_2 - 1\right)}{PCRF_2} C_{da}}{C_{out}^{2nd} - \frac{\left(PCRF_2 - 1\right)}{PCRF_2} C_{da}} \qquad \text{Eq. 9}$$

This expression (eq. 9) allows for an estimation of the contribution of background on the measured particle concentration reduction factors (*PCRF*) from the known concentrations at the inlet of the GVPR (C_{in}^{1st}), the outlet of the GVPR (C_{out}^{2nd}) and the background (C_{da}). For these estimations, $PCRF_2$ was assumed to be 10.

The three sources of uncertainty ($s_{stab}, s_{rep}, s_{bckg}$) were considered random and independent, thus contributing to the total uncertainty through:

$$s = PCRF \cdot \sqrt{\left(\frac{s_{stab}}{PCRF}\right)^2 + \left(\frac{s_{rep}}{PCRF}\right)^2 + \left(\frac{s_{bckg}}{PCRF}\right)^2} \quad \text{Eq. 10}$$

4.2.3 Golden instrumentation results

Figure 38 summarizes the average particle concentration reduction factors at 30, 50 and 100 nm determined at the different participating laboratories with the GCPC using the reference calibration setup. Also shown in Figure 38 are the dilution factors for the laboratories that performed this type of measurements.

JRC calibrated the GVPR system thrice in the start, in the middle and at the end of the measurement campaign. The particle concentration reduction factors determined in these three repetitions were found to be 99.5(±3), 101.5(±2) and 102.5(±4), respectively. These results suggest that the performance of the golden instrumentation was stable throughout the campaign, despite the change of the ET and the primary dilution air heater, as well as the three maintenances of the GCPC (before the tests at LAT, AEAT and VW).

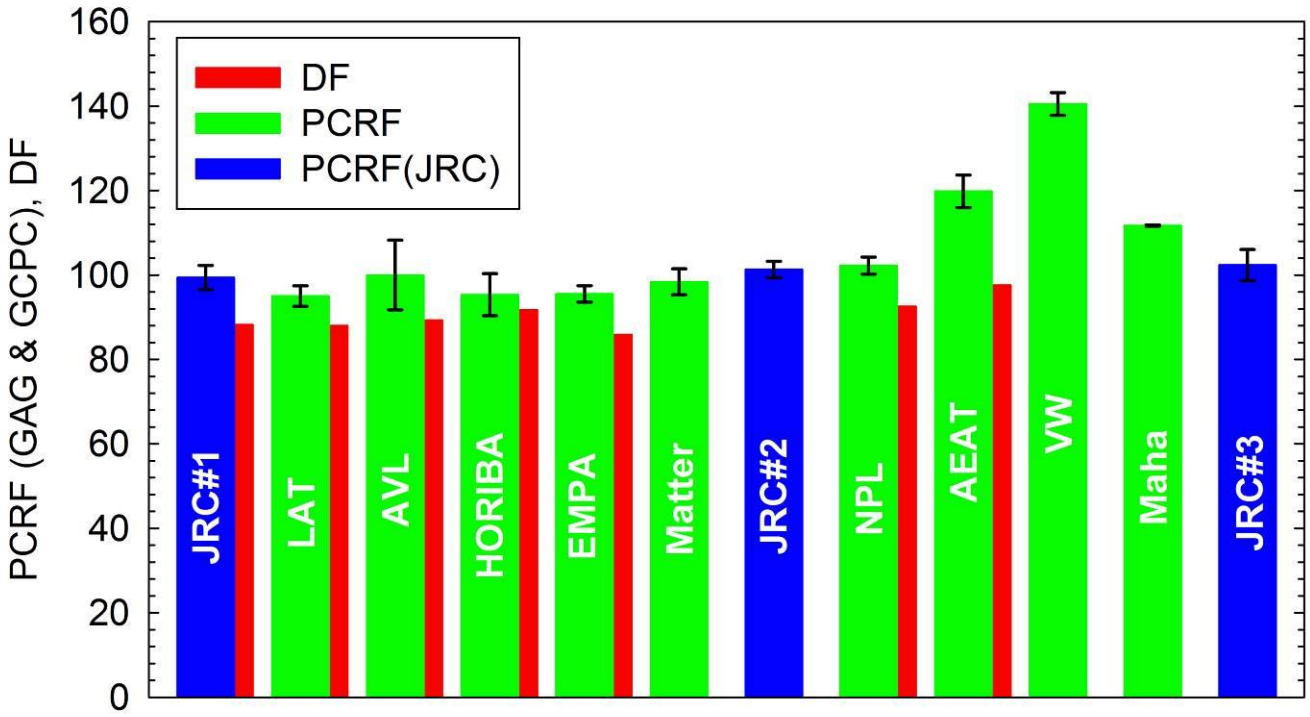

Figure 38: Average particle concentration reduction factors (*PCRF*) at 30, 50 and 100 nm graphite particles measured with the GCPC at the different laboratories (blue – green bars). The dilution factors are also shown with red bars for the laboratories that actually performed this type of measurements.

The measured particle concentration reduction factors (*PCRF*) in six (LAT. AVL, Horiba, EMPA, Matter Aerosol and NPL) out of the remaining nine labs agreed well with the results at JRC, with the individual differences lying within the experimental uncertainty. However, three laboratories measured systematically higher *PCRF* values. Namely, Maha determined a *PCRF* of 112(±0.2), AEAT measured a *PCRF* of 120(±4) while VW determined a *PCRF* of 140(±3). From these three laboratories only AEAT measured the dilution factor with gas analyzer. The measured dilution factor at AEAT was found to be 11% higher than that determined at JRC (Figure 36), in line with the ~19% higher *PCRF*. This could potentially indicate wrong settings of the GVPR, i.e. lower dilution air pressure and/or inaccurate control of the sample underpressure (Figure 28). Such inaccuracies in the control of the operating pressures of the GVPR could also potentially explain the 112 *PCRF* determined at Maha (~10% higher than that determined at JRC). However, the results determined at VW (140±3) were too high to be solely attributed to wrong settings of the GVPR. One additional source of error may lie to excessive throttling of the vented flows (i.e. by the use of long and/or narrow venting tubes). For

example, Giechaskiel et al. (2004) reported that 7 kPa built-up at the exit of the ejector may lead to a 20% increase of the dilution factor. After communication with VW it was verified that a long 8 mm diameter tubing diameter tubing was employed to vent the exhaust of the second dilutor (~44 lpm), which is expected to have introduced significant pressure drop (Figure 39). Accordingly, the results obtained at VW and AEAT were considered as outliers.

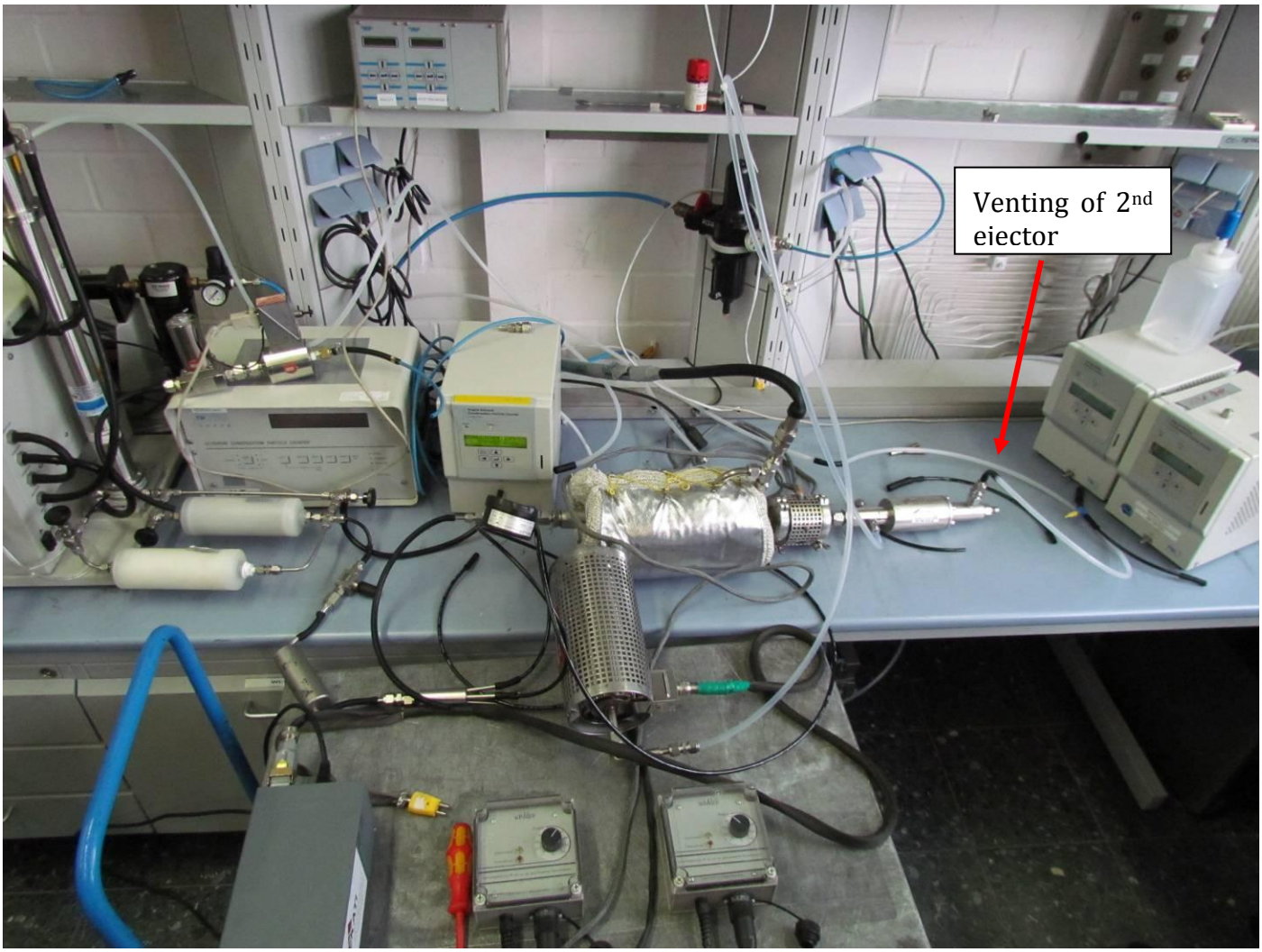

Figure 39: Experimental setup at VW illustrating the small diameter tubing employed to vent the exhaust of the second diluter.

Figure 40 summarizes the individual differences of the average particle concentration reduction factors determined at each laboratory from the grand-average determined from all laboratories except VW and AEAT. With the exception of these two laboratories (AEAT and VW), the results agreed within ±10% with the grand-average value of 100:1. A comparison with the grand-average dilution factor of 90.5:1 (Figure 36), suggests an average ~90% particle penetration.

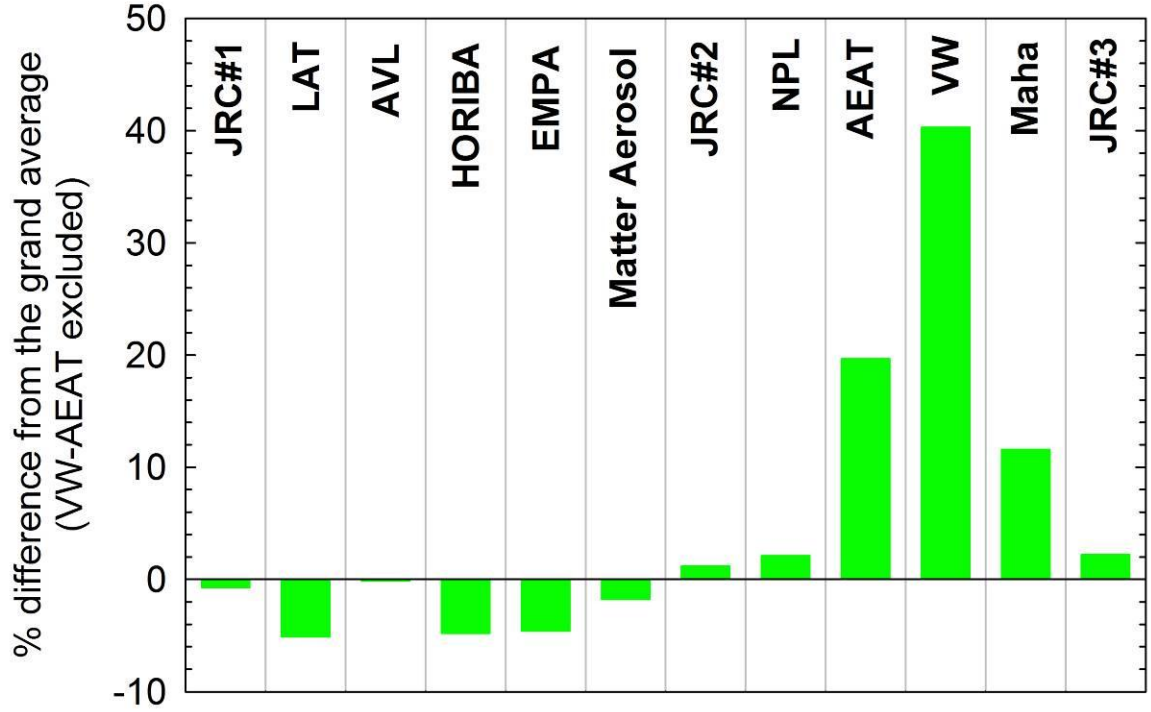

Figure 40: Percentage difference of the particle concentration reduction factors measured at each laboratory from the grand average determined from all laboratories except AEAT and VW.

Figure 41 compares the ratios of the particle concentration reduction factors at 30 nm (*PCRF*(30)) and 50 nm (*PCRF*(50)) to that at 100 nm (*PCRF*(100)). These ratios provide some information on the size specific particle losses in the GVPR, and are confined by the legislation to 95-130% for *PCRF*(30)/*PCRF*(100) and 95%-120% for *PCRF*(50)/*PCRF*(100). In the case of the GVPR, the particle losses were found to be largely independent of particle size with the two ratios lying around 100%.

Figure 42 illustrates the quantified experimental uncertainties in the measured particle concentration reduction factors at each lab. The experimental uncertainty was estimated to be less than 5% in the measurements at 50 and 100 nm but could grow up to 16% in the tests at 30 nm. The background contribution was estimated to be generally small, with the exception of the 30 nm tests conducted at JRC. This is due to the relatively low concentrations at the inlet of the GVPR (500-1000 #/cm^3), a limitation imposed from the Tandem-DMA setup employed. A limited number of tests were repeated, and the results generally agreed within 2% (again the exception being the tests at 30 nm conducted at JRC with low concentrations). The main source of uncertainty appears to be the stability of the concentrations (s_{stab}), which can exceed 15% especially if no "reference" CPC is employed to monitor the drifts of the concentration downstream of the VPR (AVL, Horiba, AEAT and VW). The more stable results were obtained at Maha where the calibration setup was at overpressure and part of the extracted sample from the DMA was vented. This approach was very effective in minimizing the contribution of pressure fluctuations (in both dilution air and sample) on the measured concentrations, which fluctuated by less than 1% over the test sequence.

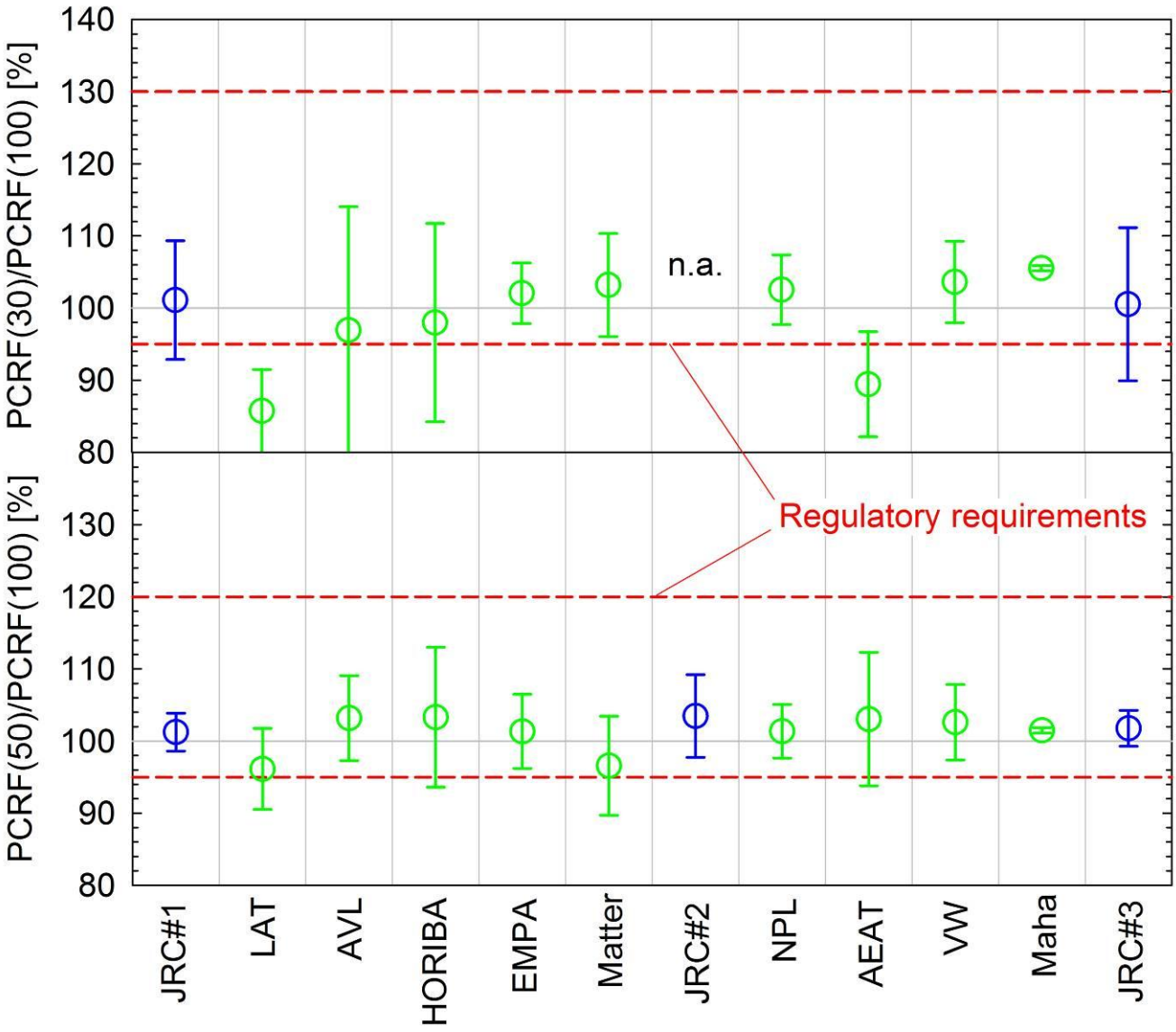

Figure 41: Ratios of the particle concentration reduction factors at 30 nm (*PCRF*(30) – upper panel) and 50 nm (*PCRF*(50) – lower panel) to that at 100 nm (*PCRF*(100)), as determined with the GCPC and the reference calibration setup at the difference laboratories.

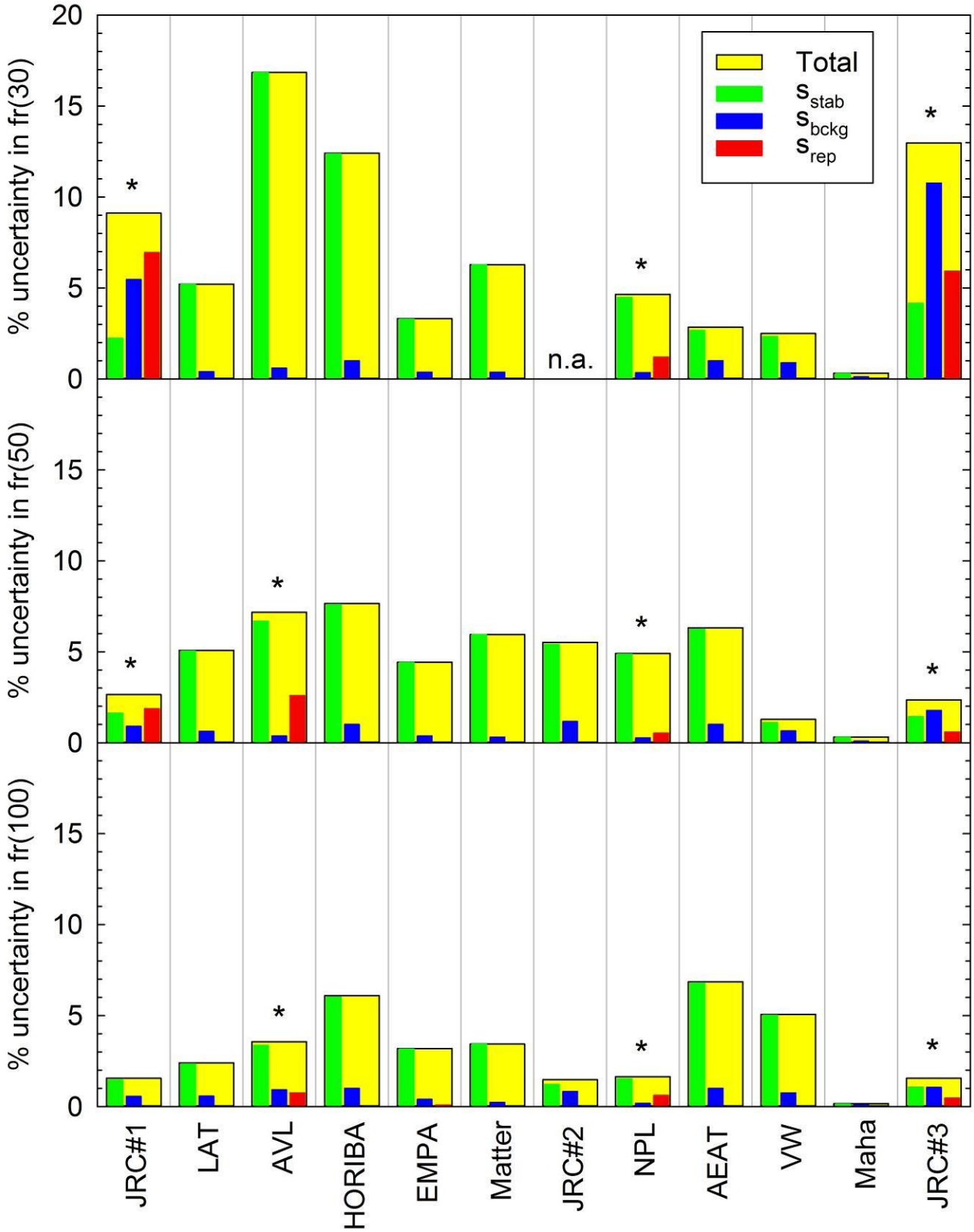

Figure 42: Experimental uncertainties (eq. 10 - yellow bars) in the measured particle concentration reduction factors at 30 nm (top panel), 50 nm (middle panel) and 100 nm (lower panel) with the GCPC using the reference calibration setup. The individual uncertainties related to s_{stab} (eq. 4c), s_{bckg} (eq. 9) and s_{rep} (eq. 4b - for labs that performed more than one repetitions and are designated with an asterisk on top of the bars) are shown with the green, blue and red bars.

4.2.4 Results with alternative CPCs

4.2.4.1 Alternative CPCs having a 50% cut-off size at 23 nm

Three of the participating laboratories employed an alternative CPC having the same nominal cut-off size with the GCPC (23 nm) in the tests with the reference calibration setup. The particle concentration reduction factors determined with the two CPCs are compared in Figure 43. The results were broadly similar. In the tests at JRC and EMPA no clear difference could be identified given the experimental uncertainty. It is worth noting that the alternative CPC employed at Maha (TSI 3790) yielded systematically 2.5% lower *PCRF* values at all sizes.

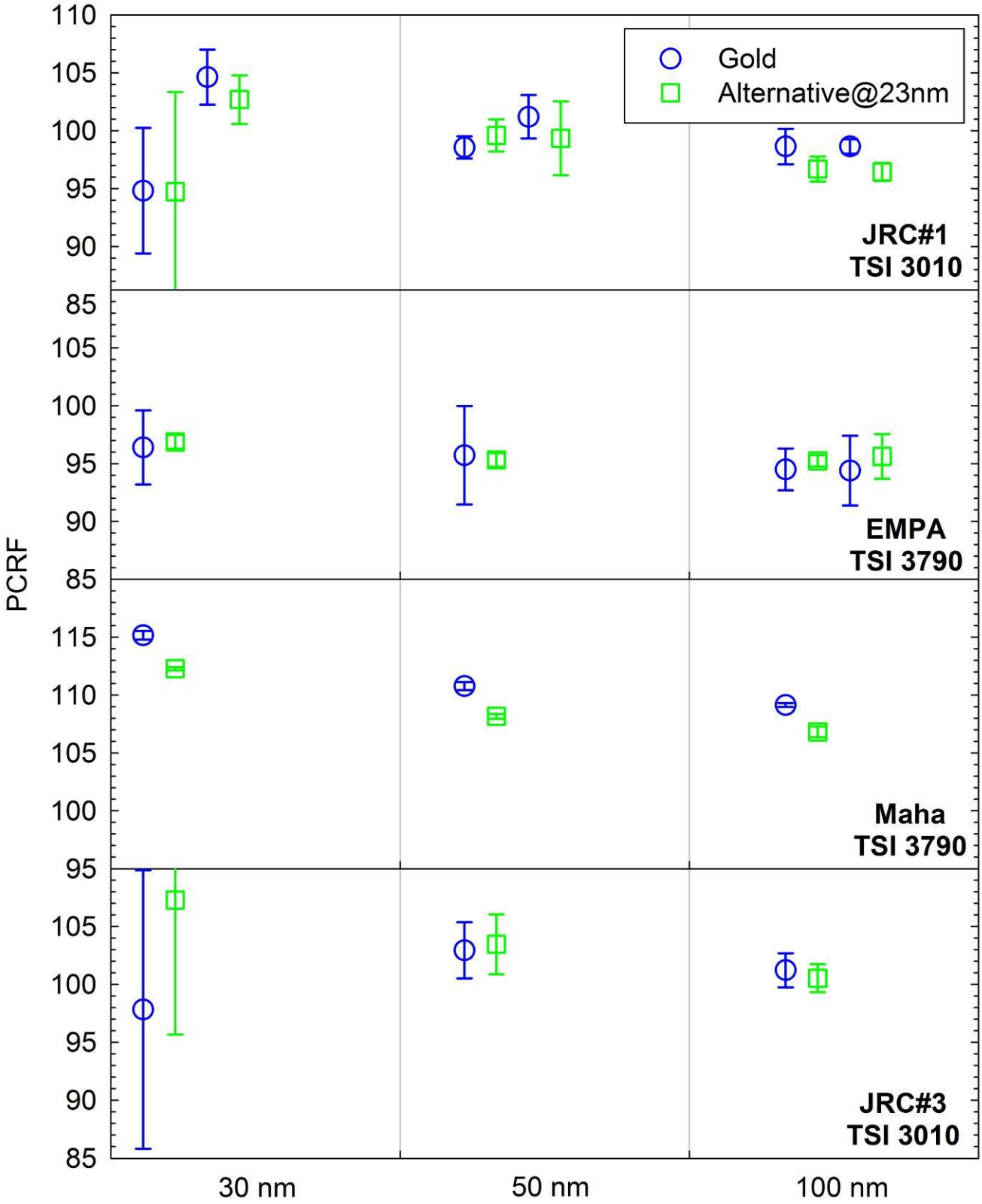

Figure 43: Comparison of the particle concentration reduction factors determined with the GCPC and an alternative CPC having the same nominal cut-off size (23 nm), using the reference calibration setup.

Interestingly, this difference agrees quantitatively with a slight non-linearity observed in some linearity cross-checks between the GCPC and the particular TSI 3790 CPC (Figure 44). No such trend could be identified in the cross checks of the other two alternative CPCs against the GCPC. The concentrations detected with the TSI 3010 CPC (operating at a temperature difference of 9°C) employed at JRC were very low (18-19% lower) but this deteriorated performance was known beforehand (e.g. Mamakos et al., 2011b). It needs to be stressed that the performance of the TSI 3790 CPC employed at Maha is well within the regulatory requirements of a ±10% accuracy.

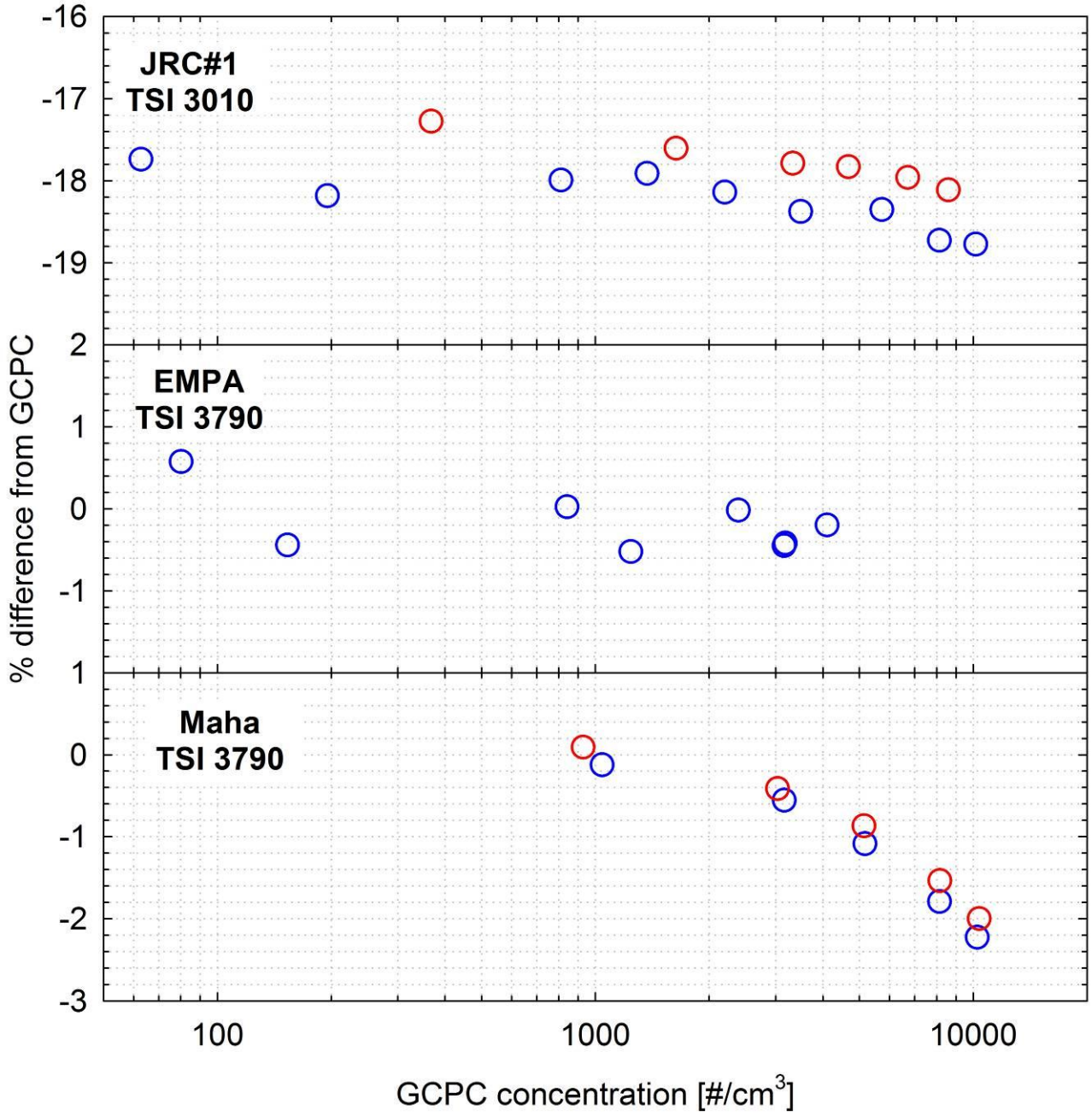

Figure 44: Linearity cross-checks between the GCPC and the alternative CPCs having a 50% cutoff size at 23 nm employed at JRC, EMPA and Maha. All these checks were conducted using 100 nm graphite particles produced by the GAG.

4.2.4.2 Alternative CPCs having a 50% cut-off size below 23 nm

Most of the laboratories employed an alternative CPC having a 50% cut-off size below 23 nm in the reference calibration setup. The Particle concentration reduction factors determined with these low cut-off size CPCs are compared to those measured with the GCPC in Figure 45. Similar results were obtained with the alternative CPCs, with the individual differences from the GCP generally lying within the experimental uncertainties.

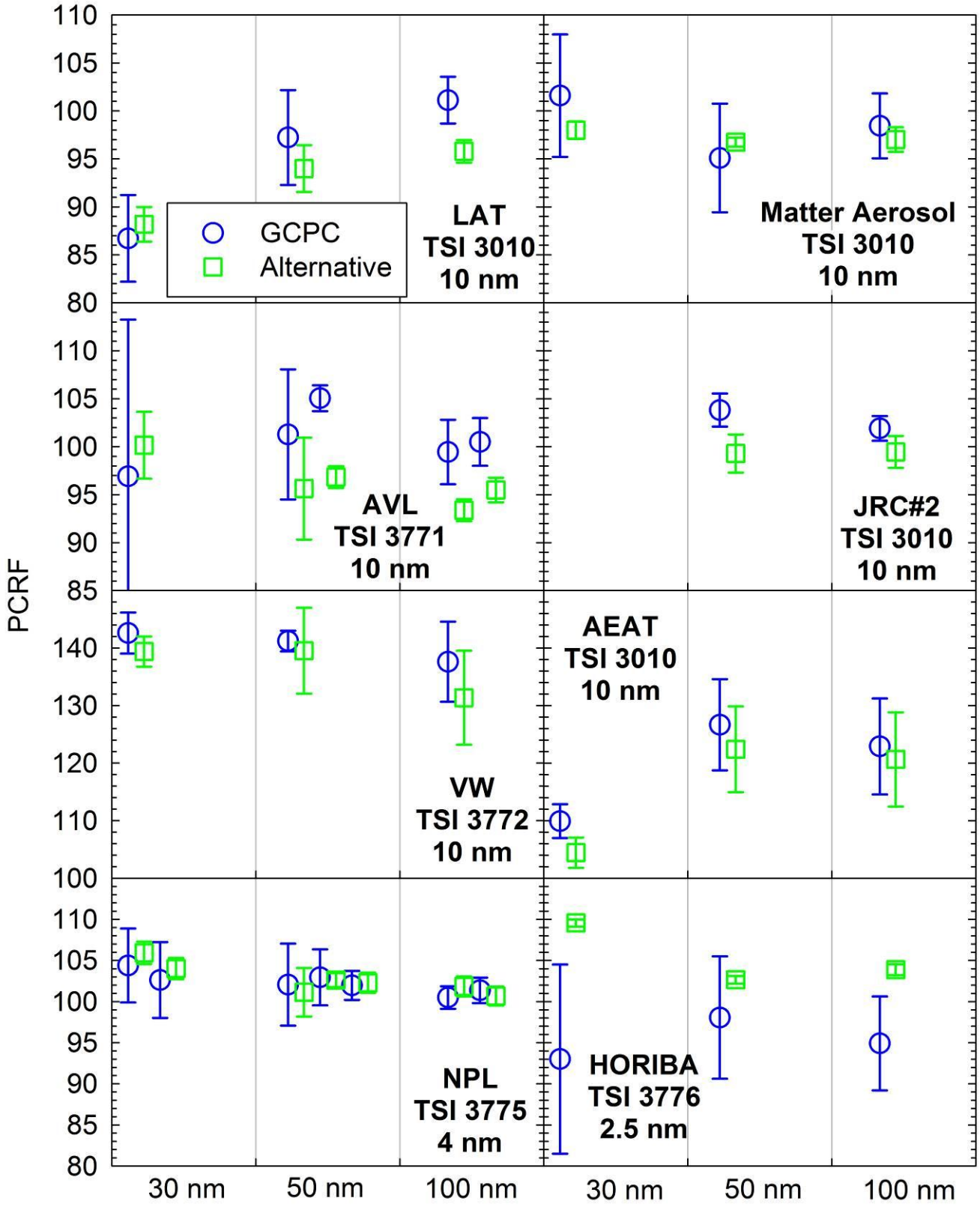

Figure 45: Comparison of the particle concentration reduction factors determined with the GCPC and an alternative CPC having a lower cut-off size, using the reference calibration setup.

Figure 46 summarizes the linearity cross-checks between the GCPC and the CPCs with a 50% cut-off size at 10 nm, for all laboratories that performed these type of experiments. Generally, the linearity performance of the alternative CPCs was equivalent to that of the GCPC and no trends could be identified in the individual differences. One notable exception was the TSI 3010 CPC employed at AEAT which exhibited a similar trend with the TSI 3790 CPC employed at Maha. The relative difference progressively increased from approximately -3% at 1000 #/cm^3 to -5% at 9000 #/cm^3. The results of the TSI 3010 were corrected for coincidence following the empirical formula suggested by

TSI. This is in line with the systematically lower average *PCRF* values determined with the TSI 3010 (2-5%), but this is rather a strong argument considering the large experimental uncertainty (7-8%).

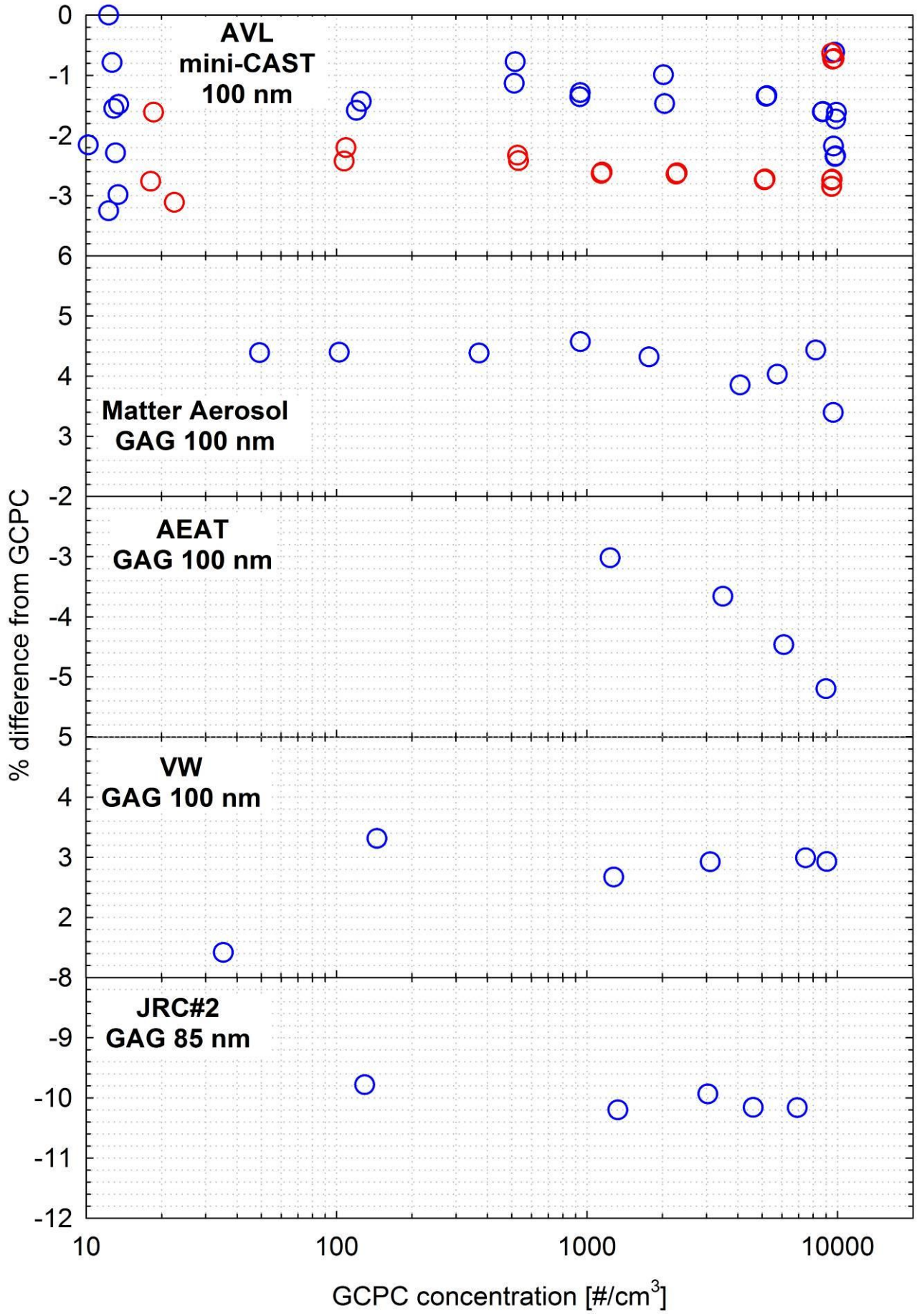

Figure 46: Linearity cross-checks between the GCPC and the low cut-off size CPCs employed at AVL (TSI 3771 – 10 nm). Matter Aerosol (TSI 3010 – 10 nm), AEAT (TSI 3010 – 10 nm), VW (TSI 3772 – 10 nm) and JRC (TSI 3010 – 10 nm).

NPL performed an absolute calibration of the GCPC and the TSI 3775 (d_{50} at 4 nm) against an electrometer using graphite particles at 30, 50 and 100 nm. The left panel of Figure 47 shows the linearity results for both CPCs with 100 nm graphite particles (left-panel). The right hand panel of Figure 47 compares the counting efficiency curves of the GCPC at 30, 50 and 100 nm graphite particles as determined at NPL to the counting efficiencies determined at JRC. No clear linearity issue could be identified for both CPCs. Interestingly, the results at NPL confirm the reduced efficiency of the GCPC to detect graphite particles, with the percentage difference from the electrometer indications ranging between -12% and -13% at 100 nm.

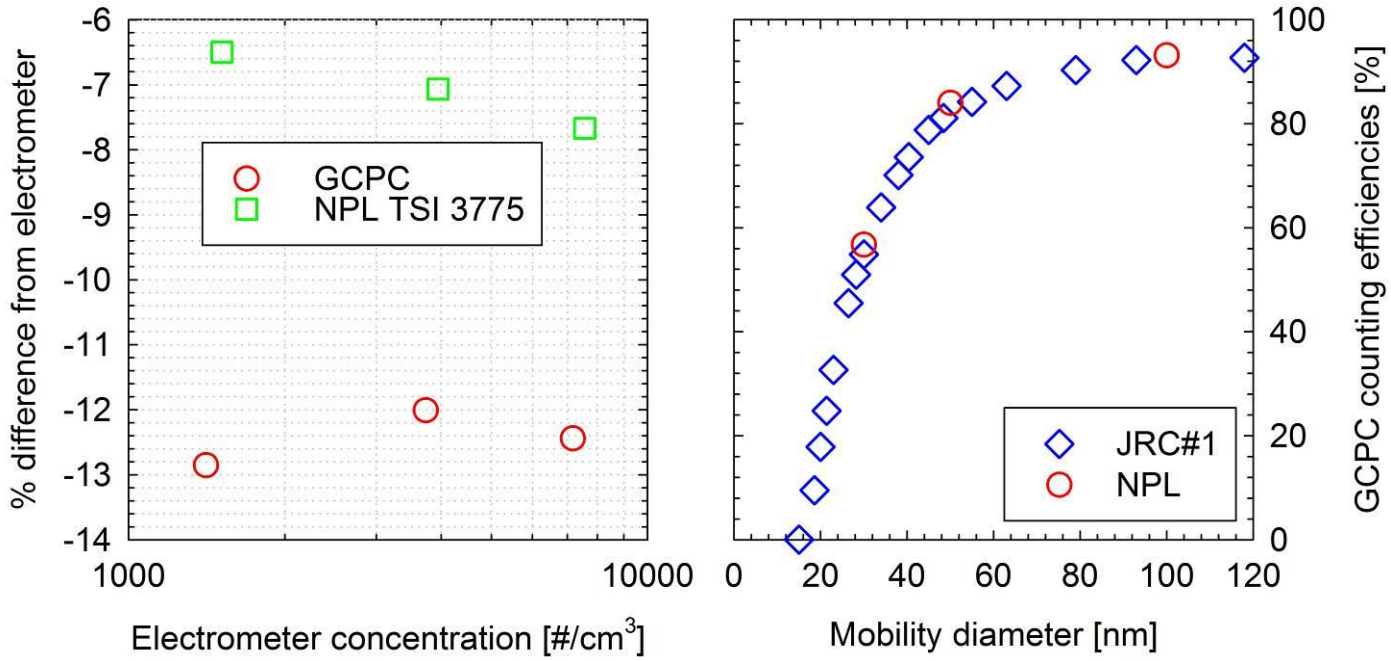

Figure 47: Left panel: Linearity checks of the GCPC and the TSI 3775 against a Grimm 5.705 electrometer for 100 nm graphite particles. Right-panel: Counting efficiencies of the GCPC determined at NPL and JRC (both corrected for the nominal slope of 0.95).

Figure 48 compares the ratios of the particle concentration reduction factors at 30 and 50 nm to those at 100 nm, determined at the different laboratories using the low cut-off size CPCs. The determined fractions had a lower uncertainty compared to the results obtained with the GCPC (Figure 41). In both cases (GCPC and low cut-off size CPCs) the agreement was better at the 50 over 100 nm ratios with the standard deviation of the mean values determined at each lab lying at 2.5%. The corresponding figure for the 30 over 100 nm ratios was ~7%. This indicates that the measurements at 30 nm are more challenging and subject to larger uncertainties.

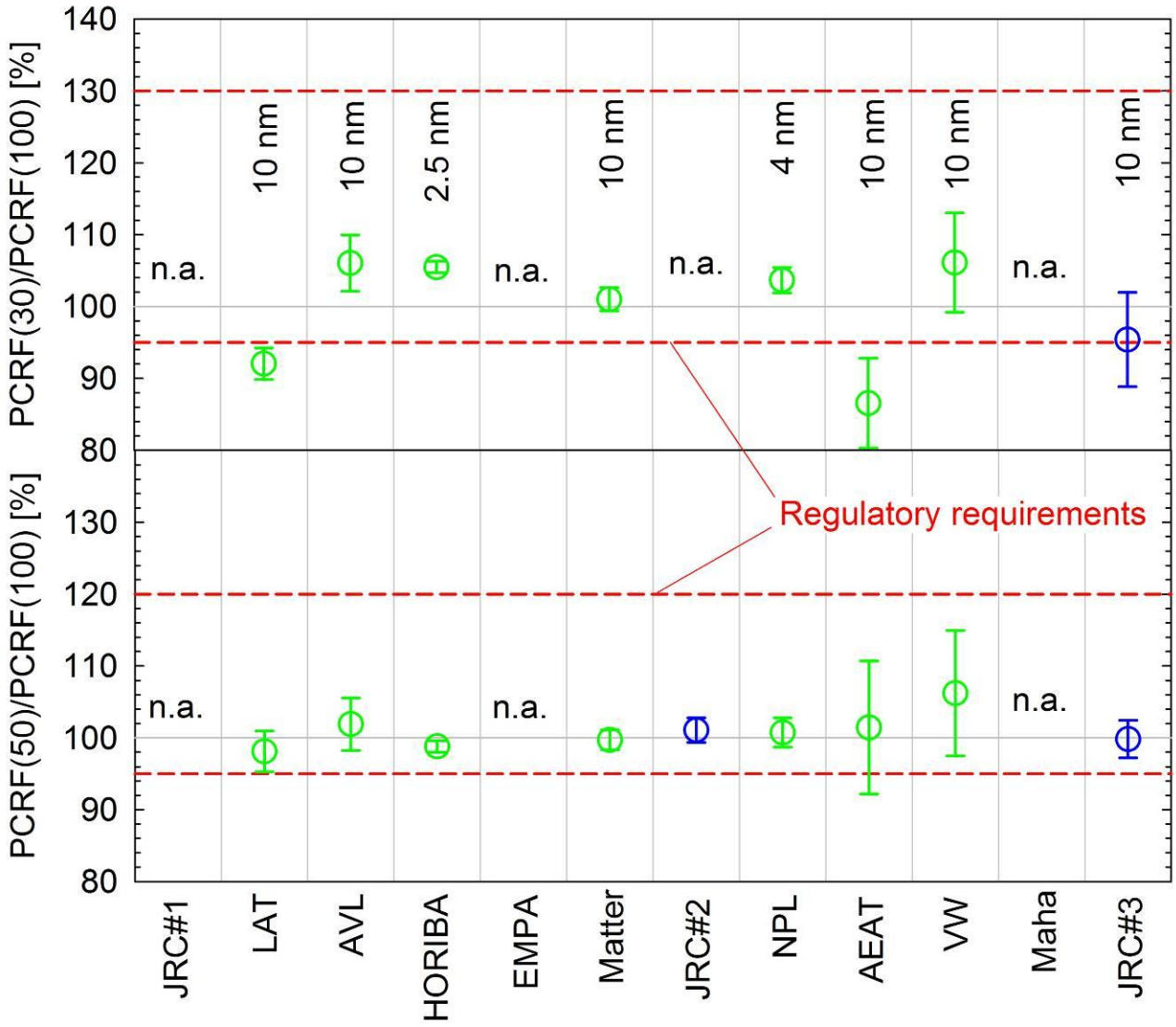

Figure 48: Ratios of the particle concentration reduction factors at 30 nm (*PCRF*(30) – upper panel) and 50 nm (*PCRF*(50) – lower panel) to that at 100 nm (*PCRF*(100)), as determined with the low cut-off size (displayed on the top panel) CPCs and the reference calibration setup at the difference laboratories.

4.2.5 Results with alternative generators

4.2.5.1 CAST

Five laboratories calibrated the GVPR using aerosol produced by CAST. Four of them (AVL, Horiba, Matter and AEAT) measured the particle concentration reduction factors with the GCPC and a low cut-off size CPC (Figure 49) while VW employed two modified TSI 3790 CPCs (Figure 50) in the calibrations with CAST.

The particle concentration reduction factors determined with the two generators at 50 and 100 nm using the GCPC (left-hand panels of Figure 49) generally agreed within ±4%. However, at 30 nm the particle concentration reduction factors determined with CAST particles were systematically higher at all three labs that performed these measurements (AEAT, Matter Aerosol and Horiba), exceeding those determined with graphite particle by 23 to 33%. This behaviour was not evident when a low cut-off size CPC was employed (right-hand panels of Figure 49 and Figure 49). In this case, the differences for the two particle types were similar at all sizes and ranged between ±10%. This apparent overestimation of the particle concentration reduction factor with 30 nm CAST particles when the GCPC was employed, is an indication that these particles were not thermally stable. A potential shrinkage (i.e. due to evaporation of any volatile content) of the 30 nm particles would have a strong effect on the indications of the GCPC as this size range lies at the steep part of the counting efficiency curve of the instrument (e.g. Figure 47). For example, based on the experimental

data collected on graphite, a shrinkage to 27 nm would result in approximately 20% lower concentrations downstream of the GVPR and consequently a 20% overestimation of the particle concentration reduction factors. While the CAST particles were thermally pre-treated in all labs, the dilution employed (internal in most cases) might not be sufficient to reduce the vapour pressures of volatile material at levels that would prohibit re-condensation.

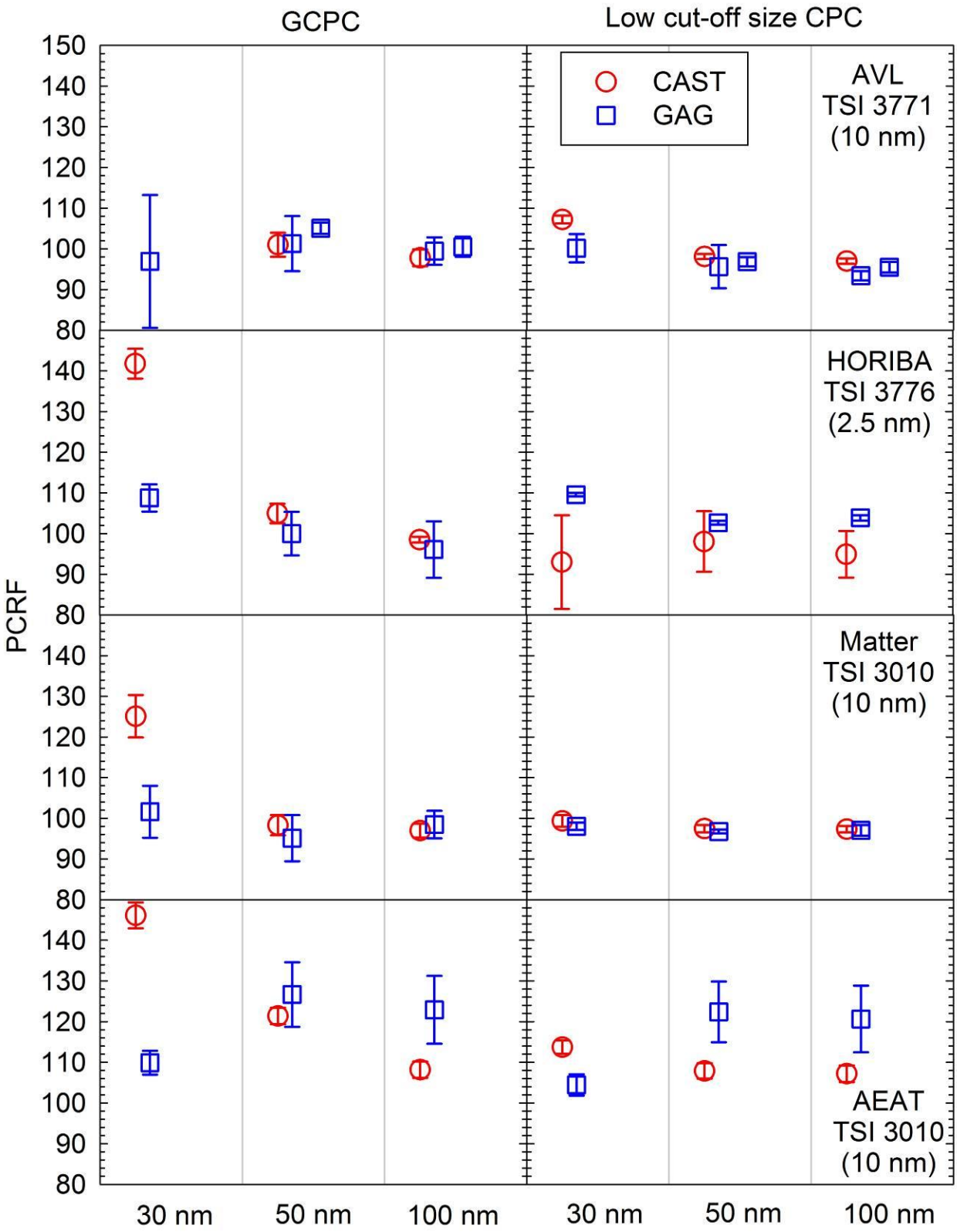

Figure 49: Comparison of the particle concentration reduction factors determined with aerosol produced by the GAG (blue dots) to those determined with CAST particles (red dots) using the GCPC (left-hand panel) and a low cut-off size CPC. The AVL results on CAST particles, were obtained using the alternative setup (Figure 13) which is also employed for the calibration of their instrumentation.

In the calibration of the GVPR with mini-CAST, VW employed two TSI 3790 CPCs that were modified to operate at elevated temperature differences of 17°C. The particle concentration reduction factors determined in these tests were found to be systematically higher by 5% (50 nm) to 10% (100 nm) compared to those determined with the GCPC and the TSI 3772 using graphite particles. This difference should potentially indicate some linearity problems, as it was observed that modification of the operating temperatures of the TSI 3790 may affect their linearity (see section 4.2.6.5 and Giechaskiel & Bergmann, 2011). VW has observed such deterioration of the performance of the two units but no information was provided on their linearity performance.

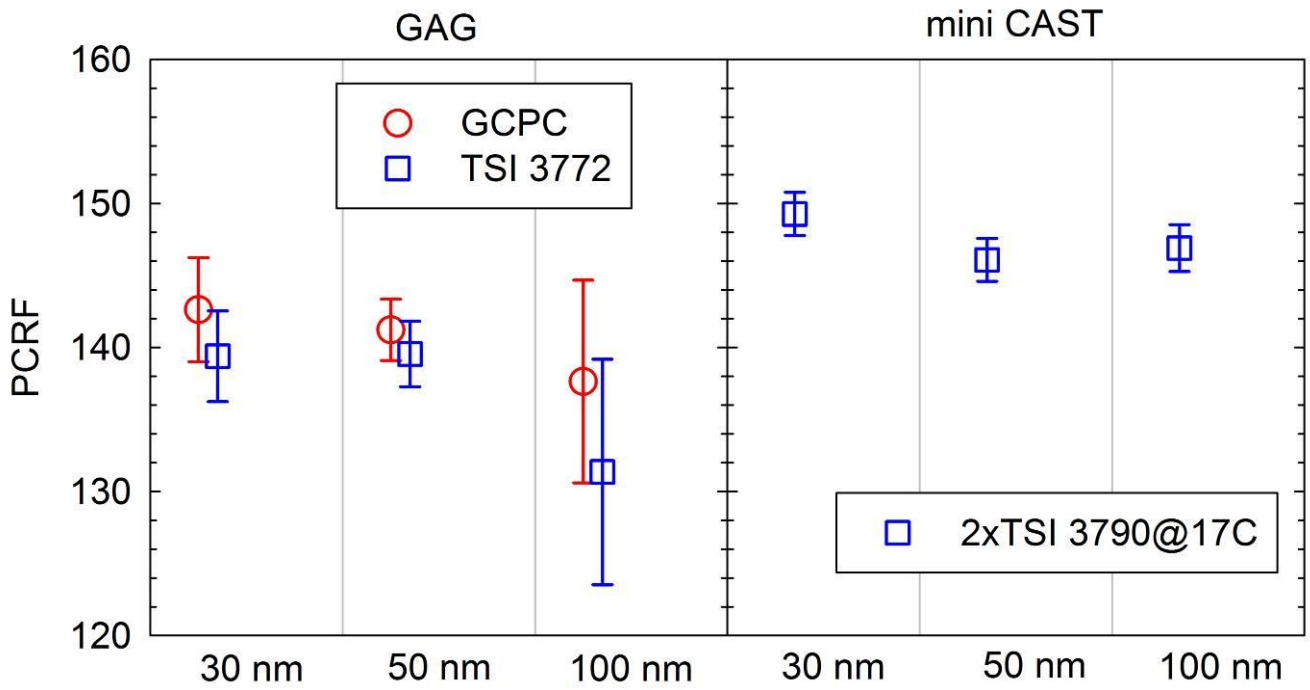

Figure 50: Particle concentration reduction factors determined at VW using graphite particles produced by the GAG (left-hand panel) and a mini-CAST.

4.2.5.2 Engine Exhaust

LAT performed some particle concentration reduction factor measurements using diesel exhaust, thermally pre-treated in a thermodenuder. Unfortunately, such measurements were not possible at 30 nm owing to the low number concentrations. The results at 50 and 100 nm are compared to those determined with graphite particles in Figure 51. No statistically significant difference could be observed in the results obtained with the GCPC for the two types of particles, with the individual differences (0% at 50 nm and 4% at 100 nm) lying within the experimental uncertainty (±5%). The TSI 3010 CPC gave systematically lower *PCRF* values compared to the GCPC, especially for engine exhaust aerosol, where the particle concentration reduction factors were found to be similar to the measured dilution factors (87-90). These small values may reflect small non-linearity problems, but there is no experimental information available to confirm this.

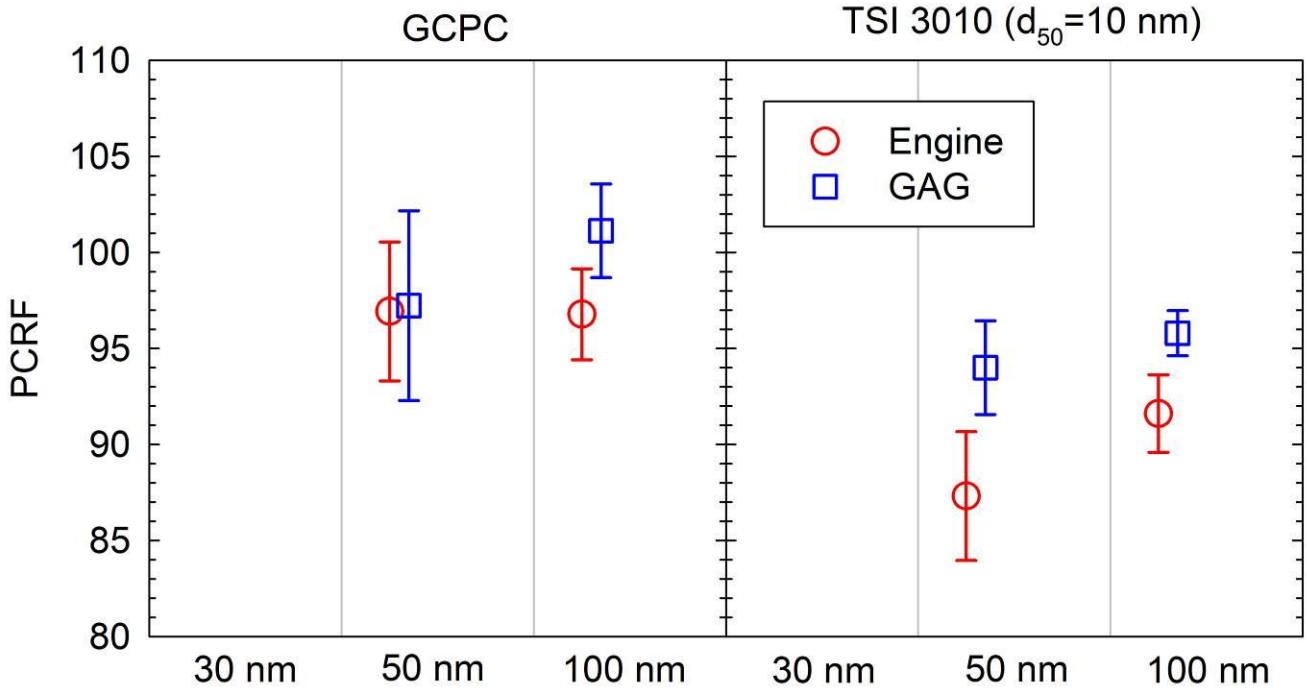

Figure 51: Comparison of the particle concentration reduction factors determined with aerosol produced by the GAG (blue dots) to those determined with diesel exhaust particles (red dots), using the GCPC (left-hand panel) and a low cut-off size CPC.

4.2.5.3 Sodium Chloride

Two laboratories (EMPA and Horiba) employed also sodium chloride particles for the calibration of the GVPR. Figure 52 compares the results obtained with the two generators and two CPCs (GCPC and TSI 3776 with a d_{50} at 2.5 nm) at Horiba. At 50 and 100 nm the results obtained with the two particle generators generally agreed within less than ±5%. This was also the case at 30 nm when the low cut-off size CPC was employed. However, the GCPC yielded a *PCRF*(30) of only 28 for 30 nm sodium chloride particles. This very low particle concentration reduction factor implies that some particle growth took place downstream of the GVPR. Considering that sodium chloride particles are highly hygroscopic, such growth could actually originate from the humidity in the dilution air. This apparent increase in particle size could be also associated with some particle restructuring and is in line with the increase in the counting efficiency detected by Sakurai et al. (2011) by preheating the particles at increasing temperatures. The results with and without neutralizer agreed within ±5%, and no systematic trend could be identified. It needs to be emphasized though that the losses in the GVPR were largely size-independent and therefore the results were not expected to be that much affected on the fraction of multiple-charged particles.

EMPA employed two TSI 3022 CPCs having a 50% counting efficiency at 7 nm in the calibration of the GVPR with sodium chloride particles. The measured particle concentration reduction factors (Figure 53) where broadly similar (differences smaller than ±3%) to those determined with graphite particles even at 30 nm.

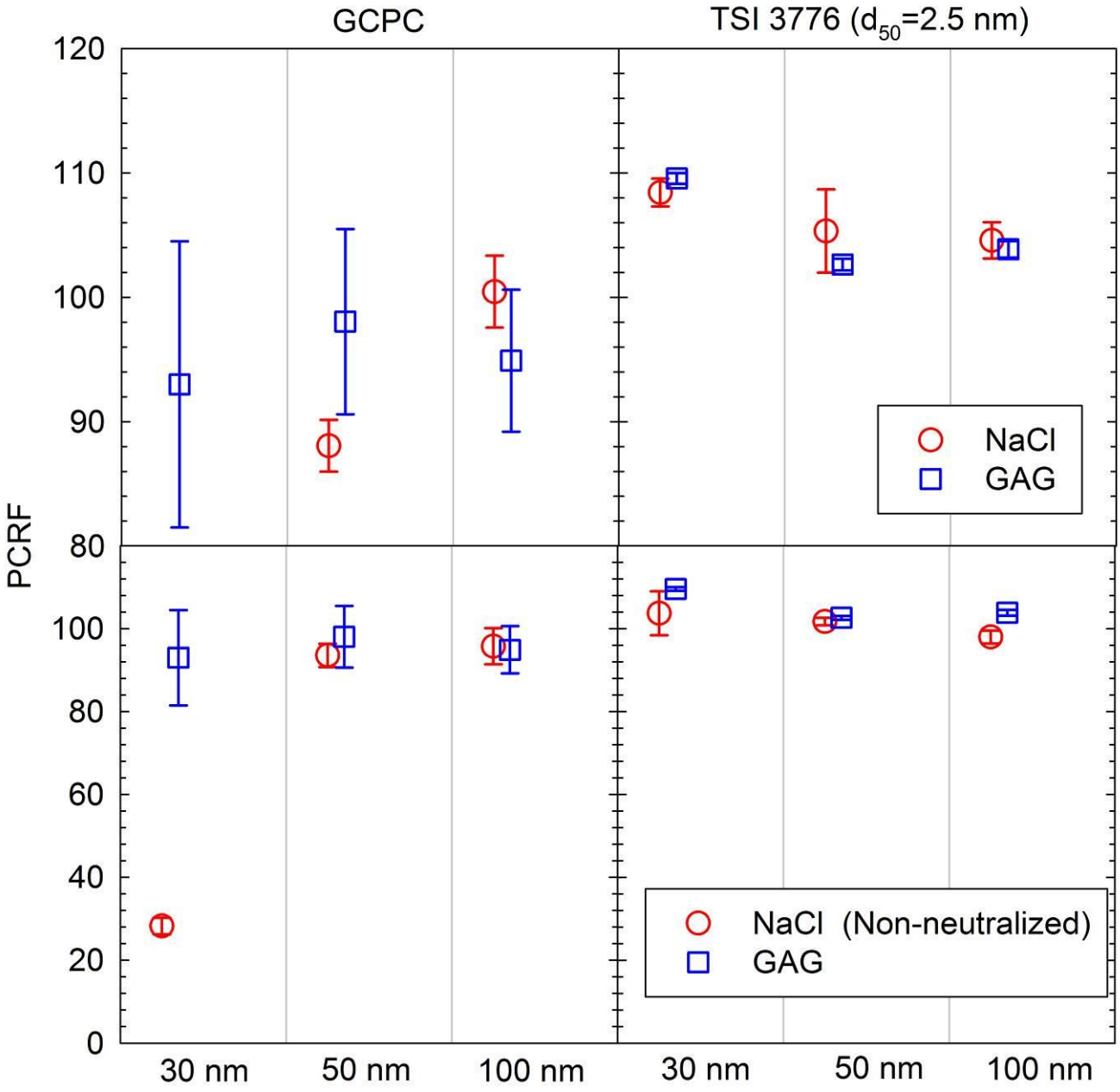

Figure 52: Comparison of the particle concentration reduction factors determined at Horiba with aerosol produced by the GAG (blue dots) to those determined with sodium chloride particles (red dots), using the GCPC (left-hand panel) and a TSI 3776 CPC having a 50% cut-off size at 2.5 nm. Tests were performed with (upper-panel) and without (lower panel) neutralizing the generated aerosol prior to entering the DMA.

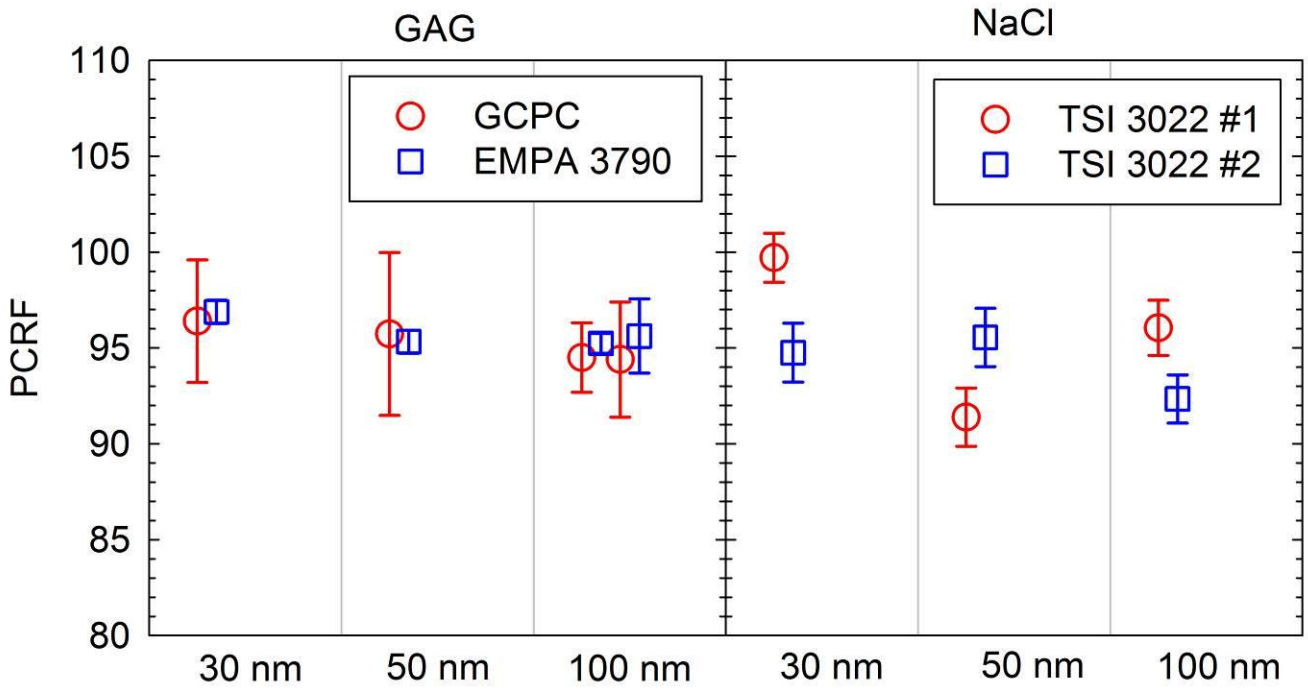

Figure 53: Comparison of the particle concentration reduction factors determined at EMPA with graphite particles produced by the GAG (left-hand panel) to those determined with sodium chloride particles (right-hand panel).

4.2.5.4 Palladium particles

EMPA employed also an in-house glow-plug generator producing palladium particles, to calibrate the GVPR. The particle concentration reduction factors dtermiend with palladium particles were broadly similar to those produced with graphite particles with the individual differences being smaller than 1% at 50 and 100 nm and less than 2-4% at 30 nm.

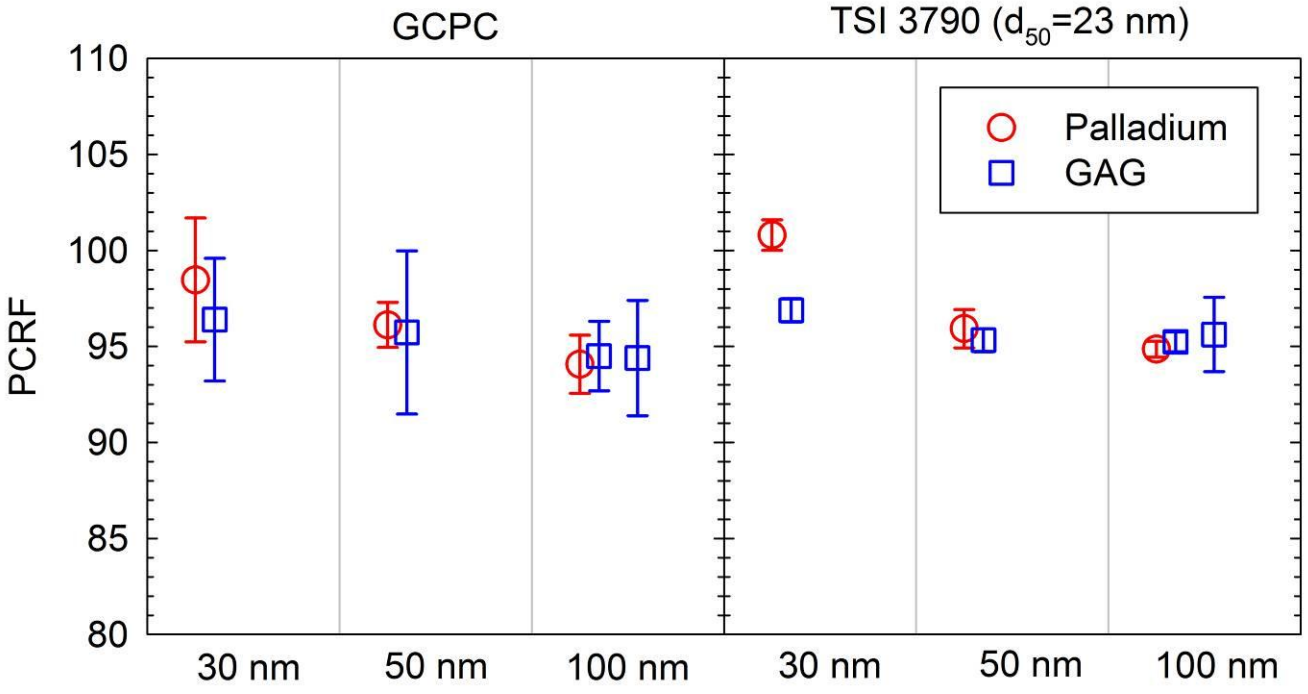

Figure 54: Comparison of the particle concentration reduction factors determined at EMPA with aerosol produced by the GAG (blue dots) to those determined with palladium particles (red dots), using the GCPC (left-hand panel) and an alternative TSI 3790 CPC (d_{50} at 23 nm).

4.2.5.5 Alternative graphite spark generators

Maha performed some calibration measurements with the older graphite spark generator model commercialized by Palas as DNP 2000. Tests were performed with and without thermal pretreatment of the generated polydisperse aerosol. The results obtained with the two generators were broadly similar and differed by less than 4% at all sizes.

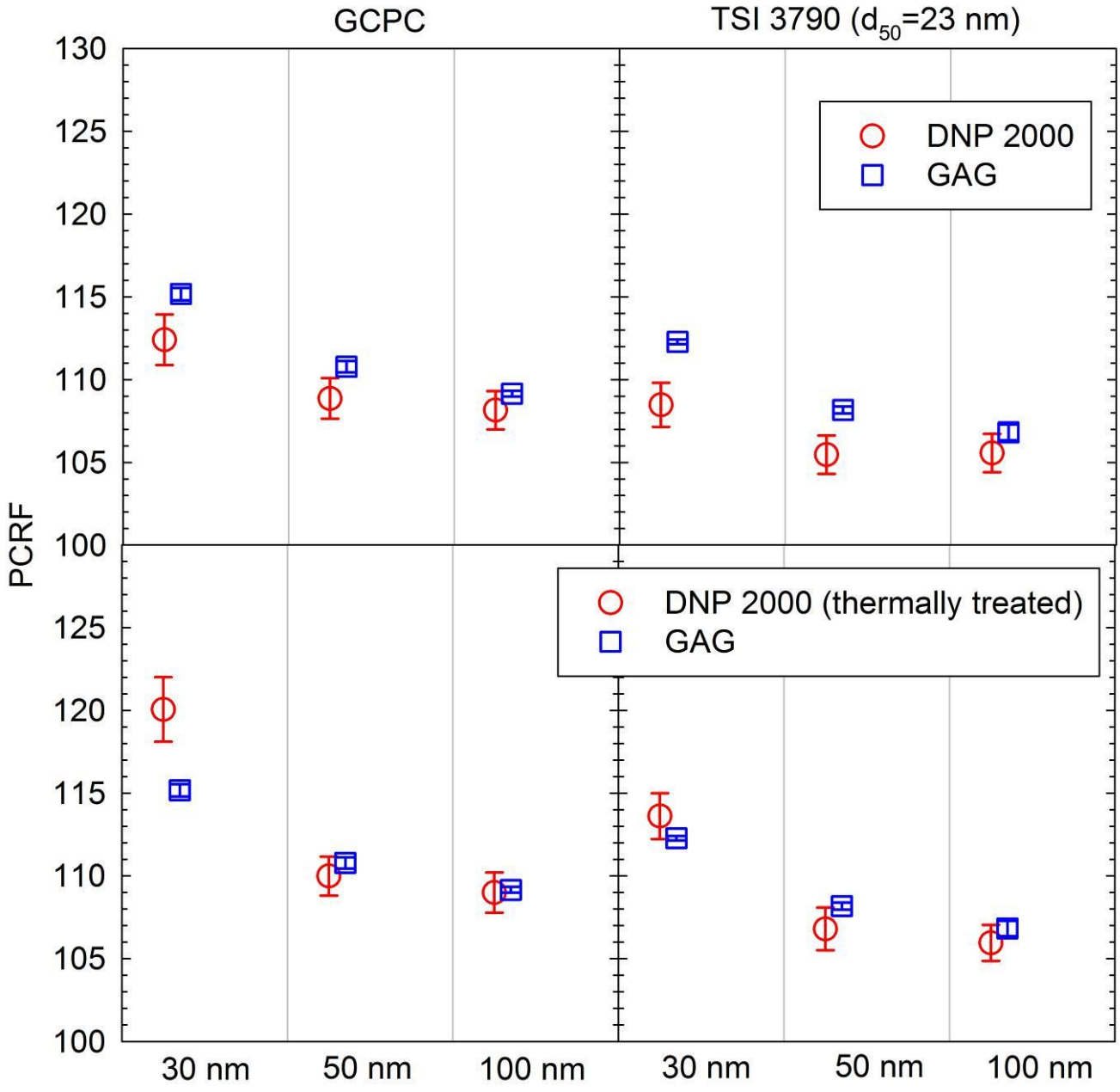

Figure 55: Top panel: Comparison of the particle concentration reduction factors determined at Maha with graphite particles produced by the GAG (blue dots) and a Palas DNP2000 generator (red dots), using the GCPC (left-hand panel) and an alternative TSI 3790 CPC (d_{50} at 23 nm). Bottom panel: As in top panel with the exception that the aerosol produced by the DNP 2000 was thermally pre-treated.

4.2.6 Additional investigations

4.2.6.1 Particle Concentration Reduction Factors at 15 nm

Matter Aerosol performed some particle concentration reduction factor measurements using 15 nm graphite particles produced by the GAG (set point 1 – 3 lpm N_2, 6 lpm air and 0.75 mA). For these tests, two TSI 3010 CPCs (d_{50} at 10 nm) were employed, as the detection efficiency of the GCPC at 15 nm was zero. The particle concentration reduction factor at 15 nm, determined with the two low cut-off size CPCs, averaged at 98.5(±1.5). This value is hardly indistinguishable from the particle concentration reduction factors at 30 (98±1), 50 (97±0.5) and 100 nm (97±0.7).

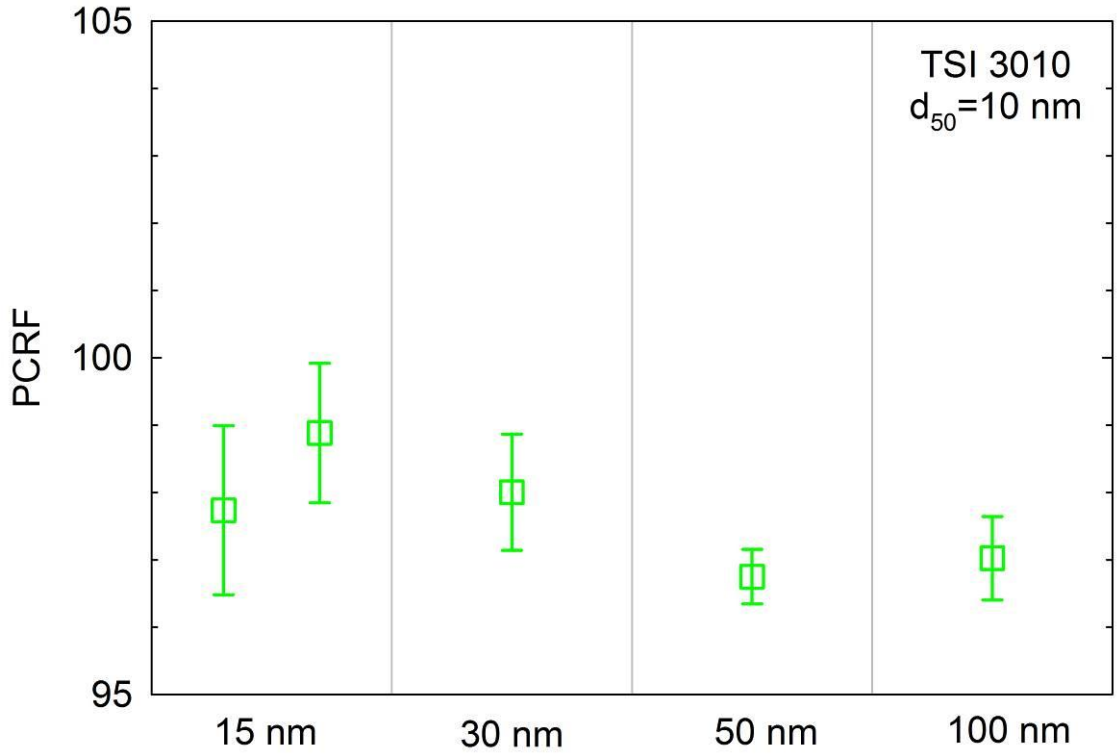

Figure 56: Particle concentration reduction factors for 15, 30, 50 and 100 nm graphite particles produced by the GAG, as determined at Matter Aerosol. The results at 15 nm were obtained with two TSI 3010 CPCs alternatively sampling upstream and downstream of the GVPR, while the results at 30, 50 and 100 nm with the GCPC.

Matter Aerosol also measured the size distribution of the extracted sample from the DMA at 15 nm, which is shown in Figure 57. The measured size distributions indicated a large fraction of multiply charged particles, with clearly identifiable peaks even at 37 nm that corresponds to quintuply-charged particles. These figures are unrealistically high, considering for example, that the nominal probability of doubly charged particles at 22.5 nm is only 0.02% while the probability that a 37 nm particle carries 5 charges is expected to be less than 2×10^{-17} (Wiedensohler A., 1988). These figures would result in unrealistically high number concentrations upstream of the DMA (up to 10^{21} #/cm^3/dlogd_p). It is therefore possible that the measured *PCRF* at 15 nm were underestimated due to the high contribution of larger multiply charged particles.

Similarly excessive high fractions of multiply-charged particles were observed in all configurations examined at Matter Aerosol (including the measurements with the CAST generator). For example, Figure 58 shows the size distributions of 100 nm CAST particles classified in the DMA of Matter Aerosol. These results are indicative of a non-properly functioning neutralizer, i.e. due to reduced radioactivity, that can not effectively neutralize highly charged particles produced by the spark and the CAST generators. Matter Aerosol confirmed that the neutralizer was more than ten years old, and its radioactivity felt below the level recommended by the manufacturer (<1 mCi).

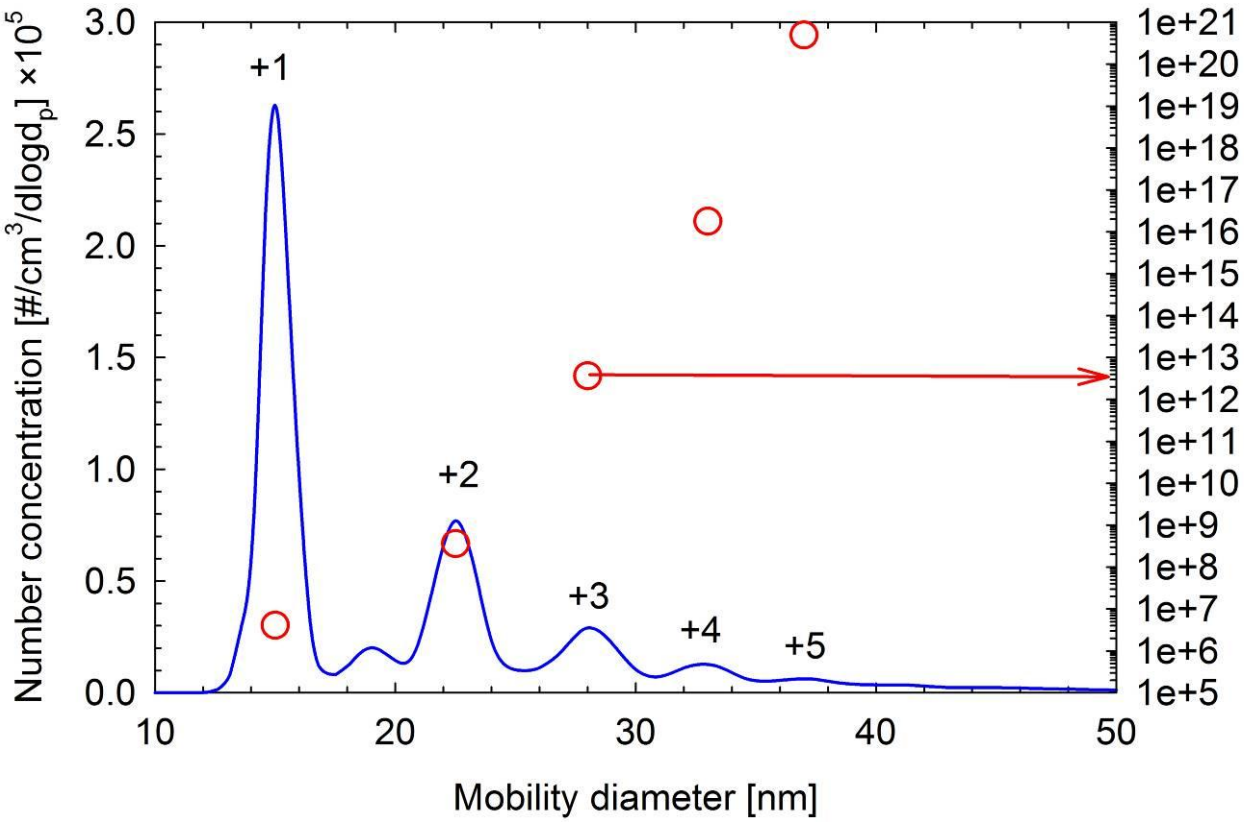

Figure 57: Particle size distribution of the extracted DMA samples at 15 nm, corrected for the multiple charged fractions, but not for diffusion losses. Also shown with red dots are the calculated concentrations upstream of the DMA based on the bipolar charging probabilities employed by TSI (Wiedensohler A., 1988).

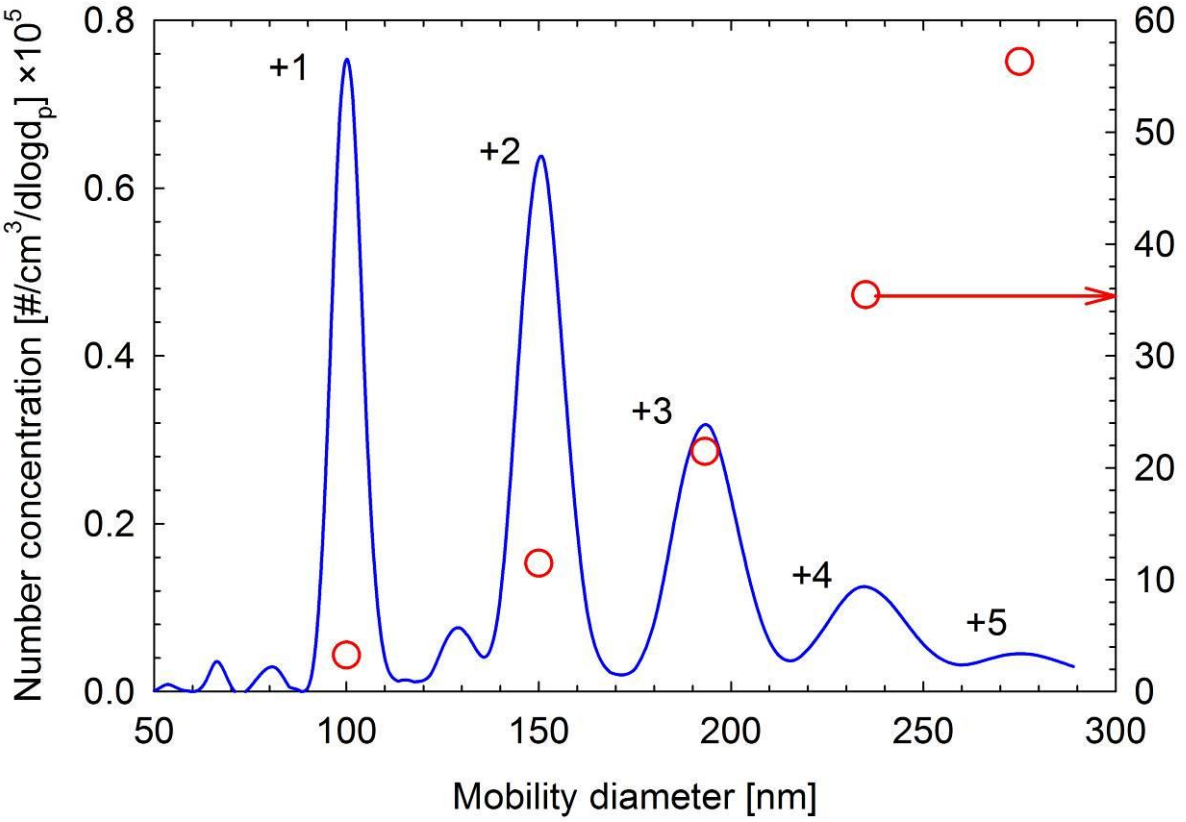

Figure 58: Particle size distributions (blue lines) of 100 nm CAST particles classified at Matter Aerosol. Also shown with red dots are the calculated concentrations upstream of the DMA based on the bipolar charging probabilities employed by TSI (Wiedensohler A., 1988).

4.2.6.2 Tandem-DMA versus DMA

The advantage of using a tandem-DMA setup to size classify calibration particles, is that it effectively reduces the fraction of larger multiple-charged larger particles. However, the GVPR is not suitable for this type of investigation due to the small (if any) dependence of the particle losses on size. This is verified by the dedicated experiments conducted at EMPA where both approaches (DMA and TDMA) were investigated (Figure 59). No difference could be identified, with the differences in the particle concentration reduction factors determined with the two methods lying within the experimental uncertainty (±3%).

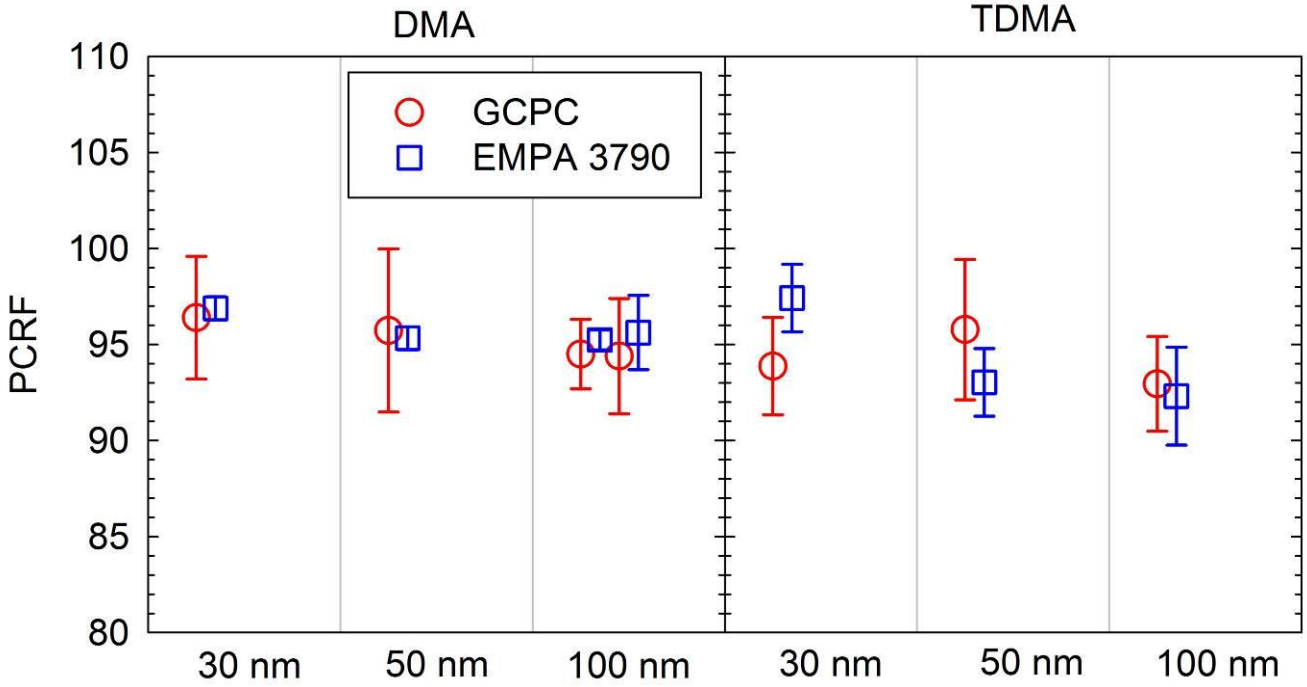

Figure 59: Particle concentration reduction factors determined at EMPA for graphite particles produced by the GAG, using a single DMA (left-hand panel) or two DMAs in series (right-hand panel).

4.2.6.3 Thermal stability of graphite particles

The thermal stability of the graphite particles generated by the GAG was verified in size distribution measurements of DMA-classified particles, upstream and downstream of the GVPR, conducted at EMPA and Maha (Figure 60). The size spectra downstream of the GVPR, corrected for the particle concentration reduction factors determined at the two laboratories, were found to be in very good agreement with the size distributions upstream of the GVPR. There was no indication of particle shrinkage downstream of the GVPR. It is worth mentioning that in line to the results obtained at JRC (Figure 33), the multiple-charge correction algorithm did not remove entirely the doubly-charged fractions below the selected size, especially at 100 nm.

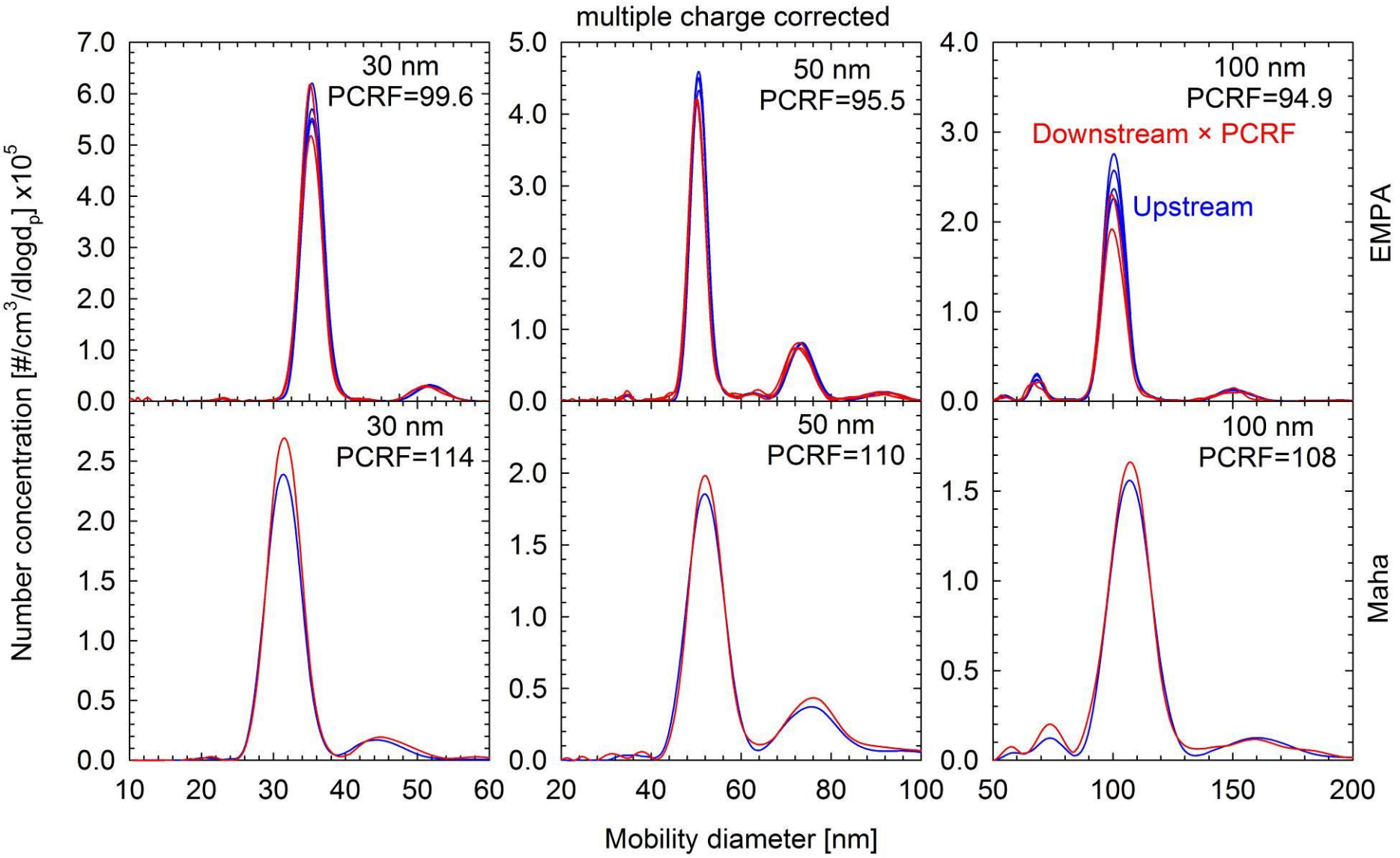

Figure 60: Particle size distributions of DMA-classified 30, 50 and 100 nm graphite particles upstream (blue lines) and downstream (red lines) of the GVPR as measured at EMPA (upper panels) and Maha (lower panels). The distributions downstream of the GVPR were corrected for the measured particle concentration reduction factors at each size.

4.2.6.4 Polydisperse measurements with SMPS

Several laboratories investigated the possibility of employing polydisperse aerosol for the calibration of the GVPR. The size distributions measured downstream of the GVPR were found to be systematically shifted towards smaller sizes. However, to a large extent this apparent shift was associated with particle growth through coagulation owing to the different sample flowrates of the GVPR (~4 lpm) and the SMPS (as low as 0.3 lpm). A characteristic case is illustrated in Figure 61 comparing polydisperse distributions of GAG and CAST aerosols upstream and downstream of the GVPR as measured at AVL. The SMPS employed in these tests, operated at sample flowrate of 0.3 lpm. When a shorter tube was employed to connect the SMPS to the GAG, the upstream distributions were shifted towards smaller sizes and the number concentrations were higher.

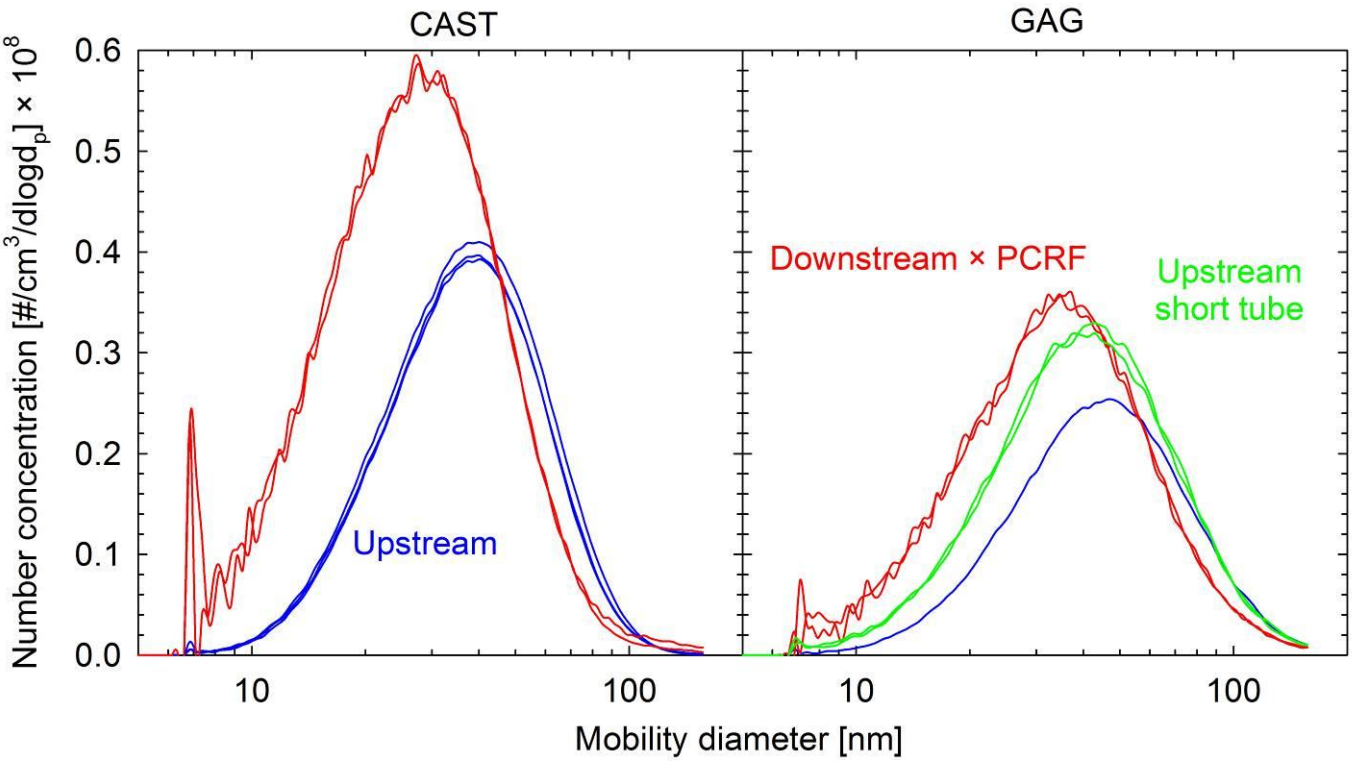

Figure 61: Measured size distributions of polydisperse CAST (left-hand panel) and GAG (right-hand panel) aerosol measured upstream (blue – green curves) and downstream (red curves) of the GVPR.

4.2.6.5 Linearity of the TSI 3790 CPC at elevated operating temperatures

Maha performed some linearity checks of the GCPC against one of their TSI 3790 units, that was employed as a "reference" (monitoring always the concentration downstream of the GVPR), with the latter operating at its nominal saturator-condenser temperature difference (~6.5°C) but also at an elevated temperature difference of 17°C. This modification should shift the lowest detectable particle size at smallest sizes and would therefore be suitable for calibration experiments with thermally unstable aerosols. However, the cross-checks conducted at Maha indicated that this change of the operating temperatures can severely affect the linearity of the instrument. While the two CPCs agreed within 4.9±0.1% at their nominal temperatures, the difference increased from ~10% at 900 #/cm^3 to ~15% at 5000 #/cm3 and 21% at 10000 #/cm^3 for the modified TSI 3790 CPC. According to the manufacturer, this behaviour is associated with the dead time (coincidence) correction of the instrument. This correction depends on the shape of the pulses (and effectively the size of the grown droplets) which changes at elevated temperatures, requiring recalibration of the units (TSI, 2010).

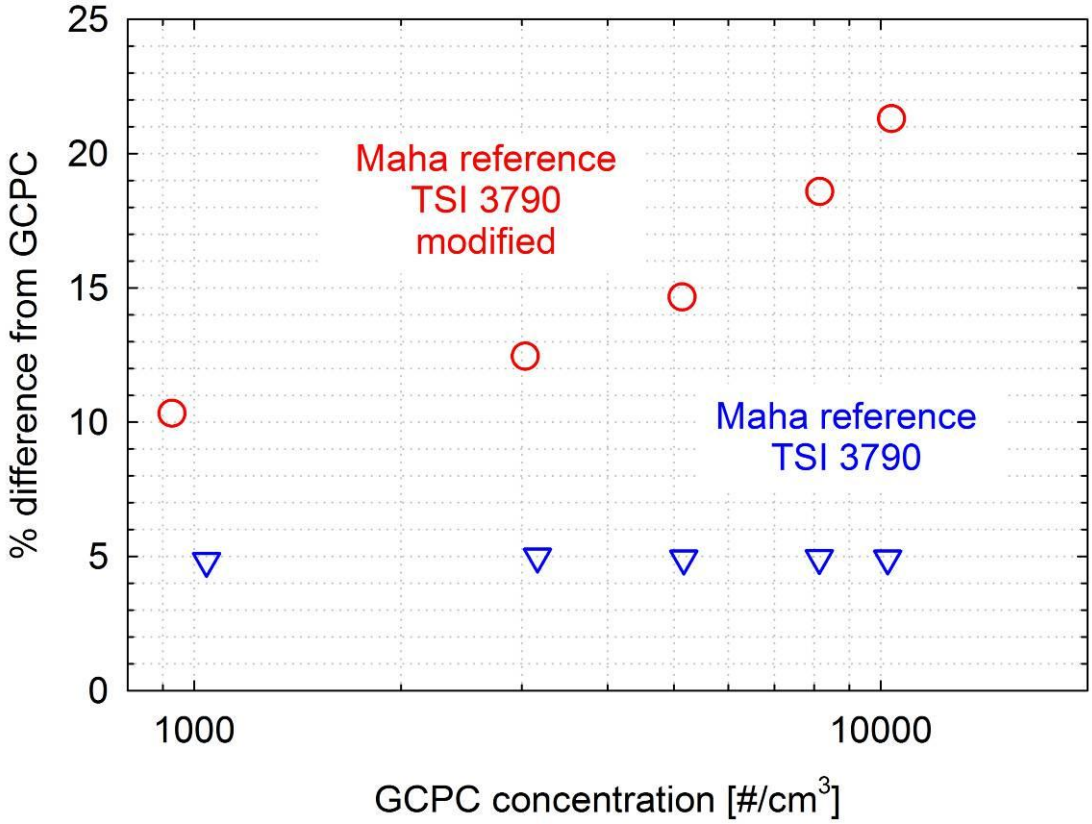

Figure 62: Linearity cross-checks between the GCPC and a TSI 3790 CPC operating at the nominal condenser-saturator temperature difference (blue symbols) and at an elevated temperature difference of 17°C (red dots), using 100 nm graphite particles.

Similar linearity issues at modified operating temperatures of the TSI 3790 were identified by VW, AVL and Horiba[2]. Interestingly though, these linearity issues were not evident in all CPC units. For example, Figure 63 compares the concentrations measured with the two TSI 3790 CPCs employed at VW against those measured with the GCPC at the nominal and at elevated operating temperature differences (between the condenser and the saturator) of the two 3790 CPCs. The increase of the operating temperature differences only affected the linearity of one of the two CPCs. This was the CPC employed to measure the upstream concentrations of the GVPR in the calibration experiments with CAST particles, and the results of these cross-checks were employed to correct the indicated concentrations.

[2] Horiba actually employed TSI 100 CPCs which are identical to the TSI 3790 models but do not include a display.

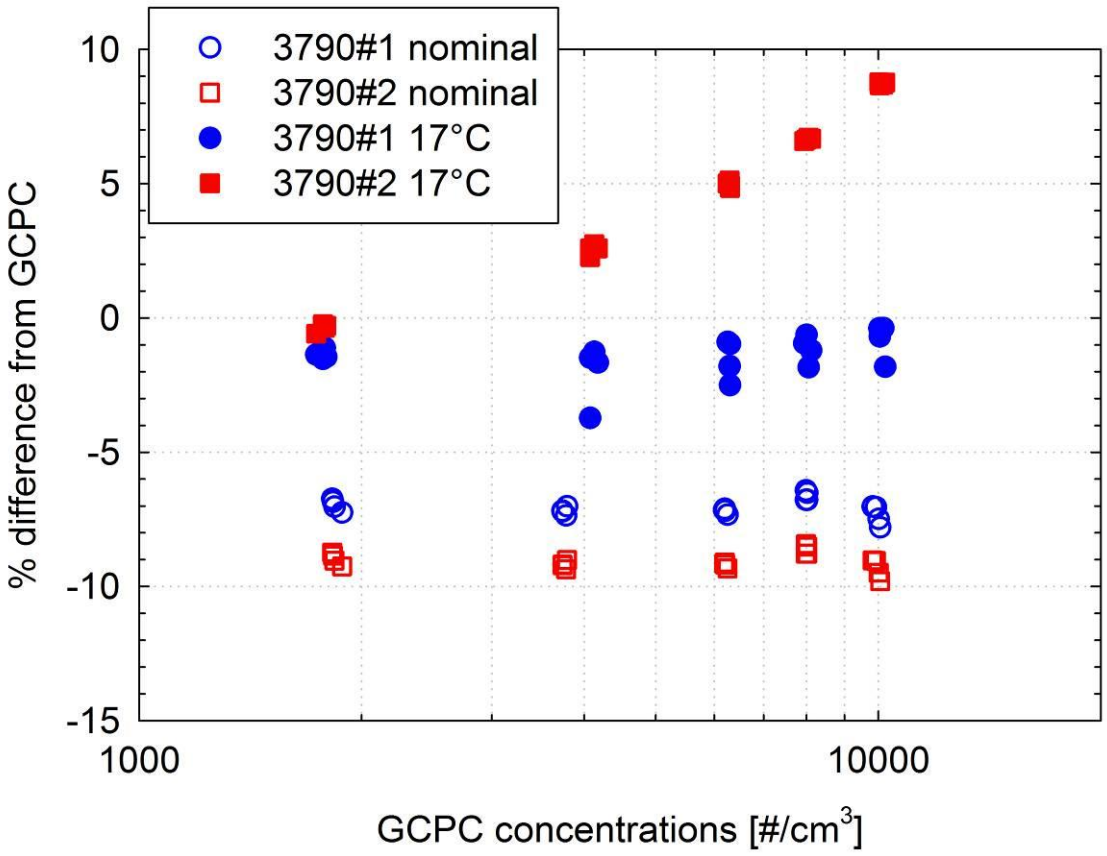

Figure 63: Linearity cross-checks between the GCPC and the two TSI 3790 CPC employed at VW operating at the nominal condenser-saturator temperature differences (empty symbols) and at an elevated temperature difference of 17°C (filled symbols) using 55 nm CAST soot particles.

5 CONCLUSIONS

A dual ejector system with an intermediate Evaporating Tube was circulated at 11 laboratories to measure the Particle Concentration Reduction Factors (*PCRF*) at 30, 50 and 100 nm (as required by the legislation). In addition to this "Golden" Volatile Particle Remover (GVPR), a PALAS DNP 3000 graphite spark generator (Golden Aerosol Generator - GAG) and a TSI 3790 Condensation Particle Counter (Golden CPC – GCPC), were also circulated to compare the performance of the different aerosol generators and CPCs employed at each laboratory.

The dilution factor of the GVPR was found to be very sensitive in the operating inlet, outlet and dilution air pressures. The effect of inlet and dilution air pressure was quantified at some preliminary calibration experiments at JRC and the participating laboratories were accordingly instructed to carefully adjust these pressures. The average PCRF at 30, 50 and 100 nm values determined at eight of the eleven in total laboratories using the golden instrumentation agreed within ±5%, but three laboratories measured systematically higher values (10%, 20% and 40%, respectively). This overestimation was most probably related to a backpressure build-up at the exit of the second ejector, as verified in the lab with the highest overestimation. This pressure built-up results in a direct increase of the dilution factor of the second ejector as explained in Giechaskiel et al. (2004).

The graphite particles produced from the GAG were found to be thermally stable as verified by size distribution measurement of DMA-classified particles, upstream and downstream of the GVPR, at least at the 300°C wall temperature of the Evaporating Tube. For this thermally stable aerosol, the GCPC having a cut-off size of 23 nm yielded similar PCRF results with low cut-off size CPCs. Sodium chloride and CAST particles were not thermally stable however, despite the pre-conditioning employed at the different laboratories. Accordingly, the use of the high cut-off size GCPC resulted in an underestimation (based on comparison with results obtained with graphite aerosols and with CAST particles using the low cut-off size CPCs) of the PCRF for 30 nm NaCl particles (by up to 70%) and an overestimation of the PCRF for 30 nm CAST particles (by up to 33%). The underestimation of the PCRF at 30 nm NaCl particles suggests that the particles grew in size downstream of the GVPR, either due to restructuring inside the evaporating tube (Sakurai et al., 2011) or due to hygroscopic growth (Biskos et al., 2006).

On the other hand, the overestimation of the PCRF with 30 nm CAST particles suggests some particle shrinkage. All labs that employed CAST aerosol, have treated it thermally at 300°C (Matter Aerosol), 350°C (AVL, Horiba, VW) or 400°C (AEAT). Accordingly it is not expected that some restructuring took place inside the evaporating tube of the GVPR. Most probably, this shrinkage is associated with the presence of some volatile material onto the particle. For the volatiles to be removed in the pre-conditioning of the sample, the thermal treatment is not sufficient. It is also necessary to sufficiently dilute the sample in order to reduce the vapour pressures of the produced volatile species at levels that would prohibit recondensation or even adsorption onto the soot particles. The necessary dilution will depend on the volatile fraction of the generated soot which also depends on the operating parameters of the CAST generator. At the same time, in calibration experiments the amount of dilution is restricted by the requirement of 10000 #/cm^3 monodisperse particles upstream of the VPR under calibration. All in all, none of the conditioning approaches employed in the campaign, which included dilution up to 10:1 before the thermal pre-treatment, were proven sufficient to remove entirely the volatile material.

Despite these thermal stability issues, when a low cut-off size CPC was employed (having a 50% counting efficiency at 10 nm or below), both the CAST and sodium chloride particles gave equivalent results with graphite. This indicates that any size or morphology modification that took place occurred at sizes where particle detection in the low cut-off size CPCs has reached the 100% efficiency. It is therefore advisable that a low cut-off size CPC is employed when CAST or NaCl particles are employed in *PCRF* calibrations.

The study also provided evidence that a temperature adjustment of CPCs having a nominal 50% counting efficiency at 23 nm to reduce the cut-off size may affect the linearity of the CPCs. Therefore such modifications must be accompanied by a thorough check of the linearity performance. On the other hand, no significant linearity issues were observed in cross-checks of 15 in total CPCs

operating at their nominal temperatures against the GCPC. The worst performing instruments exhibited a 2.5% drift in the 1000 to 10000 #/cm^3 concentration range. Interestingly, all linearity issues (including those of modified CPCs) were evident at high concentrations, and therefore could be checked even against traceable electrometers.

Some laboratories performed polydisperse characterization of the GVPR using Scanning Mobility Particle Sizers (SMPS). The characterization of the size distributions however, was found to be a rather challenging task as the high concentrations of the produced calibration aerosol can lead to significant coagulation. In these particular calibration investigations, the different sample flowrates of the GVPR (~4 lpm) and the SMPS (down to 0.3 lpm) can lead to significantly different residence times of the polydisperse aerosol on the sampling lines that can shift the size distributions by as high as 20 nm for a 2 s difference in the residence times, with an accompanied 3-fold change in the number concentration. Therefore an accurate calibration of the GVPR with polydisperse aerosol requires that all precautions are made to ensure that the residence time of the polydisperse aerosol before dilution at levels that would freeze coagulation will be the same when sampling upstream and downstream of the VPR system.

The small dependence of the particles losses on mobility size for the GVPR did not allow for definite conclusion regarding the effect of particle charge state. One laboratory however, measured the distribution spectra of particles classified in a DMA equipped with an old, inefficient neutralizer and determined very large fractions of multiply charged particles for both graphite and CAST. This is an indication that the generated particles can be highly charged and if not neutralized, the size classified particles may contain a large fraction of larger particles. The study also provided evidence that aggregate graphite particles (especially for larger sizes) acquire more charges compared to spherical droplets of the same mobility, in good agreement with published data in the literature. Therefore, if multiply charge correction is necessary, it should take into account this different charging behaviour of aggregate particles.

6 Nomenclature

CO	Carbon Monoxide
CO_2	Carbon Dioxide
CAST	Combustion Aerosol STandard
CPC	Condensation Particle Counter
CVS	Constant Volume Sampler
DF	Dilution Factor
DMA	Differential Mobility Analyzer
DPF	Diesel Particulate Filter
ET	Evaporating Tube
GAG	Golden Aerosol Generator
GCPC	Golden Condensation Particle Counter
GVPR	Golden Volatile Particle Remover
HC	HydroCarbons
HD	Heavy Duty
HEPA	High Efficiency Particulate Air filter
JRC	Joint Research Centre
LCU	Linearity Check Unit
LD	Light Duty
MFC	Mass Flow Controller
NaCl	Sodium Chloride
N_2	Nitrogen
NO	Nitrogen Monoxide
NOx	Nitrogen Oxides
O_2	Oxygen
PCRF	Particle Concentration Reduction Factor
PFDS	Partial Flow Dilution System
PM	Particulate Matter
PN	Particle Number
PMP	Particle Measurement Programme
SMPS	Scanning Mobility Particle Sizer
s_{stab}	Uncertainty in the PCRF (expressed in standard deviation) related to the stability of the concentrations
s_{bckg}	Uncertainty in the PCRF (expressed in standard deviation) related to the background concentrations
s_{rep}	Uncertainty in the PCRF (expressed in standard deviation) related to the repeatability of the measurements

TDMA	Tandem Differential Mobility Analyzer
UK	United Kingdom
UN-ECE	United Nations Economic Council for Europe
US	United States
VPR	Volatile Particle Remover
WHTC	Word-harmonized Heavy duty Transient Cycle

7 REFERENCES

Andersson, J. and Clarke, D. (2004). UN-GRPE PMP Phase 3: Inter-laboratory Correlation Exercise: Framework and Laboratory Guide. Available at: http://www.unece.org/trans/doc/2005/wp29grpe/PMP-2005-14-01e.pdf

Andersson J., Giechaskiel B., Muñoz-Bueno R., Sandback E. And Dilara P. (2007). Particle Measurement Programme (PMP) Light-Duty Inter-Laboratory Correlation Exercise (ILCE_LD) Final Report. EUR 22775 EN, Available for download at: http://ies.jrc.ec.europa.eu/uploads/fileadmin/Documentation/Reports/Emissions_and_Health/EUR_2006-2007/EUR_22775_EN.pdf

Andersson, J., Mamakos, A., Giechaskiel, B., Carriero, M. and Martini, G. (2010). Particle Measurement Programme (PMP) Heavy Duty Inter-laboratory Correlation Exercise (LCE_HD) Final Report. JRC Scientific and Technical Reports EUR 24561 EN.

Andersson, J., Wedekind, B., Hall, D., Stradling, R. and Wilson, G. (2001). DETR/SMMT/CONCAWE Particulate Research Programme: Light Duty Results. SAE Technical Paper 2001-01-3577.

Berg, W. (2003). Legislation for the Reduction of Exhaust Gas Emissions, in Handbook of Environment Chemistry, 3(Part T), Series, Anthropogenic Compounds, Traffic and Environment, Springer, pp 175-253.

Biskos, G., Paulsen, D., Russell, L. M., Buseck, P. R. and Martin, S.T. (2006). Prompt Deliquescence and Efflorescence of Aerosol Nanoparticles. Atmospheric Chemistry and Physics, 6:4633–4642.

COM 446 Final (2005). Communication from the Commission to the Council and the European Parliament. Thematic Strategy on Air Pollution. Available at: http://eur-lex.europa.eu/LexUriServ/LexUriServ.do?uri=COM:2005:0446:FIN:EN:PDF

Commission Regulation 692/2008. Available at: http://eur-lex.europa.eu/LexUriServ/LexUriServ.do?uri=CELEX:32008R0692:en:NOT

Commission Regulation 715/2007. Available at: http://eur-lex.europa.eu/LexUriServ/LexUriServ.do?uri=CELEX:32007R0715:en:NOT

EPA (2009). Integrated Science Assesment for Particulate Matter. Final Report. U.S. Environmental Protection Agency, Washington, DC, EPA/600/R-08/139F, 2009. Available at: http://cfpub.epa.gov/ncea/cfm/recordisplay.cfm?deid=216546#Download

Federal Register (2001). Control of emissions from new and in-use highway vehicles. Rules Regul, 66 (12)

Giechaskiel B., Carriero M., Martini G., Anderson J. (2009a). Heavy Duty Particle Measurement Programme (PMP): Exploratory Work for the Definition of the Test Protocol. SAE Technical Papers 2009-01-1767

Giechaskiel, B., Carriero, M., Martini, G., Krsenbrink, A. and Scheder, D. (2009b). Calibration and Validation of Various Commerical Particle Number Measurement Systems. SAE Technical Paper 2009-01-1115.

Giechaskiel, B., Wang, X., Horn, H.-G., Spielvogel, J., Gerhart, C., Southgate, J., Jing, L., Kasper, M., Drossinos, Y. and Krasenbrink, A. (2009c). Calibration of Condensation Particle Counters for Legislated Vehicle Number Emission Measurements. Aerosol Science and Technology, 43: 1164-1173.

Giechaskiel, B., Dilara, P. and Andersson, J. (2008a). Particle Measurement Programme (PMP) Light Duty Inter-Laboratory Exercise: Repeatability and Reproducibility of the Particle Number Method. Aerosol Science and Technology, 42:528-543.

Giechaskiel, B., Dilara, P., Sandbach, E. and Andersson, J. (2008b). Particle Measurement Programme (PMP) Light Duty Inter-Laboratory Exercise: Comparison of Different Particle Number Measurement Systems. Measurement Science and Technology, 19:095401.

Giechaskiel, B. and Drossinos, I. (2010). Theoretical Investigation of Volatile Removal Efficiency of Particle Number Measurement Systems. SAE Technical Paper 2010-01-1304.

Giechaskiel, B., Mamakos, A., Andersson, J., Dilara, P., Martini, G., Schindler, W., Bergmann, A. (2012). Measurement of Automotive Nonvolatile Particle Number Emissions within the European Legislative Framework: A Review. Aerosol Science and Technology, 46:719-749.

Giechaskiel, B., Munoz-Bueno, R., Rubino, L., Manfredi, U., Dilara, P., De Santi, G. and Andersson, J. (2007). Particle Measurement Programme (PMP): Particle Emissions Size and Number Emissions Before, During and After Regeneration Events of a Euro 4 DPF Equipped Light Duty Diesel Vehicle. SAE Technical Paper 2007-01-1944.

Giechaskiel, B., Ntziachristos, L. and Samaras, Z. (2004). Calibration and Modelling of Ejector Dilutors for Automotive Exhaust Sampling. Measurement Science and Technology, 15:2199–2206.

Giechaskiel, B., Wang, X., Gilliland, D. and Drossinos, Y. (2011). The Effect of Particle Chemical Composition on the Activation Probability in n-butanol Condensation Particle Counters. Journal of Aerosol Science, 42: 20-37.

Giechaskiel, B., and Bergmann, A. (2011). Validation of 14 used, re-calibrated and new TSI 3790 condensation particle counters according to the UN-ECE Regulation 83. *J. Aerosol Sci.,* 42:195-203.

Gotoh, A., Ikazaki H., and Kawamura, M. (1990) Simple Generator of Ultrafine Particles for Tests. Journal of Colloid and Interface Science, 140, 535-537.

Jing, L. (1999). Standard Combustion Aerosol Generator (SCAG) for Calibration Purposes. 3rd ETH Workshop on "Nanoparticle Measurement", ETH Hönggerberg Zürich, 9-10 August 1999.

Lall, A., A. and Friedlander, S. K. (2006). On-line Measurement of Ultrafine Aggregate Surface Area and Volume Distributions by Electrical Mobility Analysis: I. Theoretical Analysis. Journal of Aerosol Science, 37:260–271.

Mamakos, A., Giechaskiel, B. and Drossinos, I., Lesueur, D., Martini, G. and Krasenbrink, A. (2011a). Calibration and Modelling of PMP-Compliant Condensation Particle Counters. JRC Scientific and Technical Research Report, EUR 25145 EN. Available at:
http://publications.jrc.ec.europa.eu/repository/handle/111111111/25454

Mamakos, A., Carriero, M., Bonnel, P., Demircioglu, H., Douglas, K., Alessandrini, S., Forni, F., Montigny, F. and Lesueur, D. (2011b). EU-PEMS PM Evaluation Program - Second Report - Study on Post DPF PM/PN Emissions. JRC Scientific and Technical Research Report, EUR 24793 EN. Available at:
http://publications.jrc.ec.europa.eu/repository/handle/111111111/16239

Maricq, M.M. (2007). Bipolar Diffusion Charging of Soot Aggregates. Aerosol Science and Technology, 42:247-254.

Rogak, S., N. and Flagan R., C. (1992). Bipolar Diffusion Charging of Spheres and Agglomerate Aerosol Particles. Journal of Aerosol Science, 23:693–703.

Sakurai, H., Saito, K., Taishi, T., andKoyama, T. (2011). Two Sources of Error in Determination of the Particle Concentration Reduction Factor of the Volatile Particle Remover Used in Legislated Vehicle Emission Measurement. Meas. Sci. Technol., 22:085108.

TSI (2010). Live-Time Counting. CPC-001 Rev. A.

UNECE Regulation No. 49. Proposal for Supplement 4 to the 05 Series of Ammendments to Regulation No. 49 (Emissions of Compression Ignition and Gas Fuelled Positive Ignition Engines for Use in Vehicles). Available at: http://www.unece.org/trans/main/wp29/wp29regs41-60.html

UNECE Regulation No. 83. Uniform Provisions Concerning the Approval of Vehicles with Regard to the Emission of Pollutants According to Engine Fuel Requirements. Available at:
http://www.unece.org/trans/main/wp29/wp29regs81-100.html

Wang, X. and Horn, H.-G. (2008). Flow Rate Correction for the Model 3790 Engine Exhaust Condensation Particle Counter (EECPC). TSI application note Application Note EECPC-001.

Wen, H.,Y. , Reischl, G.,P. and Kasper G. (1984). Bipolar Diffusion Charging of Fibrous Aerosol Particles—I. Charging Theory. Journal of Aerosol Science, 15:89-101.

Wiedensohler A. (1988). An Approximation of the Bipolar Charge Distribution for Particles in the Submicron Size Range. Journal of Aerosol Science, 19: 387-389.

Zervas, E., Dorhene, P., Forti, L., Perrin, C., Monique, J., C., Monier, R., Ing, H. and Lopez, B. (2005). Inter-Laboratory Test of Exhaust PM Using ELPI. Aerosol Science and Technology, 39:333-346.

8 ANNEX A

8.1 Description of the minimum required calibration work to be performed at each participating laboratory

1. The instruments shall be inspected for damage on arrival at the lab. Below is a list of components you should receive:
    a. Dual ejector system:
        i. 2 × Ejectors
        ii. ET
        iii. Pressure transducer and thermocouple block
        iv. Dilution air heater
        v. Heating blanket, & rope to tide it up around the hot ejector.
        vi. Metal tubing to vent the excess flow of the hot ejector
        vii. Temperature controllers for the dilution air heater, the heating blanket and the ET.
        viii. Spare sealing o-rings.
    b. PALAS spark generator (including connection fittings, power cable and spare graphite electrodes).
    c. 3790 CPC (including manual, power cable, serial and usb cables, spare o-rings).
    d. HEPA Capsule to be employed in the dilution air line (in case the compressed air line is not filtered by any other means)
2. The dual ejector system shall be assembled upon my arrival. I want to ensure that it is properly assembled before testing.
3. Experimental work: Before each test the dual ejector systems shall be left running for at least 1 hour with the heaters on to allow for the stabilization of the temperatures. The dual ejector system shall always operate in 2 bar overpressure and at an inlet pressure of 3 kPa below ambient. The connection of the CPC(s) to the outlet of the dual ejector system shall always be performed through an T fitting in order to avoid any pressure buildup
    a. Leak check: Special care shall be taken regarding the background levels downstream the VPR. These should be below 2 #/cm3. The HEPA capsule provided should suffice for that. If not there might be some leakage problems. These tests should be performed with me present so that I can potentially assist you resolving the problem.
    b. Dilution factor measurement: The dilution factor of the dual ejector system fully assembled with the heaters on, shall be measured using a trace gas. The calibration gas should be at a concentration level that would allow accurate determination of a DF around 100, taking into account the background levels of the trace gas. The inlet pressure of the dual ejector system shall be -3 kPa gauge. This can be achieved through a valve installed upstream the pressure transducer block.
    c. PCRF measurements:
        i. Golden aerosol generator: Each lab shall provide the necessary equipment to size classify the generated polydisperse aerosol at 30, 50 and 100 nm. No thermal treatment shall be applied to ensure identical conditions at each lab. The PALAS generator setting shall be 3 lpm air, 3 lpm N_2, 2 mA and medium energy for the 50 and 100 nm tests and 6 lpm air, 3 lpm N_2, 0.75 mA at medium energy for the 30 nm tests. Due to the relatively high sample flowrate of the ejectors (~ 5 lpm) some HEPA filtered make up air will be necessary, as well as some kind of mixer (like a long silicon tubing). The sample pressure at the inlet of the ejector must be -3 kPa gauge. This can be achieved by means of a valve downstream the mixing point of the make up air and the DMA outlet flow, that could also enhance mixing.
        In these particular tests I will request from you to employ two CPCs in parallel (one being the golden one) operating on at 1 slpm. One should be sampling

downstream the ejector and one upstream in parallel with the ejector. The tubing employed to connect the two CPCs in the setup should be of exactly the same dimensions. At each setting one should interchange the position of the two CPCs at least 8 times and record the concentrations for at least 1 minute once the levels stabilize.

At the start and the end of the measurements of each size the background levels shall be recorded at both sampling positions (upstream and downstream the VPR) with both CPCs. The size distribution should also be measured, by means of extracting sample form the golden generator at the same sample flowrate and using the same plumbing with that employed during the PCRF calibration.

ii. Alternative generators: Each lab shall follow the approach they typically follow for the calibration of their equipment. They are free to use the golden CPC. The size distribution of the produced calibration aerosol shall also be recorded during the testing.

iii. Characterization of particle losses at 15 nm: Given the recent interest in sub-23 nm particles emitted by diesel and gasoline vehicles, I would like to ask each participant to perform <u>on a voluntary basis</u> some PCRF measurements at 15 nm, or provide some thoughts and suggestions in this issue.

d. CPC linearity checks: Since the linearity of the CPCs employed can potentially affect the measured PCRF values we suggest that each lab inter-correlate the CPC units employed with the golden one. This could be easily implemented by means of having the CPC under evaluation sampling in parallel with the Golden CPC monodisperse aerosol produced by the golden generator (PALAS setting: 3lpm Air, 3 lpm N2, 6 mA current, Medium Energy). The DMA shall be set at a size of >100 nm to ensure that the CPCs have reached the peak detection efficiency. The measured concentrations can be adjusted by means of a dilution bridge installed upstream the DMA. At least 6 concentration levels should be checked between 20 and 10000 #/cm3. No need for thermal treatment is required for these tests.

9 ANNEX B

9.1 Original calibration certificate of the GCPC (Page 1/2)

CPC MODEL 3790 CERTIFICATE OF CALIBRATION

70721012	Serial number	Test Aerosol: Emery Oil
06 July 2010	Date	

Inlet Flow (Volumetric)		Units	Low Limit	High Limit
1	Inlet Flow Value	L/min	0.95	1.05

Temperature and Pressure		Units	Low Limit	High Limit
21	Room Temperature	°C	-	-
48%	Room Relative Humidity	-	-	-
38.3	Saturator Temperature	°C	38	38.7
31.7	Condensor Temperature	°C	30.5	32
40	Optics Temperature	°C	39.8	40.2
25.2	Cabinet Temperature	°C	20	35
99.9	Ambient Pressure	kPa	88	108
78.9	Pressure Drop across Orifice	kPa	70	88
2.951	Pressure Drop across Nozzle	kPa	1.9	3.2

Laser Check		Units	Low Limit	High Limit
17	Laser power (measured)	mW	14	20

Optics		Units	Low Limit	High Limit
35	Laser current reading	mA	12	-
2.2	Minimum pulse height	V	1	3.65
120	Minimum pulse width	ns	110	450
3.3	Maximum pulse height	V	2	3.65
220	Maximum pulse width	ns	110	450

Zero Count Test		Units	Low Limit	High Limit
0	Concentration average over 12 hours	p/cc	0	0.001

Lower Detection & Concentration Linearity Test Results		Units	Low Limit	High Limit
58.9%	23 nm Particle Counting Efficiency	-	38%	62%
92.4%	41 nm Particle Counting Efficiency	-	90%	-
96.8%	Linearity Test: Slope (up to 10,000 p/cc)	-	90%	110%
0.9900	Linearity of Regression (R)	-	0.97	-
N/A	CPC / Electrometer Counting Ratio (25,000 p/cc nom.)	-	-	-
N/A	CPC / Electrometer Counting Ratio (50,000 p/cc nom.)	-	-	-

Final Voltage Measurements	
Pass	Analog Input and Output Voltages
Pass	Verify flash memory function (pass/fail)

			Units	Low Limit	High Limit
-6.32%	2000 p/cc	CPC Concentration	% Diff.	-10%	10%
-5.32%	4000 p/cc	CPC Concentration	% Diff.	-10%	10%
-3.52%	6000 p/cc	CPC Concentration	% Diff.	-10%	10%
-3.99%	8000 p/cc	CPC Concentration	% Diff.	-10%	10%
-1.88%	10000 p/cc	CPC Concentration	% Diff.	-10%	10%

9.2 Original calibration certificate of the GCPC (Page 2/2)

LINEARITY RESPONSE

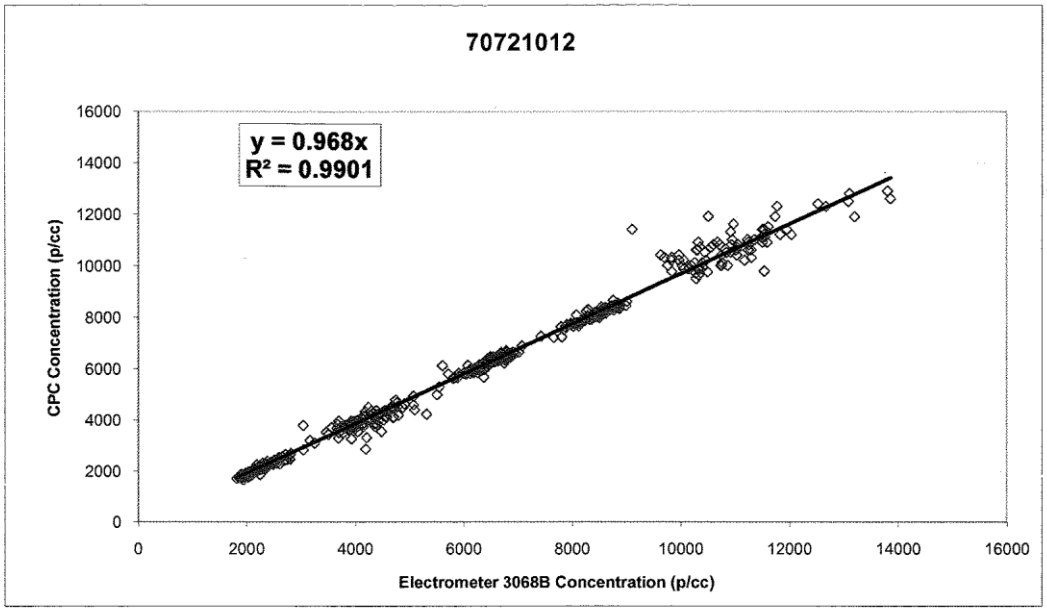

TSI Instruments does hereby certify that the above described instrument conforms to the original manufacturer's specifications (not applicable to As Found data) and has been calibrated using standards whose accuracies are traceable to the National Standards or have been derived from accepted values of natural physical constants or have been derived by the ratio type of self calibration techniques.
The calibration ratio for this instrument is at least 1:1. TSI's calibration system meets ISO-9001, Quality Assurance Requirements for Measuring Equipment. This report may not be reproduced, except in full, unless permission for the publication of an approved abstract is obtained in writing from the calibration organization issuing this report.

Measurement Variable	Sytem ID Number	Date Last Calibrated	Calibration Date Due
Voltage Measurement	UK 95650607	09/03/2010	09/03/2011
Electrometer	E006117	17/09/2009	17/09/2010
Aerosol Flow	UK 0701068-S	22/02/2010	22/02/2011
Classifier Flow	E006118	31/03/2010	31/03/2011
Temperature Measurement	UKQ231307	30/11/2009	30/11/2010

Matthew Griffin
Calibrated By

06 July 2010
Calibration Date

9.3 Calibration certificate of the GCPC after the failure at LAT (Page 1/2)

CPC MODEL 3790 CERTIFICATE OF CALIBRATION

70721012	Serial number	Test Aerosol: Emery Oil
30/11/2010	Date	

Inlet Flow (Volumetric)

		Units	Low Limit	High Limit
0.99	Inlet Flow Value	L/min	0.95	1.05

Temperature and Pressure

		Units	Low Limit	High Limit
20	Room Temperature	°C	-	-
40%	Room Relative Humidity	-	-	-
38.3	Saturator Temperature	°C	38	38.7
31.5	Condensor Temperature	°C	30.5	32
40	Optics Temperature	°C	39.8	40.2
25.2	Cabinet Temperature	°C	20	35
97.5	Ambient Pressure	kPa	88	108
80	Pressure Drop across Orifice	kPa	70	88
2.929	Pressure Drop across Nozzle	kPa	1.9	3.2

Laser Check

		Units	Low Limit	High Limit
17	Laser power (measured)	mW	14	20

Optics

		Units	Low Limit	High Limit
42	Laser current reading	mA	12	-
1.5	Minimum pulse height	V	1	3.65
120	Minimum pulse width	ns	110	450
3.3	Maximum pulse height	V	2	3.65
220	Maximum pulse width	ns	110	450

Zero Count Test

		Units	Low Limit	High Limit
0	Concentration average over 12 hours	p/cc	0	0.001

Lower Detection & Concentration Linearity Test Results

		Units	Low Limit	High Limit
61.4%	23 nm Particle Counting Efficiency	-	38%	62%
90.1%	41 nm Particle Counting Efficiency	-	90%	-
92.0%	Linearity Test: Slope (up to 10,000 p/cc)	-	90%	110%
0.9997	Linearity of Regression (R^2)	-	0.97	-
N/A	CPC / Electrometer Counting Ratio (25,000 p/cc nom.)	-	-	-
N/A	CPC / Electrometer Counting Ratio (50,000 p/cc nom.)	-	-	-

Final Voltage Measurements

Pass	Analog Input and Output Voltages
Pass	Verify flash memory function (pass/fail)

Linearity Response: CPC vs. Electrometer 3068B

			Units	Low Limit	High Limit
-8.80%	2000 p/cc	CPC Concentration	% Diff.	-10%	10%
-7.77%	4000 p/cc	CPC Concentration	% Diff.	-10%	10%
-7.77%	6000 p/cc	CPC Concentration	% Diff.	-10%	10%
-7.98%	8000 p/cc	CPC Concentration	% Diff.	-10%	10%
-8.16%	10000 p/cc	CPC Concentration	% Diff.	-10%	10%

9.4 Calibration certificate of the GCPC after the failure at LAT (Page 1/2)

LINEARITY RESPONSE

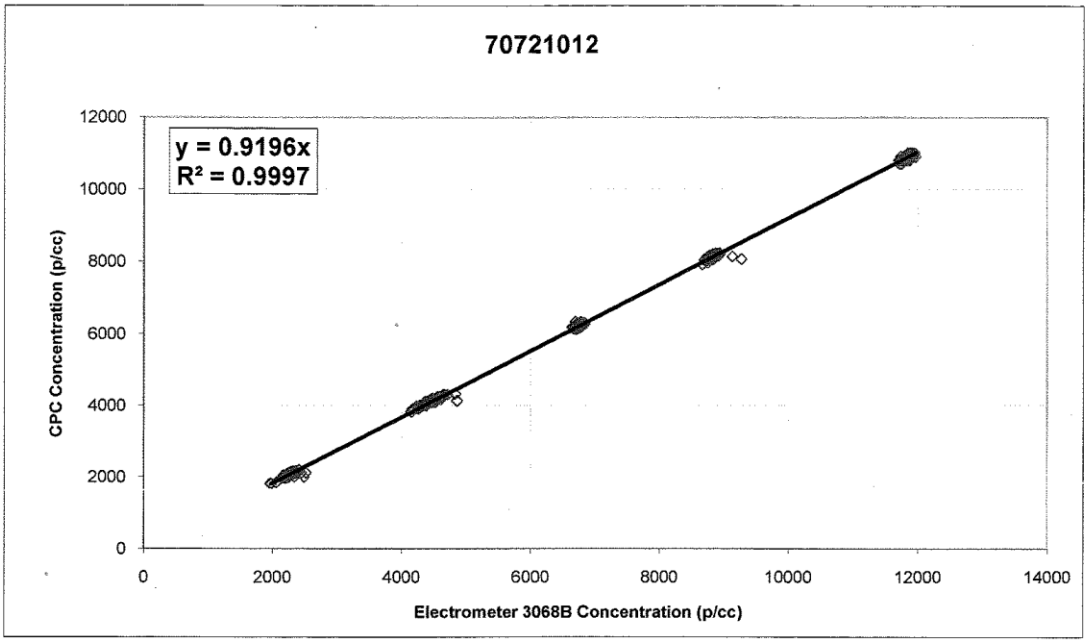

TSI Instruments does hereby certify that the above described instrument conforms to the original manufacturer's specifications (not applicable to As Found data) and has been calibrated using standards whose accuracies are traceable to the National Standards or have been derived from accepted values of natural physical constants or have been derived by the ratio type of self calibration techniques.
The calibration ratio for this instrument is at least 1:1. TSI's calibration system meets ISO-9001, Quality Assurance Requirements for Measuring Equipment. This report may not be reproduced, except in full, unless permission for the publication of an approved abstract is obtained in writing from the calibration organization issuing this report.

Measurement Variable	Sytem ID Number	Date Last Calibrated	Calibration Date Due
Voltage Measurement	UK 95650607	09/03/2010	09/03/2011
Electrometer	E006117	23/09/2010	23/09/2011
Aerosol Flow	UK 1010010-S	05/10/2010	05/10/2011
Classifier Flow	E006118	31/03/2010	31/03/2011
Temperature Measurement	UKQ231307	15/10/2010	15/10/2011

Matthew Griffin
Calibrated By

30 November 2010
Calibration Date

9.5 Calibration certificate of the GCPC after the failure at AEAT (Page 1/2)

CPC MODEL 3790 CERTIFICATE OF CALIBRATION

70721012	Serial number Test Aerosol: Emery Oil
13 October 2011	Date

Inlet Flow (Volumetric)		Units	Low Limit	High Limit
1	Inlet Flow Value	L/min	0.95	1.05

Temperature and Pressure		Units	Low Limit	High Limit
21	Room Temperature	°C	-	-
57%	Room Relative Humidity	-	-	-
38.3	Saturator Temperature	°C	38	38.7
31.7	Condensor Temperature	°C	31	32.5
40	Optics Temperature	°C	39.8	40.2
28.4	Cabinet Temperature	°C	20	35
99.3	Ambient Pressure	kPa	88	108
75.8	Pressure Drop across Orifice	kPa	70	88
2.9	Pressure Drop across Nozzle	kPa	1.9	3.2

Laser Check		Units	Low Limit	High Limit
18	Laser power (measured)	mW	14	20

Optics		Units	Low Limit	High Limit
42	Laser current reading	mA	12	-
3	Minimum pulse height	V	1	3.65
340	Minimum pulse width	ns	110	450
3.4	Maximum pulse height	V	2	3.65
360	Maximum pulse width	ns	110	450

Zero Count Test		Units	Low Limit	High Limit
0	Concentration average over 12 hours	p/cc	0	0.001

Lower Detection & Concentration Linearity Test Results		Units	Low Limit	High Limit
48.3%	23 nm Particle Counting Efficiency	-	38%	62%
90.8%	41 nm Particle Counting Efficiency	-	90%	-
95.7%	Linearity Test: Slope (up to 10,000 p/cc)	-	90%	110%
0.9996	Linearity of Regression (R^2)	-	0.97	-
N/A	CPC / Electrometer Counting Ratio (25,000 p/cc nom.)	-	-	-
N/A	CPC / Electrometer Counting Ratio (50,000 p/cc nom.)	-	-	-

Final Voltage Measurements	
Pass	Analog Input and Output Voltages
Pass	Verify flash memory function (pass/fail)

Linearity Response: CPC vs. Electrometer 3068B				Units	Low Limit	High Limit
Nominal Conc.	UUT	Electrometer	%Difference			
2000 p/cc	1917.89	2018.05	-4.96%	% Diff.	-10%	10%
4000 p/cc	4111.78	4297.42	-4.32%	% Diff.	-10%	10%
6000 p/cc	5892.44	6162.22	-4.38%	% Diff.	-10%	10%
8000 p/cc	7942.33	8286.74	-4.16%	% Diff.	-10%	10%
10000 p/cc	10038.56	10490.55	-4.31%	% Diff.	-10%	10%

9.6 Calibration certificate of the GCPC after the failure at AEAT (Page 2/2)

LINEARITY RESPONSE

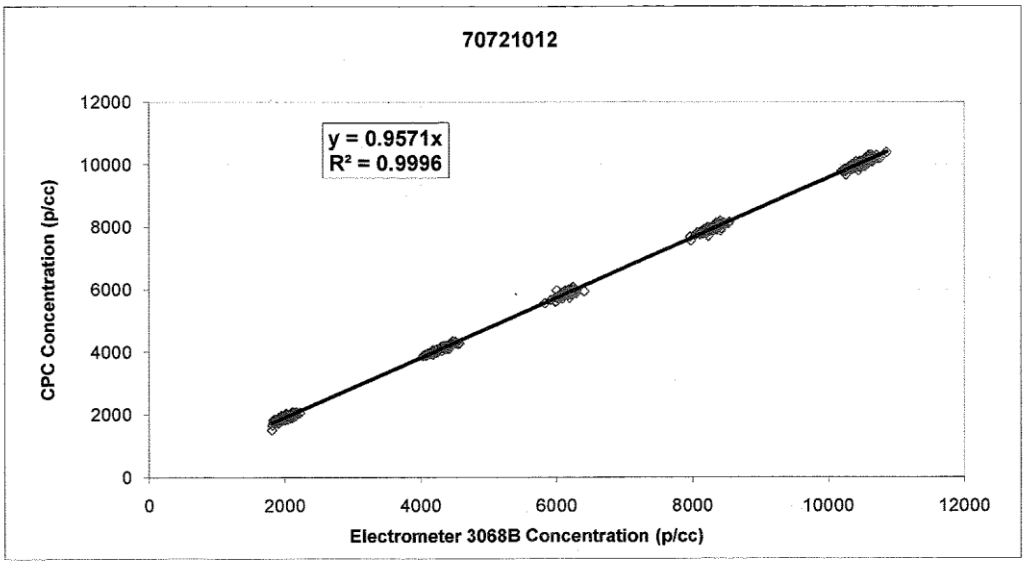

TSI Instruments does hereby certify that the above described instrument conforms to the original manufacturer's specifications (not applicable to As Found data) and has been calibrated using standards whose accuracies are traceable to the National Standards or have been derived from accepted values of natural physical constants or have been derived by the ratio type of self calibration techniques.
The calibration ratio for this instrument is at least 1:1. TSI's calibration system meets ISO-9001, Quality Assurance Requirements for Measuring Equipment. This report may not be reproduced, except in full, unless permission for the publication of an approved abstract is obtained in writing from the calibration organization issuing this report.

Measurement Variable	Sytem ID Number	Date Last Calibrated	Calibration Date Due
Voltage Measurement	UK 95650607	28 April 2011	28 April 2012
Electrometer	UK 71050219	04 January 2011	04 January 2012
Aerosol Flow	UK 1002016-S	09 February 2011	09 February 2012
Classifier Flow	UK 70711001	11 October 2011	11 October 2012
Temperature Measurement	E006164	04 May 2011	04 May 2012

Daniel Hatton
Calibrated By

13 October 2011
Calibration Date

9.7 Calibration certificate of the GCPC after the failure at VW (Page 1/2)

CPC MODEL 3790 CERTIFICATE OF CALIBRATION

70721012 Serial Number Test Aerosol: Emery Oil

16 February 2012 Date

Inlet Flow

		Units	Low Limit	High Limit
0.98	Measured Flow (Volumetric)	L/min	0.95	1.05
0.914	Calculated Flow (Standard)	SL/min	-	-

Standard Conditions: 0° C, 101.3 kPa

Temperature and Pressure

		Units	Low Limit	High Limit
21	Room Temperature	°C	-	-
22%	Room Relative Humidity	-	-	-
101.7000	Room Barometric Pressure	kPa	-	-
38.3	Saturator Temperature	°C	38	38.7
31.6	Condenser Temperature	°C	31	32.5
40	Optics Temperature	°C	39.8	40.2
30.5	Cabinet Temperature	°C	20	35
75	Pressure Drop Across Orifice	kPa	70	88
2.8	Pressure Drop Across Nozzle	kPa	1.9	3.2

Laser Check

		Units	Low Limit	High Limit
17	Laser Power (Measured)	mW	14	20

Optics

		Units	Low Limit	High Limit
41	Laser Current Reading	mA	12	-
2.6	Minimum Pulse Height	V	1	3.65
360	Minimum Pulse Width	ns	110	450
3.6	Maximum Pulse Height	V	2	3.65
420	Maximum Pulse Width	ns	110	450

Zero Count Test

		Units	Low Limit	High Limit
0	Concentration Average Over 12 Hours	p/cc	0	0.001

Lower Detection & Concentration Linearity Test Results

		Units	Low Limit	High Limit
56.1%	23 nm Particle Counting Efficiency	-	38%	62%
92.3%	41 nm Particle Counting Efficiency	-	90%	-
94.6%	Linearity Test: Slope (up to 10,000 p/cc)	-	90%	110%
0.9995	Linearity of Regression (R^2)	-	0.97	-

Final Voltage Measurements

Pass	Analog Input and Output Voltages
Pass	Verify Flash Memory Function (Pass/Fail)

Linearity Response: CPC vs. Electrometer 3068B

Nominal Conc.	UUT	Electrometer	%Difference	Units	Low Limit	High Limit
2000 p/cc	2162.36	2274.28	-4.92%	% Diff.	-10%	10%
4000 p/cc	3981.07	4207.43	-5.38%	% Diff.	-10%	10%
6000 p/cc	6098.30	6441.91	-5.33%	% Diff.	-10%	10%
8000 p/cc	8249.55	8731.62	-5.52%	% Diff.	-10%	10%
10000 p/cc	10308.62	10893.84	-5.37%	% Diff.	-10%	10%

Particle Size Used in Linearity Test: 55 nm

9.8 Calibration certificate of the GCPC after the failure at VW (Page 2/2)

LINEARITY RESPONSE

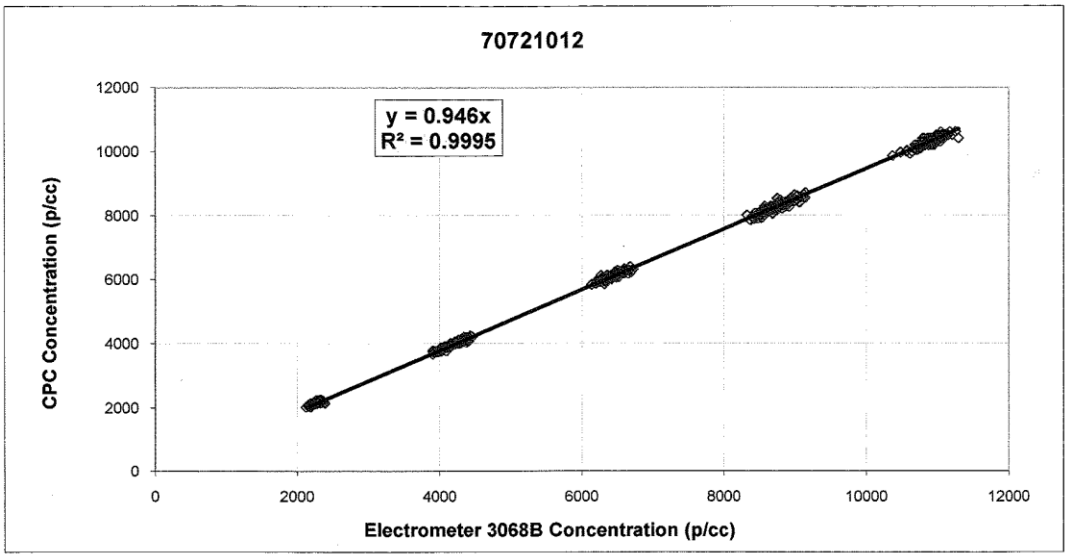

TSI Incorporated does hereby certify that the above described instrument conforms to the original manufacturer's specifications (not applicable to As Found data) and has been calibrated using standards whose accuracies are traceable to the National Institute of Standards and Technology within the limitations of NIST's calibration services or have been derived from accepted values of natural physical constants or have been derived by the ratio type of self calibration techniques. The calibration ratio for this instrument is at least 1:1. TSI's calibration system meets ISO-9001:2000 and complies with ISO 10012:2003, Quality Assurance Requirements for Measuring Equipment. This report may not be reproduced, except in full, unless permission for the publication of an approved abstract is obtained in writing from the calibration organization issuing this report

Measurement Variable	System ID Number	Date Last Calibrated	Calibration Date Due
High Voltage Divider	E003452	29 April 2011	29 April 2012
Voltage Measurement	UK 95650607	28 April 2011	28 April 2012
Electrometer	E006117	10 October 2011	10 October 2012
Aerosol Flow	UK 0507091-S	09 February 2012	09 February 2013
Classifier Flow	UK 70711001	11 October 2011	11 October 2012
Temperature Measurement	E006157	18 November 2011	18 November 2012
Barometric Pressure Gage	E006013	29 March 2011	29 March 2012

Daniel Hatton
Calibrated By

16 February 2012
Calibration Date

European Commission
EUR 25512 – Joint Research Centre – Institute for Energy and Transport

Title: Particle Measurement Programme. Volatile Particle Remover Calibration Round Robin. Final Report.

Author: Athanasios Mamakos
Editors: Giorgio Martini, Alois Krasenbrink

Luxembourg: Publications Office of the European Union

2012 – 86 pp. – 21.0 x 29.7 cm

EUR – Scientific and Technical Research series – ISSN 1831-9424 (online), ISSN 1018-5593 (print)

ISBN 978-92-79-26416-0 (pdf)
ISBN 978-92-79-26417-7 (print)

doi: 10.2788/49253

Abstract

A dual ejector system with an intermediate Evaporating Tube was circulated at 11 laboratories to measure the Particle Concentration Reduction Factors (*PCRF*) at 30, 50 and 100 nm (as required by the legislation). In addition to this "Golden" Volatile Particle Remover (GVPR), a PALAS DNP 3000 graphite spark generator (Golden Aerosol Generator - GAG) and a TSI 3790 Condensation Particle Counter (Golden CPC – GCPC), were also circulated to compare the performance of the different aerosol generators (including CAST, sodium chloride and palladium) and CPCs employed at each laboratory. The study highlighted the importance of controlling and accounting for the pressures in the calibration setup. It also highlighted the difficulties associated with the measurement of the size distribution of the polydisperse aerosols produced by the generators that due to the high number concentrations are prone to significant coagulation. The study also provided evidence that the pre-treatment of sodium-chloride and CAST particles employed in most laboratories is not sufficient, and can lead to inaccuracies in the PCRF measurements at 30 nm if a CPC with a 50% counting efficiency at 23 nm is employed. No significant linearity issues were identified in the 15 in total CPCs that were cross-checked against the GCPC. However, a change of the operating temperature of TSI 3790 CPCs to reduce the cut-off size can lead to significant linearity issues for some units, and therefore such modifications must be accompanied by linearity checks.

LB-NA-25512-EN-N

As the Commission's in-house science service, the Joint Research Centre's mission is to provide EU policies with independent, evidence-based scientific and technical support throughout the whole policy cycle.

Working in close cooperation with policy Directorates-General, the JRC addresses key societal challenges while stimulating innovation through developing new standards, methods and tools, and sharing and transferring its know-how to the Member States and international community.

Key policy areas include: environment and climate change; energy and transport; agriculture and food security; health and consumer protection; information society and digital agenda; safety and security including nuclear; all supported through a cross-cutting and multi-disciplinary approach.

Publications Office

ISBN 978-92-79-26416-0